Pion-pion scattering and the diffractive production of nucleon resonances

Macgregor, B. R.

P I O N - P I O N S C A T T E R I N G

AND THE

D I F F R A C T I V E P R O D U C T I O N

OF

N U C L E O N R E S O N A N C E S

THESIS SUBMITTED TO

THE UNIVERSITY OF DURHAM

BY

B.R.MACGREGOR, B.Sc. (DUNELM)

FOR

THE DEGREE OF DOCTOR OF PHILOSOPHY

DEPARTMENT OF PHYSICS
UNIVERSITY OF DURHAM

JULY 1976

CONTENTS

ABSTRACT

The physics related to two aspects of the $\pi N \to \pi\pi N$ reaction is studied.

We first consider the imposition of the constraints of analyticity, unitarity and, in particular, crossing, on the pion-pion scattering amplitudes, as extracted from studies of the low dipion mass kinematic region of the $\pi N \to \pi\pi N$ reaction. The application of the Roy equations to pion-pion scattering is discussed, then physical region crossing sum rules are systematically derived and applied, in conjunction with finite energy sum rules, to obtain information on the asymptotic pion-pion scattering amplitudes. The amplitudes are found to be well described in terms of Regge and pomeron exchange, with rho-f strong exchange degeneracy broken and an asymptotic total cross section for pion-pion scattering rather smaller than that expected from naive factorization arguments.

Other evidence for a small meson-meson scattering asymptotic total cross section is collected, and possible explanations for the apparent failure of the pomeron to factorize are discussed.

The second part of this thesis deals with diffraction dissociation processes. We discuss how the Deck-Drell-Hiida mechanism, in conjunction with the diffractive production, and subsequent decay, of resonances provides a good qualitative explanation of many of the features of inelastic diffractive scattering. Detailed data on the angular distributions of the diffractively produced pion-nucleon system in the 16 GeV. $\pi N \to \pi\pi N$ reaction are then interpreted quantitatively in terms of a simple model based on the above ideas, with full account taken of spin and interference effects. Information is obtained on the pomeron couplings, and the high energy t channel isospin zero pion-pion scattering amplitude, directly determined, is found to be consistent with the sum rule calculation results and a small asymptotic pion-pion scattering total cross section.

ACKNOWLEDGEMENTS

I am very grateful to Alan Martin for much encouragement and helpful advice. I also thank Penny Estabrooks, Fred Gault and Mike Pennington for helpful discussions, as well as all the other members of the Durham particle physics group for their continued enthusiasm about high energy physics.

The support of the Science Research Council is also gratefully acknowledged.

I: INTRODUCTION

The division of physics into the spheres of influence of four distinct interactions may be one of the most unphysical distinctions ever made.(1) Nevertheless, in spite of ambitious unification schemes (see eg. ref. (2) and references therein), a realistic unified theory is probably a very long way off, and it remains useful to consider the interactions separately when interpreting experimental data. It is currently fashionable (once again) to use field theory in attempts to understand the strong interaction, and the literature is full of quarks, gluons and gauge theories. However, as Bjorken points out (3), there is in fact little direct evidence for these things, and so it is still useful to work with the general principles of S-matrix theory, which should be true whichever underlying theory turns out to be correct.

S-matrix ideas have been extremely successful in organizing and interpreting a great deal of strong interaction data, in addition to providing rigorous results like the dispersion relations and the Froissart bound (4). Only recently has the S-matrix approach led, via the dual models, back to field theory. The basic S-matrix theory assumptions provide a way of bypassing the step from quark-gluon ideas to hadronic interactions, by being concerned only with the properties of the observable amplitude for scattering from a given 'in' state to a given 'out' state. It is required that the amplitude be Lorentz invariant, T, C, P invariant, crossing symmetric, unitary, and analytic in the complex plane (for $2 \rightarrow 2$ scattering) of Mandelstam variables, with the only singularities being particle poles and those required by unitarity. (See ref.(5) for more details.)

We shall work, in this thesis, within the framework of S-matrix phenomenology of strong interactions. (The term 'phenomenology' is used here to denote the organization of data and its interpretation in terms of empirical rules and models.) We shall be mainly concerned with the 16 - 17 GeV/c $\pi N \rightarrow \pi\pi N$ reaction; this simple process contains a surprising amount of interesting physical information.

Firstly, as briefly discussed in section 1.7, the properties of $\pi\pi \rightarrow \pi\pi$ scattering (See refs.(13) for reviews of pion-pion scattering.) may be extracted by studying the $\pi N \rightarrow \pi\pi N$ reaction in the appropriate kinematic region, when

the mass of the outgoing pion-nucleon system is large. Since there are no pion targets, pion-pion scattering can only be studied indirectly by this, or a similar, means. Pion-pion scattering is the simplest possible strong interaction process, as it involves spinless equal mass particles. The general S-matrix principles are thus most easily applied, and constrain the reaction strongly. Models for the strong interaction are most easily constructed for pion-pion scattering, and their predictions are simple and easily tested. One of the few strong interaction calculations which may be performed from 'first principles' uses current algebra ideas to obtain predictions for the pion-pion scattering lengths (6); these predictions are now beginning to be tested as information on low energy pion-pion scattering becomes available. The duality predictions of linear Regge trajectories, exchange degeneracy, daughter resonances and straight line amplitude zero paths may be easily checked if good pion-pion scattering data is available. This role of pion-pion scattering as the proving ground for strong interaction phenomenology provides the motivation for the enormous effort devoted to detailed pion-pion phase shift analyses based on such reactions as $\pi N \longrightarrow \pi\pi N$ (7-12).

The application of the general S-matrix principles to pion-pion scattering will be the concern of the first part of this thesis. In particular we shall be concerned with the use of sum rules which, as a consequence of analyticity and crossing, link the low and high energy scattering amplitudes by integral equations. Finite energy sum rules for a $2 \rightarrow 2$ elastic scattering process such as $\pi N \longrightarrow \pi N$, are well known. (14) They tend to suffer from dependence on the energy chosen as the boundary between low and high energy descriptions of the amplitude, and to weight unfairly the higher energy region of the low energy amplitudes. Less well known are the physical region crossing sum rules, which may be obtained by imposing full three channel crossing on the amplitude for an equal mass $2 \rightarrow 2$ elastic scattering process such as pion-pion scattering. The sum rules resemble, but are independent of, finite energy sum rules, have a more even weighting, and are very much less dependent on the choice of boundary between low and high energy amplitudes. Together, crossing and finite energy sum rules are very useful for obtaining information

about high energy pion-pion scattering; this will be the subject of much of chapter two.

The $\pi N \rightarrow \pi\pi N$ reaction displays many interesting features in the kinematic region where the incident pion suffers little change in momentum in scattering from the nucleon, which dissociates into a low mass pion-nucleon system. A simple physical picture of the processes contributing to this 'diffraction dissociation' reaction may be obtained by considering the nucleon as a loosely bound state of pion and nucleon. Either of these particles may then be 'hit' by the incident pion, leaving the other as a 'spectator'. Alternatively an excited state of the pion-nucleon system may be formed, which subsequently decays to a free pion and a nucleon. The contributions of these three processes may be separated by considering the angular distributions of the outgoing pion-nucleon system. Direct information on high energy pion-pion scattering is obtained from the spectator nucleon process; information on how the pomeron (which mediates the interaction between the incoming pion and the nucleon) couples to the nucleon to excite a nucleon resonance may also be extracted. We shall show in the second part of this thesis how the detailed distributions of the outgoing low mass pion-nucleon system may be understood suprisingly well in terms of, basically, the simple mechanisms outlined above.

In the remainder of this introductory chapter, after a very brief discussion of the kinematics of a $2 \rightarrow 2$ scattering process, we consider in more detail how the principles of analyticity, crossing and unitarity constrain a scattering amplitude, emphasizing the simplest case of pion-pion scattering. We show how analyticity relates the asymptotic and low energy forms of a scattering amplitude by the finite energy sum rules, and how these may be applied to the pion-pion scattering amplitudes. We discuss the processes contributing to the $\pi N \rightarrow \pi\pi N$ reaction, and show how the partial wave amplitudes for pion-pion scattering may be extracted.

1.1: Kinematics

There are 3n - 4 independent kinematic variables available to describe a general 2 → n particle reaction. It is often convenient to choose these as Lorentz scalars, which may easily be related to experimental observables in any frame of reference. For the 2 → 2 reaction, two out of the three usual Mandelstam variables s, t, u, (see eg.ref.(15)) are often chosen. The three variables obey the relation:-

$$s + t + u = \sum_{i=1}^{4} m_i^2 \tag{1.1}$$

When the four particles all have the same mass, the variables are simply related to the centre of mass momenta, $\underline{q}$, and scattering angle θ by:-

$$s = 4\left(m^2 + |\underline{q}|^2\right) \tag{1.2}$$

$$t = -2|\underline{q}|^2(1 - \cos\theta) \tag{1.3}$$

$$u = -2|\underline{q}|^2(1 + \cos\theta) \tag{1.4}$$

Thus physical scattering (in the 's-channel') occurs when $s > 4m^2$, $t < 0$, $u < 0$. We choose our normalization (see appendix (A)) such that, for 2 → 2 equal mass scattering, the differential cross section is related to the transition matrix T by:-

$$\frac{d\sigma}{d(\cos\theta)} = \frac{1}{32\pi s}|T|^2 \tag{1.5}$$

We show how to derive the analagous result for 2 → 3 scattering in appendix 1B, and discuss the kinematics of 2 → 3 scattering in later chapters.

1.2: Analyticity, crossing and dispersion relations

As a consequence of unitarity, the elastic scattering amplitude, considered as a complex valued function of the complex variable s, must have a branch point at every value of s corresponding to the threshold for a kinematically allowed reaction. (See eg.ref.5) To make the amplitude a single valued function it is simplest (and conventional) to cut the complex s plane from the lowest energy branch point to $s = \infty$.

For simplicity, we now specialize to equal mass scatter-

ing, as exemplified by the $\pi^0\pi^0 \longrightarrow \pi^0\pi^0$ process. The scattering amplitude, T (s, t, u), is single valued in the complex s plane cut from s = 4 to $s = \infty$ (where we take the pion mass to be unity). The crossing postulate implies that the same amplitude must also describe 'u channel' $\pi^0\pi^0$ scattering, when $u > 4$, $s < 0$, $t < 0$; thus in order that the amplitude be single valued a cut must be made in the complex u plane from u = 4 to $u = \infty$, which appears in the s plane, by eq.(1.1) as cut from s = -t to $s = -\infty$.
The singularity arising from t-channel scattering when $t > 4$ may similarly be taken care of. We take the physical (s-channel) scattering amplitude as the limit, as $\varepsilon \to 0+$, of $T(s+i\varepsilon, t)$.

The Mandelstam hypothesis (16) states that the only singularities in the physical amplitude are those required by unitarity (a slightly less stringent condition may be derived from the postulates of axiomatic field theory (5)) and so the singularities outlined above are the only ones present in the $\pi^0\pi^0$ scattering amplitude. (In general 2 → 2 scattering,

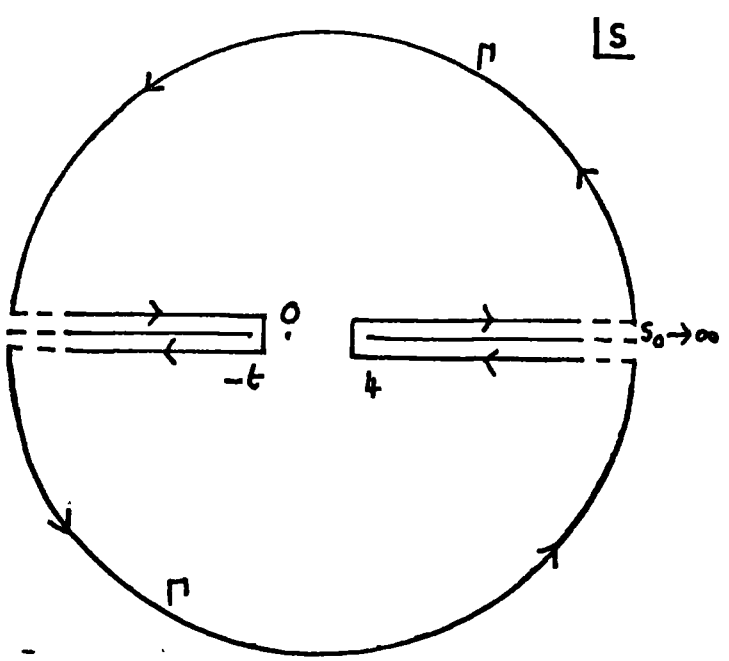

Fig.1.1. Dispersion relation contour of integration. The same contour, with a finite cutoff, is used in the derivation of finite energy sum rules.

there may also be poles on the real 's' axis corresponding to particles C, of mass less than the sum of the masses of A and B, formed in the AB $\rightarrow$ C reaction. No such particles can be formed from two pions.) We may summarize these properties by integrating the function $T(s, t_0, u)/(s - s_0)$, with t fixed at $t = t_0$, around the contour shown in fig.1.1 (maintaining the mass-shell condition (1.1)) and using Cauchy's theorem, to obtain the unsubtracted fixed t dispersion relation:-

$$Re\,T(s_0, t_0, u_0) = \frac{1}{\pi}\int_4^\infty \left(\frac{A(x, t_0)}{x - s_0} + \frac{A(x, t_0)}{x - u_0}\right) dx + \int_\Gamma \frac{A(x, t)}{x - s_0} \qquad (1.6)$$

The s - u crossing property $T(s, t, u) = T(u, t, s)$ has been used to write the integral over the left-hand cut in terms of the integral over the right-hand cut; the absorptive part of the amplitude, $A(s, t, u)$ is defined as:-

$$A(s, t, u) = \lim_{\varepsilon \to 0_+} \frac{T(s + i\varepsilon, t) - T(s - i\varepsilon, t)}{2i} \qquad (1.7)$$

This is equal to the imaginary part of the amplitude if s, t and u have such values that the scattering is physical. Eq.(1.6) is only meaningful if $\int_\Gamma dx\, T(x, t)/(x - s) = 0$. For this to be true, $T(s, t) \rightarrow 0$ as $s \rightarrow \infty$; if this is not the case we may repeat the above procedure, replacing $T(s, t, u)$ by $T(s, t, u)/(s - s_1)$ to obtain the once-subtracted dispersion relation:-

$$Re\,T(s_0, t_0, u_0) - Re\,T(s_1, t_0, u_1) = \frac{s_0 - s_1}{\pi}\int_4^\infty A(x, t)\left[\frac{1}{(x - s_0)(x - s_1)} - \frac{1}{(x - u_0)(x - u_1)}\right] dx + \int_\Gamma \frac{T(x, t)\, dx}{(x - s_0)(x - s_1)} \qquad (1.8)$$

The integral over Γ now converges if $T(s, t)/s \rightarrow 0$ as $s \rightarrow \infty$. This procedure may in general be carried out with n subtractions so that the integral over Γ converges if $T(s, t)/s^n \rightarrow 0$ as $s \rightarrow \infty$. For pion-pion scattering, Martin (17) has shown, from the postulates of axiomatic field theory, the important result that at most two subtractions are needed in dispersion relations for the amplitude when $s_0 > 4$, $4 > t_0 > -28$ (this includes an energy region where the scattering is unphysical).

1.3: Further consequences of crossing

In elastic pion-pion scattering it is possible (since all the particles are the same) to impose t - u crossing at the same time as s - u crossing, thus obtaining extra constraints on the scattering amplitude. We shall discuss these constraints in more detail in the next chapter; here we indicate the idea. Suppose that the $\pi^0\pi^0$ scattering amplitude obeys an unsubstracted dispersion relation; we may then write, for fixed $t = u_0$:-

$$Re\, T(s_0, u_0, t_0) = \frac{1}{\pi} \int_4^\infty \left(\frac{A(x, u_0)}{x - s_0} + \frac{A(x, u_0)}{x - t_0} \right) dx \qquad (1.9)$$

where the s - u crossing property has been used. Using t - u crossing, $T(s_0, u_0, t_0) = T(s_0, t_0, u_0)$, and equating eq. (1.9) to eq. (1.6) we find the crossing sum rule:-

$$\int_4^\infty \left(A(x, u_0) \left(\frac{1}{x - s_0} + \frac{1}{x - t_0} \right) - A(x, t_0) \left(\frac{1}{x - s_0} + \frac{1}{x - u_0} \right) \right) dx = 0 \qquad (1.10)$$

A similar operation may be carried out using once-subtracted dispersion relations, resulting in a more rapidly convergent integral - this will be left as an exercise for the reader.

For charged pions, the application of crossing is complicated by the fact that the scattering is described by three independent amplitudes, $T^I(s, t, u)$, where I(= 0, 1, or 2,) is the total isospin of the state in which scattering occurs. Whereas for $\pi^0\pi^0$ scattering we had simply $T_t(s,t,u) = T_s(t,s,u)$ (the suffix indicating the channel in which scattering is physical) we now need to define the combination of s channel amplitudes:-

$$T_t^I(s, t, u) = \sum_{I'} C_{II'}^{st} T_s^{I'}(s, t, u) \qquad (1.11)$$

such that, when continued into the t channel,

$$T_t^I(s, t, u) = T_s^I(t, s, u) \qquad (1.12)$$

Likewise, we must define the combination of s channel amplitudes:-

$$T_u^I(s,t,u) = \sum_{I'} C^{su}_{II'} T^{I'}(s,t,u) \tag{1.13}$$

such that, when continued into the u channel,

$$T_u^I(s,t,u) = T_s^I(u,t,s) \tag{1.14}$$

the crossing matrix, C^{su} for example, is obtained by writing the s - u crossing postulate for the ab → cd reaction as:-

$$\langle c\,d|T_s|a\,b\rangle = \langle c\,\bar{b}|T_u|a\,\bar{d}\rangle \tag{1.15}$$

where $\bar{b}$, $\bar{d}$, are the charge conjugate states of b, d. Taking great care with phases, and expanding each side of the equation into isospin amplitudes, the relation between s and u channel isospin amplitudes is obtained (see ref. (15) for details). For completeness we note here the crossing matrices:-

$$C^{st} = \begin{pmatrix} \frac{1}{3} & 1 & \frac{5}{3} \\ \frac{1}{3} & \frac{1}{2} & -\frac{5}{6} \\ \frac{1}{3} & -\frac{1}{2} & \frac{1}{6} \end{pmatrix}, \quad C^{su} = \begin{pmatrix} \frac{1}{3} & -1 & \frac{5}{3} \\ -\frac{1}{3} & \frac{1}{2} & \frac{5}{6} \\ \frac{1}{3} & \frac{1}{2} & \frac{1}{6} \end{pmatrix} \tag{1.16}$$

(we have used the phase convention that $|\pi^+\rangle \equiv +|1\ 1\rangle$ and $|\pi^-\rangle \equiv +|1\ -1\rangle$) . Crossing sum rules for charged pion scattering may now be obtained; these will be discussed in detail in the next chapter.

The imposition of s - u crossing allows a reduction in the number of subtraction constants needed in dispersion relations for charged pion-pion scattering amplitudes. The t-channel isospin amplitudes $T_t(s, t)$ have the simple s - u crossing property $T_t^I(s, t, u) = (-1)^I T_t^I(u, t, s)$. Now it is believed that $T_t^1(s, t, u)$ is well described by rho Regge

exchange as $s \to \infty$; thus $T_t^1 \sim \sqrt{s}$ and the amplitude will require a once subtracted dispersion relation. However the s - u crossing - odd property allows the subtraction constant to be removed (18) and so an unsubtracted dispersion relation may be written. Likewise T_t^0 (s, t, u), controlled asymptotically by pomeron exchange (thus T_t^0 (s, t, u) $\sim$ s), needs at first sight a twice subtracted dispersion relation, but in fact the s - u crossing even property allows a once-subtracted relation to be written.(18)

1.4: Unitarity and the partial wave expansion

Unitarity of the S matrix implies that a scattering amplitude for spinless (distinguishable) particles may be written as an infinite sum of Legendre polynomials of the form (see eg.ref.(15)):-

$$T(\theta,\phi) = \frac{8\pi k\sqrt{s}}{|q|} \sum_\ell (2\ell+1) f_\ell P_\ell(\cos\theta) \qquad (1.17)$$

where k = 1 when T is normalised as in appendix 1A, k = $1/32\pi$ when T is normalised as in the next chapter. The partial wave amplitude is

$$f_\ell = \frac{1}{2i}\left(\eta_\ell e^{2i\delta_\ell} - 1\right) \qquad (1.18)$$

with $0 < \eta_\ell < 1$.

For pion-pion scattering in a state of total isopin I, eq.(1.17) must be modified to take account of the fact that pions obey Bose statistics. In fact:-

$$T^I(\theta,\phi) = \frac{\varepsilon_f}{\sqrt{2}} \frac{k\,8\pi\sqrt{s}}{|q|} \sum_\ell (2\ell+1)\left(1+(-1)^{\ell+I}\right) f_\ell^I P_\ell(\cos\theta) \qquad (1.19)$$

$\varepsilon_f = \sqrt{2}$ if the final state pions are not distinguished, $\varepsilon_f = 1$ if they are. The total cross section is given by:-

$$\sigma_T^I = \frac{1}{\varepsilon_f^2} \int_{4\pi} |T|^2 \, d\Omega \qquad (1.20)$$

The optical theorem then takes the form:-

$$\sigma_T^I = \frac{1}{k\sqrt{s}\sqrt{s-4}} \, Im\, T^I(0) \qquad (1.21)$$

The analytic properties of the amplitudes, together with unitarity can be shown (15) to imply that $f_\ell \sim q^{2\ell}$ as $q \to 0$; thus only the partial wave amplitudes of small ℓ are important in low energy scattering, and the partial wave expansion eq.(1.17) converges rapidly. For pion-pion scattering, values of $\ell > 3$ are unimportant at energies of up to 1.8 GeV (19).

The partial wave expansion is valid in a larger region of the complex Z (= $\cos\theta$) plane than the physical region. In general the domain of convergence of a Legendre polynomial expansion of a function is the interior of the largest ellipse with foci at ± 1 which can be drawn in the Z plane without including any singular points of the function (20). The nearest (to Z = 0) singularity of the pion-pion scattering amplitude comes from the branch point at t = 4; thus the semi-major axis of the largest ellipse is of length $1 + 8/(s - 4)$. It has been shown (21) that the partial wave expansion of the absorptive part of the amplitude is in fact valid for $-28 < t < 4$ and for any s such that $4 < s < \infty$; this result, combined with that of Martin (17) shows that it is rigorously correct to write down twice subtracted fixed 't' dispersion relations for pion-pion scattering amplitudes and to describe the absorptive parts in terms of a partial wave expansion, for $-28 < t < 4$. An interesting and phenomenologically useful application of these ideas has been made by Roy (22) who, making partial use of the three-channel crossing property of pion-pion scattering to remove the subtraction constants in twice subtracted dispersion relations, obtained a set of integral equations for the partial wave amplitudes. Imposing full three channel crossing yields three of the family of crossing sum rules, as supplementary conditions. We shall discuss the Roy equations and their applications in rather more detail in the next chapter.

1.5: Finite energy sum rules and the pomeron

High energy 2-body scattering processes fall into two distinct groups; those with cross-section decreasing rapidly

with energy and those with cross section approximately constant. The former group can qualitatively be well understood with the aid of the dynamical assumption that the amplitude is dominated by the exchange of one or two Regge poles* (with more complicated singularities also present but of less importance) with intercept $\alpha_0 \simeq \frac{1}{2}$; features such as shrinkage of the forward peak, fixed t structure and factorization may also be explained. The second group of processes are diffractive in character and occur when the outgoing particles retain the same quantum numbers as the incoming, and when little momentum is transferred between the incoming particles. These properties are characteristic of the exchange of the pomeron which, though probably not a simple pole in the angular momentum plane, shows many of the features to be expected from a Regge pole of intercept $\alpha_0 \simeq 1$. We write, for the simplest asymptotic description of the spinless $2 \to 2$ scattering amplitude:-

$$T(s,t,u) \sim \sum_i \beta_i(t)\left(\frac{1+\gamma_i e^{-i\pi\alpha_i(t)}}{\sin \pi\alpha_i(t)}\right)\left(\frac{s}{s_0}\right)^{\alpha_i(t)} \qquad (1.22)$$

where, for the i^{th} Regge pole, $\beta_i(t)$ is the residue function, $\alpha_i(t) = \alpha_0 + \alpha' t$ is the trajectory function and $\gamma_i = \pm 1$ is the signature.

Assuming that, for $s \gg s_0$, the above description becomes a good approximation to the physical amplitude, we may relate the Regge description to the low energy amplitudes by integrating the quantity T (s, t, u) -T (Regge approx.) around the contour of fig.1.1, taking Γ at the finite energy $s = s_0$ instead of at $s = \infty$ as before. By assumption, $\int_\Gamma = 0$ and we have, for pion-pion scattering in a state with isospin I in the t channel, the finite energy sum rule (FESR):-

$$\int_4^{s_0} dx\, A_t^I(x,t)(2x-4+t)^{n+I} = \int_4^{s_0} A(Regge) \qquad (1.23)$$

I = 0, 1, 2; n + I is odd and positive.

The same expression occurs on the right-hand side as on the left, but with the amplitudes replaced by their Regge

* for a good introduction to Regge theory, see ref.(15).

approximations. We have defined an integrand symmetric under s - u crossing in order that the integral along the left hand cut of fig.1.1. maps onto that along the right hand cut. Since only s - u crossing has been used, similar relations may be obtained for any AB → AB reaction. Any suitable integral value of n, the 'moment' of the FESR may be chosen, however in practice a choice of $n > 1$ results in a severe dependence of the integral on the cutoff energy, s_o.

For an 'ideal' scattering amplitude we might hope to describe the low energy amplitude purely as a sum of resonances, and the high energy amplitude as a sum of simple Regge poles, without the pomeron. The FESR then shows that either description is valid if the amplitude is averaged over a range of energy - we say that the Regge poles are dual to the resonances. Explicit examples of amplitudes which satisfy the FESR's exactly and show simultaneously Regge behaviour and resonance saturation, - (but violate unitarity) have been constructed and studied in great detail; these are the dual resonance models, and the reader is referred to refs.(23) for more information. Specialising again to pion-pion scattering, we note that the absence of 'exotic' isospin two pion-pion resonances and Regge trajectories, implies that (if the right and left hand cut contributions can be treated independently):-

$$0 \simeq \int_4^{s_0} A_s^2(x,t)\,dx = \int_4^{s_0} \left[\tfrac{1}{3}A_t^0(x,t) - \tfrac{1}{2}A_t^1(x,t)\right] dx \qquad (1.24)$$

and so, if rho and f exchange dominate the t-channel isospin one and zero amplitudes respectively:-

$$\alpha_\rho(t) = \alpha_f(t) \quad , \quad Im\,\beta_\rho(t) = \frac{2}{3}\,Im\,\beta_f(t) \qquad (1.25)$$

The rho and f Regge trajectories are strongly exchange degenerate.

Of course, in a real scattering process, both low energy background and high energy pomeron exchange are present. Harari and Freud (24) suggested that these contributions to the amplitude may be dual, in that their FESR integrals are equal; this idea is given weight by the appearance of a new singularity in the angular momentum plane (the pomeron ?) when

non-planar dual diagrams (with t-channel vacuum quantum numbers and no s-channel resonances) are calculated in specific dual models. In practical calculations, including the full low energy amplitudes and with rho, f and pomeron trajectories exchanged at high energy, eq.(1.25) should be tested rather than assumed. A lack of high energy pion-pion scattering data means that the FESR type of calculation is almost the only way of determining the properties of the Regge exchanges in pion-pion scattering. While the rho trajectory can be determined from the FESR eq.(1.23) (with $I = 1$, $n = 0$), the contributions to the amplitude from the exchange of pomeron and f Regge trajectories, which possess the same quantum numbers, cannot be easily separated without assuming the strong exchange degeneracy condition eq.(1.25) or attempting the unstable cutoff dependent procedure of solving between FESR's of different moment. As will be seen in the next chapter, the crossing sum rules provide extra constraints which make this separation a possibility.

The pomeron singularity, as well as having a special role in duality schemes, differs from normal Regge poles in having an intercept of unity (or near), a less steep slope and no associated particles. Recent results show that the total cross section of several elastic scattering processes is rising at the highest experimentally available energies. For instance, the proton-proton total cross section may be parametrised as (25, 26):-

$$\sigma_T(s) \simeq \sigma_0 + \sigma_1 \ln^2(s/s_0) \qquad (1.26a)$$

$$\text{or} \quad \sigma_T(s) \simeq \sigma_0 s^{0.07} \qquad (1.26b)$$

Froissart has shown (4) that any rise of cross section faster than $\ln^2(s)$ will eventually violate unitarity. The pomeron cannot thus be a simple Regge pole of intercept 1.07, as suggested by eq.(1.26b) and must be a more complicated object. If the pomeron were a simple pole, we would expect the residue function to factorize, leading to the prediction (27):-

$$\sigma_T(\pi\pi) = \sigma_T^2(\pi p)/\sigma_T(pp) \qquad (1.27)$$

in the energy region where the processes are dominated by pomeron exchange. If the intercept of the pomeron trajectory is unity, the relation eq.(1.27) is energy independent, (once the pomeron contribution to the amplitudes is dominant) and predicts $\sigma_T(\pi\pi) \simeq 15\,mb$. which, as will be seen in later chapters, is rather too large. The question of factorization of the pomeron will be discussed in more detail in chapter 3.

For most of our purposes it will be sufficiently accurate to treat the pomeron as a Regge pole of intercept unity. The optical theorem, eq.(1.21) shows that the imaginary part of the scattering amplitude is very large in the forward direction (t =0); thus the pomeron must be mainly imaginary at t = 0 and so has even signature.

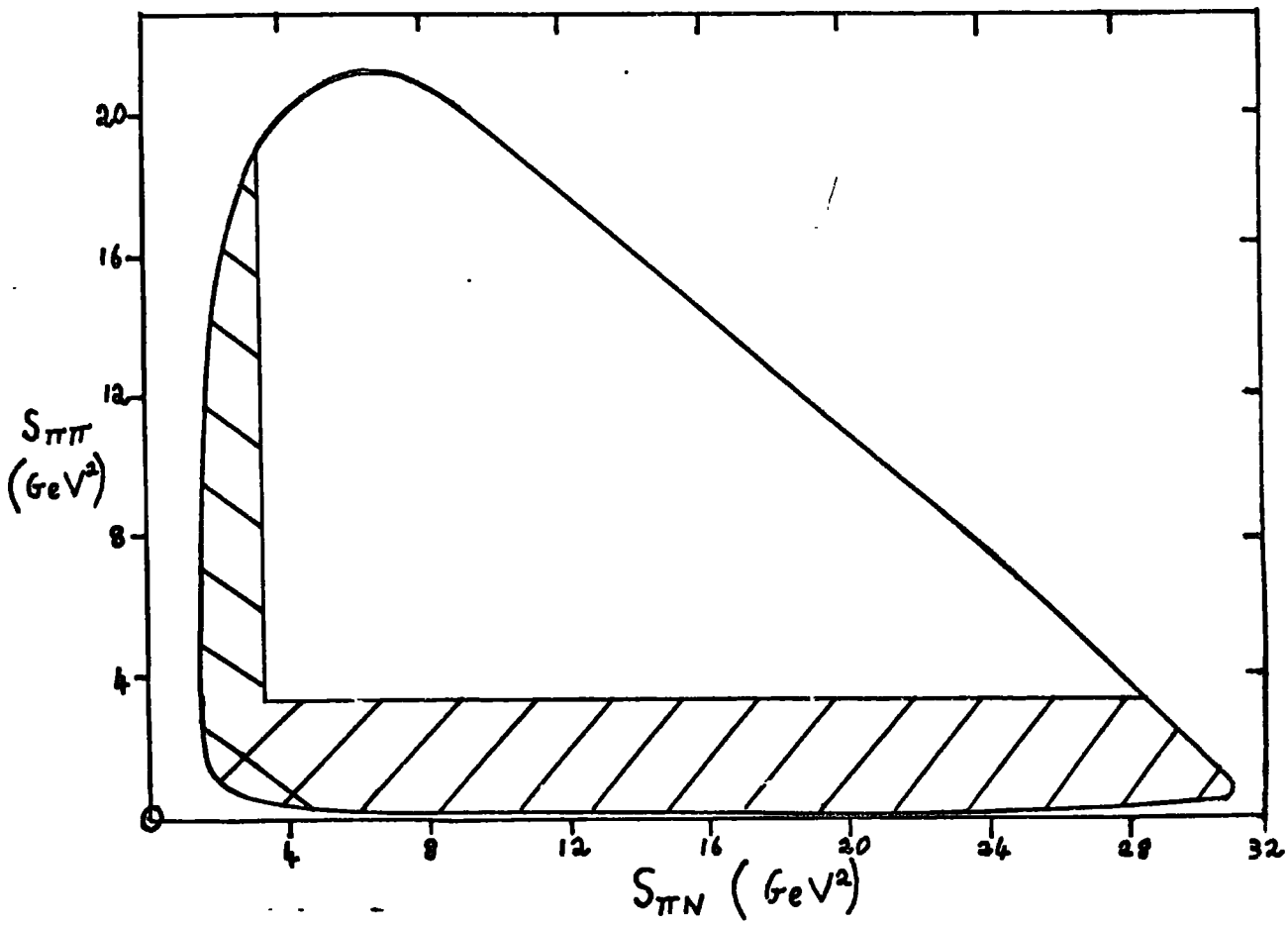

Fig.1.2. Dalitz plot of the 16GeV/c $\pi N \to \pi\pi N$ reaction. The shaded areas correspond to the kinematic regions studied in this thesis.

1.6: Processes contributing to the $\pi N \rightarrow \pi\pi N$ reaction

The $\pi N \rightarrow \pi\pi N$ reaction contains a great deal of physically interesting information. In fig.1.2 we show the Dalitz plot for this reaction at 16 GeV/c; the two shaded regions, corresponding to the production of a pion-nuclear system of mass 1-2 GeV/c^2 and a dipion system of mass 0.3 - 1.8 GeV/c^2 are of particular interest. Most of the low mass pion-nucleon production occurs when the dipion mass is large (and vice versa). An isospin analysis (see chapter 3) may be carried out to separate the isospin zero exchange component of the pion-nucleon production amplitude; for sufficiently high sub-energy this will be dominated by pomeron exchange. We shall present evidence in later chapters that the amplitudes for three processes - pion exchange, or spectator nucleon (fig.1.3a), nucleon exchange, or spectator pion (fig. 1.3b) and N* resonance production and decay (fig.1.3c) - provide the major contributions to the diffractive production of a low mass pion-nucleon system. (Analagous amplitudes will be present in other inelastic diffraction dissociation reactions).

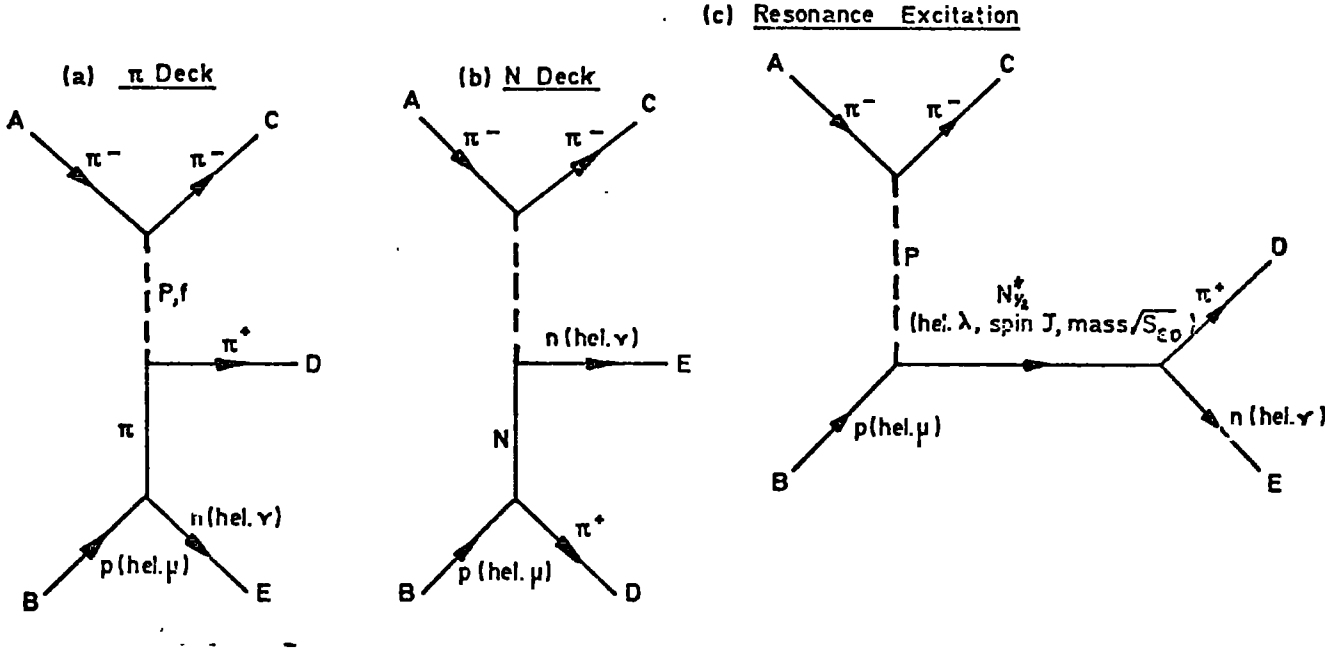

Fig.1.3. The three processes taken to contribute to the $\pi^- p \rightarrow \pi^-$ ($\pi^+ n$) reaction, in the kinematic regions shaded in fig.1.2. Process 'a' dominates when the outgoing dipion mass is low.

The first and third amplitudes are of particular interest as, if their relative contributions can be separated, we shall have information on how the pomeron behaves in high energy pion-pion scattering, as well as how it couples to the NN* system. In fact, since the two diagrams lead to different angular distributions of the pion-nucleon system, their contribution can be separated - but it is necessary to consider the spins of the particles involved (and thus a model for the pomeron couplings is needed), interference, duality, and the role of the nucleon exchange diagram, fig.1.3b. This procedure and the results obtained are discussed in detail in chapters 4 and 5.

For high mass pion-nucleon systems (and low mass dipion systems) the resonance production and decay amplitudes will become small as the pion-nucleon decay width of the N* resonances decreases. If in addition the momentum transfer between the ingoing and outgoing nucleons, t_{NN}, is restricted to small values, then only the pion exchange amplitude (fig.1.3a) will be important and, since the exchanged pion is not far off shell, the angular distribution of the dipion system should be very near to that which would be obtained were the pion-pion scattering physical, with a pion target (an experimental impossibility)[+]. We see from the Dalitz plot of fig. 1.2 that overlap between the production of a low mass dipion system, and of N* resonances in the 1-2 GeV/c^2 mass region, will be small. This indicates a means of obtaining information about pion-pion scattering without the need for a pion target. We outline below, very briefly, one procedure for extracting $\pi\pi$ partial waves from data on the $\pi N \rightarrow \pi\pi N$ reaction, and refer the reader to refs.(7 - 9) for more details.

1.7: $\pi\pi$ partial waves from $\pi N \rightarrow \pi\pi N$

It is assumed that the one pion exchange mechanism dominates the $\pi N \rightarrow \pi\pi N$ reaction when t_{NN} is small and the outgoing pion-nucleon sub-energy is large. After making corrections for small off-shell and absorptive effects, the modulus of the pion-pion scattering amplitude may be obtained at each required dipion mass from the angular distributions of the outgoing dipion system. The procedure for obtaining the

---

[+] We now consider isospin one and two, as well as isospin zero, exchange.

$\pi\pi$ partial wave amplitudes is then precisely the same as if real pion-pion scattering had been measured. The coefficients of the Legendre polynomials in the partial wave expansion eq.(1.17) are found by taking moments of the angular distribution. The overall phase of the amplitude may be fixed by requiring that the leading partial waves be consistent with unitarity and resonance behaviour (7), or by requiring the amplitude to have the correct analyticity properties (28, 29). Usually the $\pi^- p \longrightarrow \pi^- \pi^+ n$ reaction is studied to obtain information on isospin zero and one pion-pion scattering, with information on the small isospin two amplitude input from a study of $\pi^+ p \longrightarrow \pi^+ \pi^+ n$ (see eg.ref.(52)); the $\pi^+ p \longrightarrow \pi^+ \pi^- \Delta^{++}$ (10), $\pi^- p \longrightarrow \pi^- \pi^+ X^0$ (11) and $\pi^- p \longrightarrow \pi^0 \pi^0 n$ (12) reactions have also been used.

Unitarity provides a severe constraint on the solutions for the amplitude in the region where the scattering is mainly elastic, at energies below about 1GeV (the threshold for the $\pi\pi \longrightarrow K\bar{K}$ process), but has less effect at higher energies when inelasticity is large. In the analysis of ref.(7) it is shown that an unavoidable 4 - fold ambiguity arises, because it is not known which of three roots from the three complex conjugate pairs of roots of the sixth order polynomial equation $|T(\cos\theta)|^2 = 0$ to choose as the solution for $T(\cos\theta)$. Physical considerations on the path of the zeros of $T(\cos\theta)$ in the complex energy plane then reduce the 8-fold ambiguity to a 4-fold one. The authors of ref.(7) suggest that accurate measurements of $\pi^- p \longrightarrow \pi^0 \pi^0 n$ are required to select the physical solution; however recent results have shown that the imposition of analyticity may allow the correct solution to be selected. Froggatt and Petersen (28), by carrying out a partial wave analysis of the pion-pion scattering amplitude at energies between 1.1 and 1.8 GeV and simultaneously demanding that the amplitude possess the correct analyticity properties, obtain a solution similar to solution B of ref.(7), with a large ρ' daughter resonance in the P wave under the 'g' resonance. Johnson, Martin and Pennington (29) find that only solutions B and D of ref.(7) can be made consistentwith analyticity (as embodied in fixed 't' dispersion relations for $\pi^- \pi^+ \longrightarrow \pi^- \pi^+$ and $\pi^- \pi^+ \longrightarrow \pi^+ \pi^-$ scattering); their calculation deter-

mines the overall phase of the solutions. Both solutions B and D possess the ρ' resonance; to decide between them good $\pi^- p \longrightarrow \pi^0\pi^0 n$ data is still required. Shimada (30) finds solution A of ref.(7) (without a ρ' resonance) preferable, on the grounds that this solution is the most consistent with $\pi^-\pi^0 \longrightarrow \pi^-\pi^0$ data around 1.3 GeV and that unitarity constraints obtained from studying the $\pi\pi \longrightarrow K\bar{K}$ process are better satisfied by solution A. It is important that the ambiguity be decisively resolved, as the ρ' resonance is an important prediction of dual models; furthermore, quark models which describe the ψ' (3700) as a 'radial excitation' of the J/ψ (3100), of necessity predict the existence of the ρ' as a radial excitation of the ρ .

2: CROSSING AND THE PHYSICAL PION-PION SCATTERING AMPLITUDES

In this chapter we discuss how, in practice, the principle of crossing, in addition to analyticity and unitarity, constrains the $\pi\pi \longrightarrow \pi\pi$ scattering amplitudes. We shall concentrate on those constraints which apply to the physical scattering amplitudes; much work has been carried out on unphysical region crossing constraints (see eg.refs. (31 - 33) but these are generally harder to use and probably contain no more information than the physical region constraints.

The Roy equations (22) are of great value in determining the range of possible pion-pion scattering amplitudes consistent with analyticity, crossing, and unitarity, embodying as they do these properties in a manner which is easy to apply. They may also be used both to compute partial wave amplitudes in experimentally unknown regions and to check the consistency of phase shift analysis results. We discuss in section 2.1 the Roy Equations and some of the results which have been obtained from their application.

To enforce total crossing on the amplitudes it is still necessary to impose a set of supplementary conditions to the Roy equations; these are a subset of the family of crossing sum rules. Crossing sum rules have been derived in a variety of ways, usually from dispersion relations (33 - 38); we shall present a systematic derivation for all crossing sum rules in section 2.2. These sum rules provide extra constraints on the amplitudes, and it is possible that their systematic application might enable the ambiguity in the $\pi^-\pi^+$ phase shift solutions to be resolved. It turns out, however, that the leading partial waves, which are very similar in all phase-shift solutions, provide the dominant contribution to the crossing sum rules and that uncertainty in the poorly known isospin two pion-pion scattering amplitude is more important than the difference between the $\pi^-\pi^+$ phase-shift solutions.

The crossing sum rules are found to be of most use when applied to study the asymptotic form of the scattering amplitudes. Such a study may be attempted using only FESR's (39) or continuous moment sum rules (40), however results depend strongly on the poorly known phase shifts at the high energy end of the data, and on the cutoff[+] chosen. Crossing sum

---

[+] s_0 in eq.(1.23).

rules provide valuable extra independent constraints and in general have a more even weighting and are very much less dependent on the cut-off than normal FESR's.

2.1: The Roy Equations

The Roy equations are a set of integral equations for the pion-pion scattering amplitudes embodying the analyticity, crossing and unitarity properties of the amplitudes.

To derive these equations, a twice subtracted fixed t dispersion relation (rigorously valid for $0 < s < \infty$, $4 \geqslant t \geqslant -28$) is written for the amplitude, and s - u, with partial t - u, crossing is imposed to allow the amplitude at the subtraction points to be determined. The amplitudes are then expressed in terms of partial waves to arrive at an equation of the form:-

$$Re\, f_\ell^I(s) = \text{consts.} + \sum_{I'}\sum_{\ell} \int_4^N G_\ell^{I'}(x,s,t)\, Im\, f_\ell^{I'}(x)\, dx + \sum_{I'} \int_N^\infty H^{I'}(x,s,t) A^{I'}(x,t)\, dx \qquad (2.1)$$

We illustrate this procedure for the $\pi^0\pi^0$ scattering amplitude in appendix 2A. The constants are simply related to the $\pi\pi$ S and P wave scattering lengths[+] and the 'cutoff', N, is chosen at any convenient value, above which a high-energy parametrisation of the amplitudes is used. Since $H^I(x) \sim 1/x^3$, the equations are not very sensitive to the form of this parametrisation. The equations are valid for $0 < s < 60$ (1.08GeV) but, as mentioned in appendix 2A, small errors may arise in practical calculations unless this range is restricted to $0 < s < 32$ (0.8 GeV) (41). Full t - u crossing may be imposed, as indicated in appendix 2A, and leads to three supplementary conditions (crossing sum rules).

A detailed study of the uses of the Roy equations has

+ The scattering lengths are defined as (in units where the pion mass is unity):-

$$a_\ell^I = \lim_{q \to 0} \frac{\delta_\ell^I}{q^{2\ell+1}} \quad \text{with} \quad q = \tfrac{1}{2}\sqrt{s-4}$$

been carried out by Basdevant, Froggatt and Petersen(42). These authors start by assuming that the mass and width of the ρ resonance is known, inelasticity below the $\pi\pi \rightarrow K\bar{K}$ threshold is negligible and that there is no isospin two resonance below this threshold. They construct a unitary, analytic, crossing symmetric function and use this to solve the Roy equations iteratively. A wide range of allowed values for the $\pi\pi$ scattering lengths is found, with an infinity of solutions for the amplitudes below 1.08 GeV. This result shows, that the solutions obtained in ref.(43) using the unphysical region constraints and with an input similar to the above, form only a small subset of the class of possible solutions. The authors of ref.(42) then consider the effect of including extra experimental information in the calculation, namely a set of isospin zero S-wave phase shifts in the region $500\ MeV \leqslant M_{\pi\pi} \leqslant 1100$ MeV. The Roy equations then lead to a very narrow band of solutions for a_0^0 and a_0^2 in the (a_0^0, a_0^2) plane, a result very similar to the 'universal curve' of solutions for a_0^0 and a_0^2 found by Morgan and Shaw (44) from simple forward dispersion relation calculations. Indeed, by strict adherence to one input set of phase-shifts Pennington and Protopopescu (45) find the near unique values for the scattering lengths of $a_0^0 = 0.15 \pm 0.07$ and $a_0^2 = -0.05 \pm 0.028$, however a larger range is found if realistic errors are allowed. The pion-pion scattering amplitudes at energies below 1 GeV are essentially determined by the Roy equations once a_0^0, and a particular set of phase shifts, are chosen. The first order current algebra predictions for the scattering lengths are (6) $a_0^0 = 0.16$, $a_0^2 = -0.05$; unitarity corrections (46) lead to the values of $a_0^0 = 0.21$, $a_0^2 = -0.043$. These values are consistent with the results of the Roy equation calculations and with the latest experimental determination of a_0^0, from a study of the decay process $K^+ \rightarrow \pi^+\pi^- e\nu$, (47) which gives a value of 0.31 ± 0.1.

The D and F wave phase shifts in the energy region below 1GeV. are well determined by the Roy equations, better in fact than by experiment, (42) and may be used as input to phase shift analyses, as in ref.(7). Since the Roy equations closely relate the partial waves in different energy regions, it is possible to check the consistency of phase shift solutions.

A disturbing feature to emerge is that all experimentally determined P wave phase shifts in the energy region below 600 MeV are inconsistent with the results of Roy equation calculations. (48) The present belief is that the experimental analysis giving the low energy P wave must be incorrect; if this analysis is in fact confirmed then serious fundamental problems must be faced.

The simple Roy equations cannot be used to determine partial wave amplitudes at energies greater than $\sim$ 1.1 GeV. Mahoux, Roy and Wanders (49) have generalised the equations, basing them on curved dispersion paths to obtain a (more unwieldy) set of equations valid for $-28 < s < 125$ ($\sim$ 1.56 GeV). There is no reason why, by a process of analytic continuation, the analagous equations to those of ref.(49) cannot be extended to arbitrarily high energies (paying the price of increasing complexity, however) thus providing another possible tool for resolving phase-shift solution ambiguities.

Dispersion relations and sum rules may also be written for the inverse of the pion-pion scattering amplitudes (50, 51), however it is not clear that such relations contain any more information than the Roy equations with the physical region crossing sum rules.

2.2: Derivation of $\pi\pi$ crossing sum rules

In this section we present a systematic derivation of physical region crossing sum rules for pion-pion scattering. We normalize the pion-pion scattering amplitudes throughout this chapter so that:-

$$A_s^I(s,t,u) = \frac{1}{2}\sum_\ell \left(1+(-1)^{\ell+I}\right)\sqrt{\frac{s}{s-4}}\,(2\ell+1)\,P_\ell(z)\,a_\ell^I \qquad (2.2)$$

and so that the optical theorem (eq.1.21) reads:-

$$\sigma_{TOT}^I(s) = \frac{32\pi}{\sqrt{s(s-4)}}\,A_s^I(s,0) \qquad (2.3)$$

We choose units so that the charged pion mass is unity, and always impose the mass shell condition eq.(1.1):-

$$s + t + u = 4 \qquad (2.4)$$

Physical region crossing sum rules for pion-pion scattering are derived using the property special to this process that crossing may be enforced among all three channels.

It is most convenient to work with the combination of s channel amplitudes $T_t^I(s, t, u)$ defined in eq.(1.11). Total crossing may be enforced by the two independent constraints

$$T_u^I(s,t,u) \equiv (-1)^I \sum_{I'} C_{II'}^{su}\, T_t^{I'}(s,t,u) = (-1)^I T_t^I(s,u,t) \qquad (2.5)$$

$$T_t^I(s,t,u) = (-1)^I T_t^I(u,t,s) \qquad (2.6)$$

The simplest interpretation of crossing sum rules is as negative moment FESR's. Consider

$$\oint_C \frac{dx}{x-s}\left(A_t^I(x,u) - (-1)^I A_u^I(x,t)\right) = \int_{cuts} + \int_{\Gamma} = 0 \qquad (2.7)$$

where C is the usual FESR contour of fig.1.1 with Γ at finite energy s = N, and I takes values 0, 1, 2. Eq.(2.5) implies that the numerator of the integrand vanishes at x = s. We assume, in the usual FESR manner, that a Regge approximation for the amplitudes is valid for x greater than some cutoff, N, and on Γ. Using Eq.(2.6) the left-hand cut is mapped onto the right-hand cut[+] after collapsing Γ on to the

---

[+]There is a slight problem in choosing the contour such that the integral of both A (x, t) and A (x, u) along the left hand cut maps onto that along the right hand cut. In order that the lower limit maps to '4' in each case, take the contour around - min (/t/, /u/) at the right hand end. Choose the centre of the contour such that Γ joins the left hand cut at (4-N-t) for (t-u) > 0 or at (4-N-u) for (t-u) < 0. The additional assumption $\int_N^{N+|t-u|} F^I(x,t)\,\beta(x,t,u)\,dx = 0$ is then required to obtain eq.(2.8).

real axis, to obtain

$$\int_4^N dx \left\{ A_t^I(x,u)\left(\frac{1}{x-s}+\frac{(-1)^I}{x-t}\right) - (-1)^I A_u^I(x,t)\left(\frac{1}{x-s}+\frac{1}{x-u}\right) + \frac{2}{x-u}\, C_{I1}^{su}\, A_t^1(x,t)\right\} = \int_4^N A_{Regge} \tag{2.8}$$

Clearly eq.(2.8) could have been alternatively obtained by equating unsubtracted dispersion relations for F_t^I (s, u, t) and $\sum_I C_{II}^{su} F_t^{I'}$(s, t, u) where $F^I(s,t,u) \equiv T^I(s,t,u) - T^I_{Regge}(s,t,u)$, the 'centre' variable is fixed, and we assume $\int_N^\infty F^I(x,t)\, f(x,t,u)\, dx = 0$ (Cf. eq.(1.10)).

At t = u, the three sum rules eq.(2.8) for I = 0, 1, 2 all reduce to the same equation

$$\int_4^N dx \left\{ A_t^1(x,t)\left(\frac{1}{x-t}\right) - A_6^1(x,t)\left(\frac{1}{x-4+2t}+\frac{1}{x-t}\right)\right\} = \int_4^N A_{Regge} \tag{2.9}$$

The properties of sum rules (2.8) and (2.9) will be discussed in more detail in section 2.5.

Formally take $(\partial/\partial s)_t$ of eq.(2.8) to obtain

$$\int_4^N dx \left\{ \frac{\partial A_t^I}{\partial u}(x,u)\left(\frac{1}{x-s}+\frac{(-1)^I}{x-t}\right) - \frac{A_t^I(x,u)}{(x-s)^2} + \frac{2\, C_{I1}^{su}\, A_t^1(x,t)}{(x-u)^2} + (-1)^I A_u^I(x,t)\left(\frac{1}{(x-s)^2}-\frac{1}{(x-u)^2}\right)\right\} = \int_4^N A_{Regge} \tag{2.10}$$

These three equations are now independent at t=u.

These are just the relations considered by Wanders,(18) who obtained them by combining unsubtracted and once-subtracted dispersion relations for the scattering amplitude; thus he has $-\int_N^\infty A_{Regge}$ in place of $\int_4^N A_{Regge}$ and, as noted by him, their use in such a form may not be valid.

We could have obtained the Wanders sum rules eq.(2.10) by subtracting from eq.(2.7) the identity

$$\oint_C \frac{dx}{x-s'} \left\{ A_t^I(x,u') - (-1)^I A_u^I(x,t) \right\} = 0$$

It is clear that if the $I_t = 1$ amplitude increases less rapidly than x, or if the $I_t = 2$ amplitude tends asymptotically to zero, then for the resulting equation the contour Γ can be expanded to infinity for I = 1 or 2 respectively. We thus obtain $\int_N^\infty A_{Regge}$ in place of $\int_4^N A_{Regge}$, and reproduce eq.(2.10) on taking the limit $s' \to u'$.+

Now take $(\partial/\partial s)_u$ of eq.(2.10) to obtain

$$\int_4^N dx \left\{ \frac{2}{(x-s)^3} \left((-1)^I A_u^I(x,t) - A_t^I(x,u) \right) + \frac{\partial A_t^I}{\partial u} \left(\frac{1}{(x-s)^2} - \frac{(-1)^I}{(x-t)^2} \right) \right.$$

$$\left. -(-1)^I \frac{\partial A_u^I(x,t)}{\partial t} \left(\frac{1}{(x-s)^2} - \frac{1}{(x-u)^2} \right) - \frac{2 C_{I1}^{su}}{(x-u)^2} \frac{\partial A'}{\partial t}(x,t) \right\} = -\int_N^\infty A_{Regge} \qquad (2.11)$$

We can now take all the Regge integrals over $x > N$. Eq.(2.11) has again been quoted in ref.(18). It may alternatively be obtained by combining once subtracted dispersion relations. Note that at t = u, the three equations reduce to one:-

$$\int_4^N dx \left\{ A_s'(x,t) \left(\frac{2}{(x-4+2t)^3} \right) - \frac{1}{(x-t)^2} \frac{\partial A_t'}{\partial t}(x,t) \right.$$

$$\left. - \frac{\partial A_s'}{\partial t}(x,t) \left(\frac{1}{(x-4+2t)^2} - \frac{1}{(x-t)^2} \right) \right\} = -\int_N^\infty A_{Regge} \qquad (2.12)$$

Clearly this process may be continued indefinitely. Taking $(\partial/\partial s)_u$ of eq.(2.11) produces a set of three equations, independent at t = u, which may otherwise be obtained by combining once and twice subtracted dispersion relations. Then taking $(\partial/\partial s)_t$ produces the set of equations obtained from combining twice subtracted dispersion relations; these are the Roy equations supplementary conditions (22) written in a form containing derivatives. Again at t = u, these collapse

---

+It is more convenient to integrate over $x > N$ when possible.

to one equation.

As this process is continued, the convergence of the integral is increased and the lower partial waves are systematically removed from the expansion of the absorptive parts of the amplitudes - for instance eq.(2.11) has no S waves; and the Roy equation supplementary conditions have no S or P waves. This may be viewed as a consequence of the differentiation process, or as a result of the relation of the sum rules to subtracted dispersion relations.

Note that our equations (2.8 - 2.10) do not depend on the validity of unsubtracted or once-subtracted dispersion relations for the scattering amplitudes, but on the assumption that the asymptotic amplitudes are well described by a Regge form. These equations are thus more akin to FESR's than to the rigorously valid crossing sum rules obtainable from twice subtracted dispersion relations, but in numerical applications, because of the extra factors of $1/\alpha$ in the integrands, results are much less cut-off dependent than those obtained from FESR's. However care must be taken in the use of these equations near t = 0 where the lower limit of the integral over Regge amplitudes can cause complications.

In the following sections we shall evaluate appropriate combinations of these rules and discuss their properties in more detail. First however we turn to a consideration of the phase shift solutions which will be used as input to the sum rules, and which we shall attempt to distinguish.

2.3: Phase Shifts

We consider three phase shift solutions; the solution of Hyams et al (8) and solutions A and B of Estabrooks and Martin (7). These describe S_o, P, D_o and F waves in the energy range 1.0 to 1.8 GeV, covering the f and g resonances. The solution of Hyams also describes these partial waves in the region 0.6 to 1.0 GeV, covering the ρ resonance; we use only this solution in this energy range. Below 0.6 GeV simple scattering length approximations for the phases are used such that the solutions match at 0.6 GeV. The contribution to the sum rules from the region below 0.6 GeV is usually unimportant; where it is significant it is assigned large errors. Solution A of ref.(7) differs from the other two considered in having no ρ' resonance under the g. Solution B is similar to

that of Hyams et al. Fig.2.1 shows the total $\pi^+\pi^-$ cross sections $\sigma_T(\pi^+\pi^-)$ (taking an intermediate isospin 2 amplitude - see below) for these solutions. It is seen that at 1.8 GeV $\sigma_T(\pi^+\pi^-)$ is between 12 and 15 mb, and falling fast.

The s channel isospin 2 amplitudes are not determined in the above phase shift analyses and unfortunately turn out to be important in several of the sum rules. We shall present results using two extreme possibilities for these amplitudes. For energies lower than 1.1 GeV we take scattering length approximations to give an S_2 wave of -25° and D_2 wave of -3.5° at 1.1 GeV, consistent with the results of Hoogland et al (52). For our one extreme solution (the small I = 2) we assume that these values remain constant up to 1.8 GeV, resulting in a total $\pi^+\pi^+$ cross section $\sigma_T(\pi^+\pi^+)$ of 2.5 mb at that energy. This appears, from the results of ref.(52), a reasonable assumption. Asymptotically $\sigma_T(\pi^+\pi^+)$ is expected to approach $\sigma_T(\pi^+\pi^-)$ which from Fig.2.1 could be as large as 12 mb. There is nothing in the analysis of

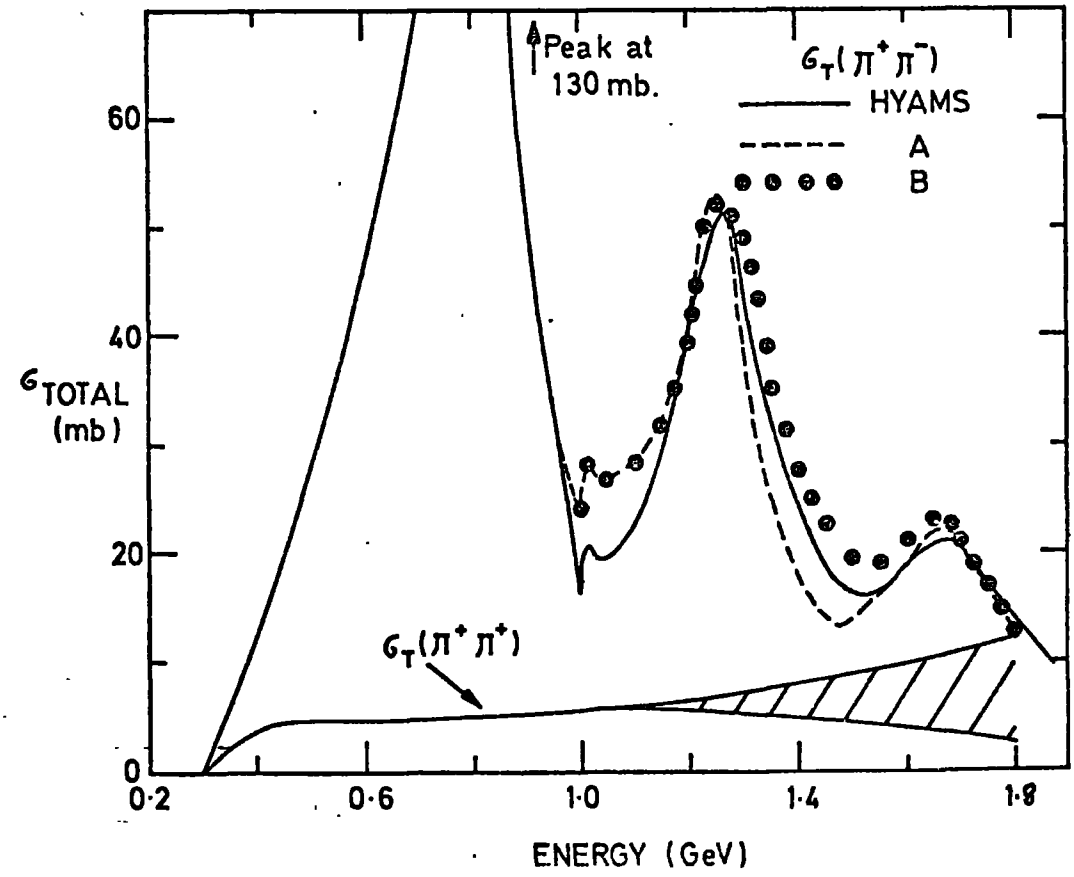

Fig.2.1 Total $\pi^+\pi^-$ cross-section for the phase-shift solutions of Hyams et.al., and solutions A and B of Estabrooks et.al., and range of possible $\pi^+\pi^+$ total cross-sections.

ref.(52) to prevent a rotation of overall phase of the S_2 and D_2 waves whilst keeping their relative phase unchanged; this corresponds to an onset of inelasticity and leads to an increased $\sigma_T(\pi^+\pi^+)$. These considerations motivate us to take the other extreme isospin two amplitude (the large I=2), from a steady rise of $\sigma_T(\pi^+\pi^+)$ up to 12.5 mb at 1.8 GeV. Fig.2.1 shows the range of $\sigma_T(\pi^+\pi^+)$ between the two extremes. Physically, a large inelasticity of the $\pi^+\pi^+$ scattering amplitude seems unlikely, as few coupled inelastic channels are available.

As discussed in section 2.1, $\pi\pi$ partial waves may be calculated in the energy range between 500 and 1100 MeV using the Roy equations (42, 45), with information about the rho resonance, S_o phase shifts and the expected asymptotic forms of the amplitudes. The energy region below 500 MeV is always unimportant in the sum rules, and those rules which have an important contribution from the 500-1100 MeV range are dominated by the rho resonance, which is taken as given in the calculations of refs.(42, 45). Thus there is no significant difference in the results obtained by taking these partial waves or those of Hyams et.al. in this low energy region (see eg. ref.51).

Most of the contributions to the sum rules come from partial waves when resonating, thus the neglect of $\ell \geq 4$ partial waves for energies less than 1.8 GeV is justified unless large cancellations occur between the dominant resonance contributions.

2.4: The asymptotic $I_t = 1$ and $I_t = 2$ amplitudes

We discuss in this section how the crossing sum rules and FESR's may be used to study the properties of the t channel isospin one and isospin two pion-pion scattering amplitudes.

To evaluate a particular sum rule, the phase shifts from a given solution are substituted into the integrand to obtain 'the low-energy sum', while 'the high energy sum' is obtained by numerically evaluating the integral with the amplitudes written in a form describing simple Regge pole exchange. The cutoff, N, is taken as 1.8 GeV unless otherwise stated.

The asymptotic t channel isospin two amplitude can only contain contributions from exchanges with exotic quantum numbers; it is usually assumed that these contributions may

be represented by the exchange of trajectories with zero or negative intercepts. In Fig.2.2 we show the integrand of the low energy part of the isospin two, first moment FESR[+] evaluated at t=0. The oscillatory nature of the integrand means that the sum will increase only slowly, if at all, as the cutoff energy N is increased; this is consistent with the above assumption. From now on we assume that the asymptotic I_t=2 amplitudes may be neglected compared with I_t=0 or I_t=1, unless occurring in a sum rule where the former is excessively weighted.

We shall now consider which combinations of crossing sum rules are of most use to us for a study of the I_t=1 asymptotic amplitude.

We find, as will be seen in the next section, that no such useful rule can be obtained from eq.(2.8). Next, consider eq.(2.10). For I=1, we find the well known rule (18, 51, 53-56) for t=u:-

$$\int_4^N d\alpha \left\{ A_s'(\alpha,t)\left(\frac{4-t-2\alpha}{(\alpha-4+2t)^2(\alpha-t)^2}\right) + \frac{\partial A_t'}{\partial t}(\alpha,t)\,\frac{1}{(\alpha-4+2t)(\alpha-t)}\right\} = -\int_N^\infty A_{Regge} \qquad (2.13)$$

The high energy sum is clearly dominated by the I_t=1 amplitude, thus this sum rule is of immediate use to us.

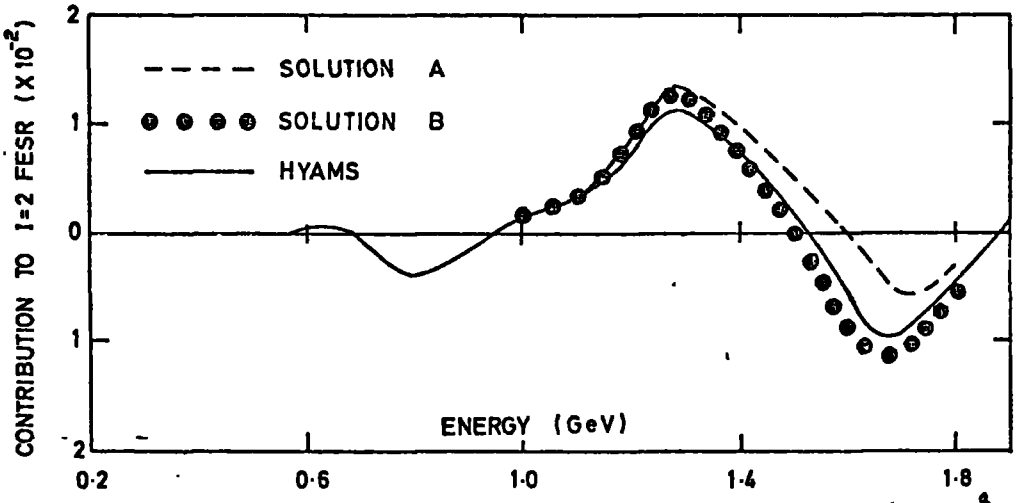

Fig.2.2. Integrand of first moment isospin 2 FESR (in m_π^a=1 units) for the phase shift solution of Hyams et.al. and solutions A and B of Estabrooks et.al. An intermediate low energy isospin 2 amplitude is used.

[+]Take I = 2, n = -1 in eq.(1.23)

We may obtain another rule, containing only $I_t=1$ and $I_t=2$ amplitudes, by taking the combination (I=1) - (I=2) of eqs.(2.10) for t=u.

$$\int_4^N d\alpha \left\{ \frac{1}{(\alpha-t)^2}\left(A_t^1(\alpha,t) - A_t^2(\alpha,t)\right) + \frac{2}{\alpha-4+2t}\frac{\partial A_t^2}{\partial t}(\alpha,t) \right.$$
$$\left. + \frac{4-3t}{(\alpha-t)(\alpha-4+2t)}\left(\frac{\partial A_t^1}{\partial t}(\alpha,t) - \frac{\partial A_t^2}{\partial t}(\alpha,t)\right)\right\} = -\int_N^\infty A_{Regge} \qquad (2.14)$$

Unfortunately this will be of little use to us as the $I_t=1$ amplitude is suppressed with respect to the $I_t=2$; thus the contribution to the high energy sum from exotic exchanges may be important.+ We also find large cancellations between the dominant partial wave contributions in the low energy sum; thus it may not be correct to neglect partial waves of $\ell > 3$. This rule is very similar to that obtained by writing eq.(2.10) for I=2, which has been found of little use because of large cancellations and cutoff dependence.(53, 54) We do not consider sum rule (2.14) any further.

We may obtain a useful rule from eq.(2.11) by taking the (I=1) + (I=2) combination. For convenience the limit $t \to u$ is taken to replace differences by derivatives (we could alternatively have taken the (I=1) + (I=2) combination, at t=u, of $(\partial/\partial s)_u$ of eq.(2.11)).

$$\int_4^N d\alpha \left\{ \left(\frac{1}{(\alpha-4+2t)^3} + \frac{1}{(\alpha-t)^3}\right)\left(2\frac{\partial A_t^1}{\partial t}(\alpha,t) + 2\frac{\partial A_t^2}{\partial t}(\alpha,t)\right)\right.$$
$$\left. - \left(\frac{1}{(\alpha-4+2t)^2} + \frac{1}{(\alpha-t)^2}\right)\left(\frac{\partial^2 A_t^1}{\partial t^2}(\alpha,t) + \frac{\partial^2 A_t^2}{\partial t^2}(\alpha,t)\right)\right\} = -\int_N^\infty A_{Regge} \qquad (2.15)$$

This is essentially a 'higher moment' form of eq.(2.14) but the differentiation has resulted in sign changes so that the $I_t=1$ amplitude is no longer suppressed. We shall use the sum rules of eqs.(2.13) and (2.15) in conjunction with the FESR's to study the asymptotic $I_t = 1$ amplitude. First we consider the use of the FESR's.

+We mention the analogous rule from eq.(2.8) in the next section.

We take for the imaginary part of the asymptotic $I_t=1$ amplitude the Regge form

$$A'_t(s,t) = \gamma(t)\left(\frac{s-4}{s_0}\right)^{\alpha(t)}$$
$$\alpha(t) = \alpha_0 + \alpha' t \quad ; \quad s_0 = 51/\mu^2 \ (= 1\ GeV^2) \qquad (2.16)$$

First, following Schmid (39) we attempt to determine the slope α' and intercept α_0 of the trajectory by solving the second moment $I_t=1$ FESR with the zeroth moment FESR. The former is unfairly weighted towards high energies, and severely cutoff dependent. The same partial waves dominate in each rule, thus the solution is unstable, depending for instance strongly on the isospin 2 low energy amplitudes.

We find an intercept of between 0.1 and 0.3, the result depending on phase shift solution and isospin 2 amplitudes, for a cutoff of 1.8 GeV. The slope is poorly determined, being dependent on t, but not inconsistent with the canonical $\alpha' = 1 GeV^{-2}$.

Rejecting the use of the second moment FESR as unreliable, we could alternatively solve the zeroth moment FESR with a crossing sum rule to determine α_0 and α'. For simplicity, however, we try inputting the 'conventional' values for a rho trajectory, $\alpha_0 = 0.5$ and $\alpha' = 0.9\ GeV^{-2}$, determining $\gamma(t)$ and checking the results for consistency with the crossing sum rules. Similar calculations have been presented in refs. (51, 53, 55, 56).

We determine $\gamma(t)$ by evaluating both sides of the zeroth moment FESR at a range of t values between zero and $-0.55\ GeV^2$ $(-28\mu^2)$. Fig.2.3 shows $\gamma(t)$ for solutions A and B, and for the two extreme I=2 amplitudes; the main uncertainty in $\gamma(t)$ comes from the uncertainty in the I=2 amplitudes. We see that $\gamma(t)$ is well described by the form.

$$\gamma(t) = a + bt \ , \quad a = 0.74 \pm 0.15 \qquad (2.17)$$
$$b = 1.9 \pm 0.15\ GeV^{-2}$$

A very similar $\gamma(t)$ is found using an intercept $\alpha_0 = 0.25$. Our cutoff is about midway between the g and the expected $\ell = 4$ resonance predicted from a linear ρ - f trajectory;(57)

the value of 'a' varies inversely, slowly, with the cutoff. For example, had we chosen a cutoff of 1.9 GeV, at the end of the data of Hyams et.al., with a large I=2 amplitude, a value of 'a' of 0.6 would have been obtained. (This was found as the 'central' value of 'a in ref.(51) where a very large I=2 contribution was used to obtain an extreme). The errors in eq.(2.17) allow for cutoff dependence.

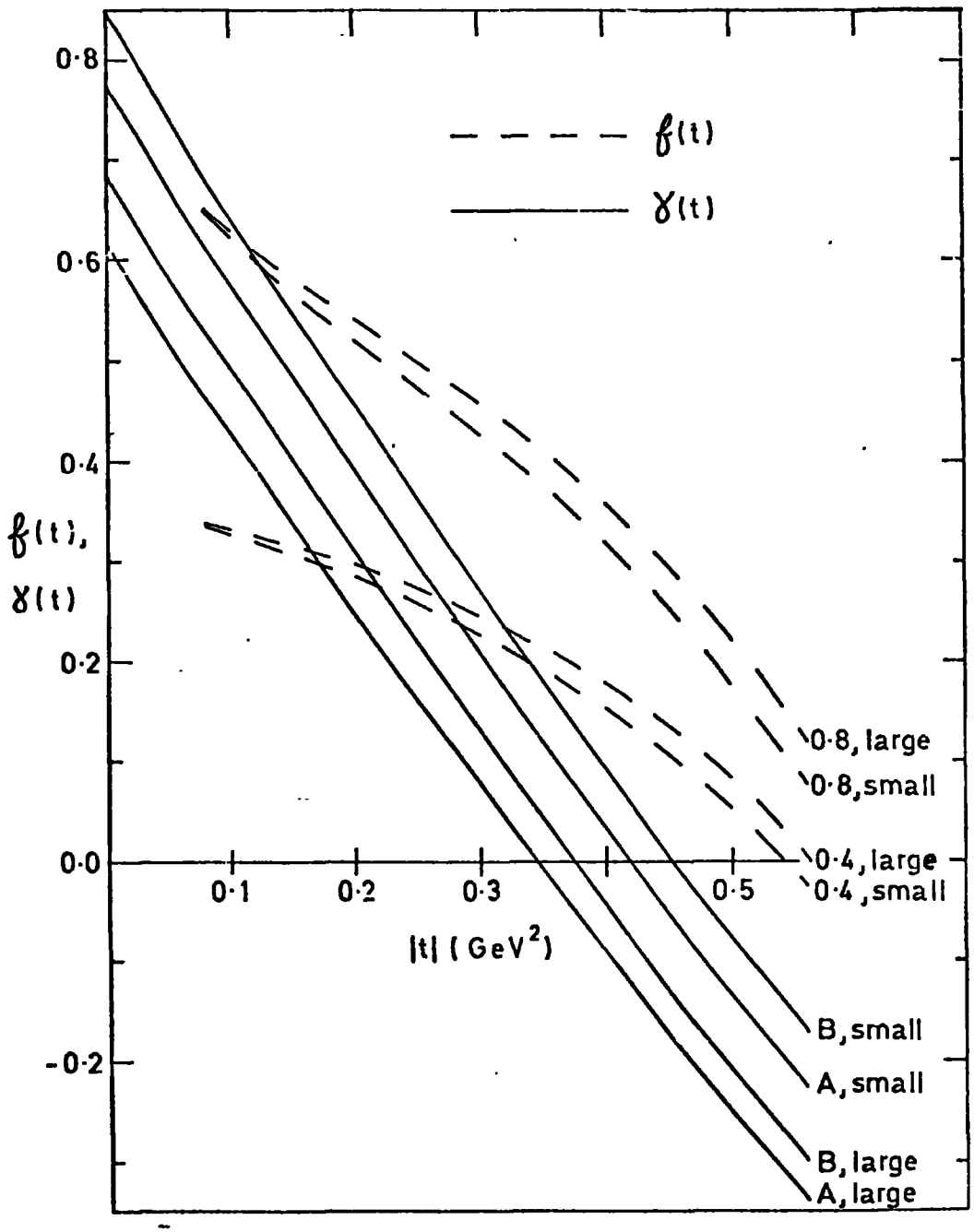

Fig.2.3. Rho ($\gamma(t)$) and f ($f(t)$) residue functions. $\gamma(t)$ is shown for soutions A and B of Estabrooks et al. for the small and large extreme isospin 2 amplitudes; it is well described by the form a + bt. Results for the Hyams et al solution lie in between those for solutions A and B. $f(t)$ is shown as obtained using solution B with the two extreme isospin 2 amplitudes and $f(o)$=0.4 and 0.8. Solution A and the Hyams et al. solution produce very similar results, with slope of $f(t)$ a little steeper.

We now check our results for the asymptotic I_t=1 amplitude with the crossing sum rules. Consider sum rule (2.13). The low energy sum has contributions from P, D_0, D_2 and F waves, the P wave dominating; we show these contributions in table (2.1). Results are very similar for the three phase shift solutions. The contribution from energies below 600 MeV is significant; we allow a 50% uncertainty on this. The high energy sum is calculated using the parameters.

$$\gamma(t) = 0.74 + 1.9t \quad \text{with (i)} \quad \alpha(t) = 0.5 + 0.9t \qquad (2.18)$$

$$\text{(ii)} \quad \alpha(t) = 0.25 + t$$

t is in units of GeV^2.

Figure 2.4a shows the low and high energy sums of the sum rule of eq.(2.13) as functions of t.[+] Good agreement is obtained using the parameters of eq.(2.18(i)) but there is disagreement when the parameters of eq.(2.18(ii)) are used.

Next consider the sum rule of eq.(2.15). This contains double derivatives and may thus be very sensitive to the t dependence of the amplitude; however, since we think this is

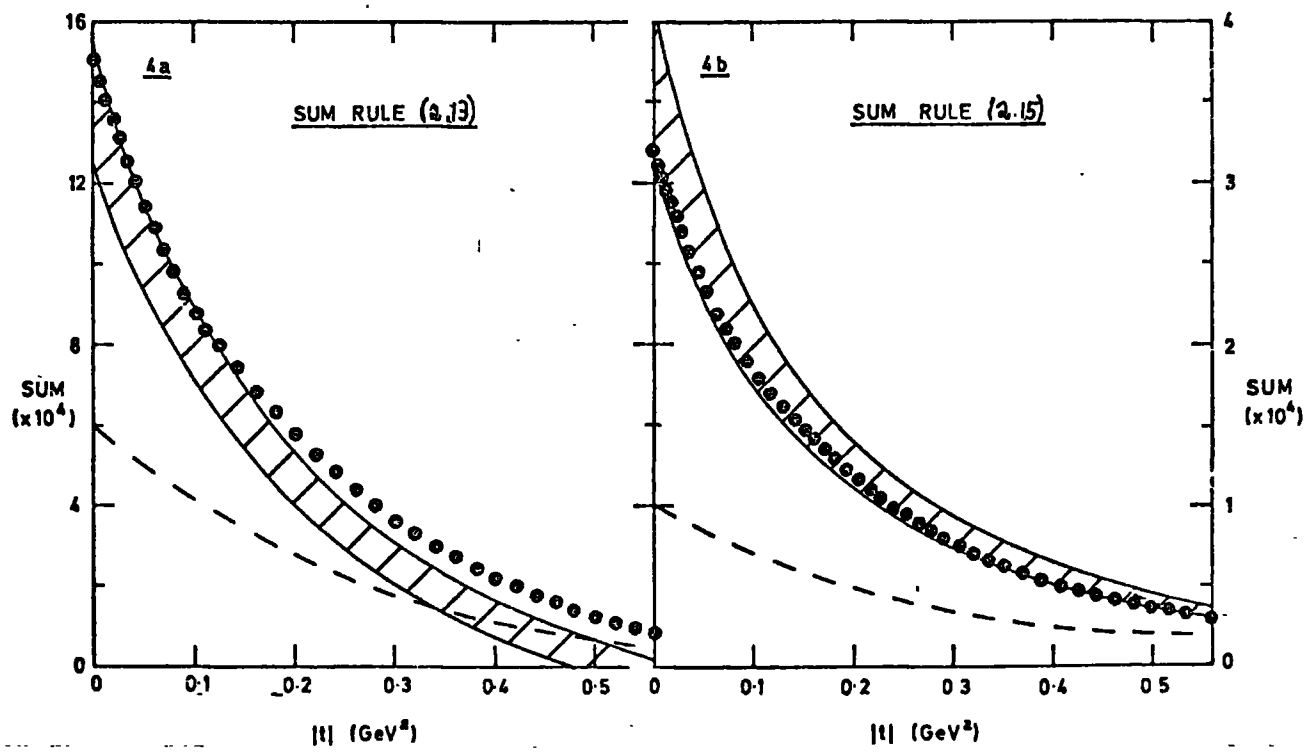

Fig.2.4 Low and high energy sums of (a) sum rule (2.13) and (b) sum rule (2.15) (in m_π^2 = 1 units), The hatched bands indicate the range of low-energy sums resulting from the uncertainty in the phase shifts below 600 MeV and in the isospin two amplitudes. The high energy sums use the parameters (2.18(i)), with α_0 = 0.5, (dotted curve) and (2.18(ii)), with α_0 =0.25 (dashed curve). Results are identical for a cutoff taken anywhere between 1.4 and 1.8 GeV

TABLE 2.1

Sum Rule	$\|t\|$ (GeV^2)	S_o	P	D_o	F	S_2	D_2	TOTAL	x
2.13	0.0	-	2.3*	-0.7	-0.1	-	0.0	1.5*	10^{-3}
	0.24	-	1.1*	-0.6	-0.1	-	0(0.05)	0.4*(0.35)	
2.15	0.0	-	3.8*	-	-0.1	-	0.0	3.7*	10^{-4}
	0.24	-	1.1*	-	-0.1	-	0.0	1.0*	
2.21	0.0	-	-	-	-	-	-	-	1
	0.24	-0.55*	-	3.5	-	0.0(-0.1)	0.1 (0.3)	3.0 (3.1)	
2.9	0.0	-0.7*	3.5	-0.7	0.7	0.2(0.4)	0.0 (0.1)	3.0 (3.3)	1
	0.24	-0.5*	2.7	-0.1	0.1	0.2(0.3)	0.0 (0.1)	2.4 (2.6)	
I=0 1st Moment FESR	0.0	2.0	8.9	6.3	9.5	4.7(8.1)	0.4 (4.9)	31 (40)	10^3
	0.24	1.8	5.7	2.0	1.8	3.7(7.8)	0.2 (2.4)	15 (21)	10^3
2.22	0.0	-	-	11.3	-2.7	-	-0.3 (-0.8)	8.3 (7.8)	10^{-6}
	0.24	-	-	7.8	-2.1	-	-0.1 (-0.5)	5.6 (5.2)	
2.23	0.0	-	-	4.9	-	-	0.3 (0.4)	5.2 (5.3)	10^{-6}
	0.24	-	-	24.9	-	-	0.6 (1.4)	25.5 (26.3)	

Contributions to sum rules from partial waves with $\ell \leq 3$. A cutoff of 1.8 GeV is taken, and solution B of Estabrooks et al. with the small extreme I=2 amplitude is used, results for the large I=2 amplitude being shown in brackets. An asterisk denotes that more than 10% of the contribution comes from the energy region below 600 MeV. The sums are expressed in units where $m_\pi^2 = 1$.

fairly well known it should be a reasonable check. The low energy sum has contributions from P, D_2, and F waves; these are shown in table 2.1 for t=0. The P wave dominates completely. The contribution to the sum from energies above 1 GeV is negligible, thus the three sets of phase shifts give the same results. There is again a significant contribution to the sum from below 600 MeV; we assign a possible error of 50% to this. Fig.2.4b shows the low and high energy sums of sum rule (2.15), again agreement is good for the parameters of eq.(2.18(i)) and poor for those of eq.(2.18(ii))[+].

The above results are not greatly affected by varying $\gamma(t)$ within its range of uncertainty. A rho intercept of 0.25 is clearly inconsistent with the crossing sum rules; the fact that this value is consistent with a higher moment FESR is probably an indication of the uncertainties inherent in the use of the latter.

We thus conclude that a form of the imaginary part of the asymptotic I_t=1 amplitude consistent with analyticity, crossing, and unitarity is

$$A'_t(s,t) = \left(\frac{s-4}{s_0}\right)^{\alpha(t)} (a + \beta t)$$

with
$$\alpha(t) = 0.5 + 0.9t$$
$$a = 0.74 \pm 0.15$$
$$\beta = 1.9 \pm 0.15 \text{ GeV}^{-2}$$

This form corresponds to the exchange of a rho trajectory with a zero at $t=0.39 \pm 0.05$ GeV^2.

These results are consistent with those of refs.(51, 53, 55, 56).

2.5: The Asymptotic $I_t = 0$ amplitude

We discuss in this section how the FESR's and crossing sum rules may be used to study the t channel isospin zero asymptotic pion-pion scattering amplitude, and how we may attempt to separate the pomeron and f exchange contributions to this

---

[+]We avoid the region $0 < t < 4$ where the lowest energy phase shifts are excessively weighted.

amplitude. First we consider which crossing sum rules are dominated by this amplitude, and thus of most use.

The sum rule of eq.(2.8) appears immediately useful as the high energy sum of this is dominated by the required amplitude. At first sight eq.(2.8) appears to be not independent of eq. (2.9), the respective high energy sums being related by

$$\left[8(t)\right]_{HE} - \left[9(t)\right]_{HE} = \int_4^N dx \left\{ \left(A_t^1(x,t)\right) O\left(\frac{1}{x^2}\right) + A_t^2(x,t) O\left(\frac{1}{x}\right) \right\} \qquad (2.19)$$

(where the abbreviation $\left[8(t)\right]_{HE}$ means 'the high energy sum of eq.(2.8) evaluated at a given value of t'). The right hand side of eq.(2.19) is small compared with either of the terms on the left hand side. The low energy sums of eqs.(2.8) and (2.9) are not trivially equal, however, as they contain contributions from different partial waves. This suggests that it is worth taking combinations of eq.(2.8) to isolate further $I_t=0$ (and $I_t=1$) dominated rules, which may provide additional constraints.

Before considering the $I_t=0$ rule we shall first dispose of the $I_t=1$ possibility. The only rule dominated by the $I_t=1$ amplitude is obtained from the (I=1) + (I=2) combination of eq.(2.8):-

$$\int_4^N dx \left\{ \left(A_t^1(x,t) - A_t^1(x,u)\right)\left(\frac{1}{x-u} - \frac{1}{x-s}\right) + A_t^2(x,u)\left(\frac{1}{x-s} + \frac{1}{x-t}\right) - A_t^2(x,t)\left(\frac{1}{x-s} + \frac{1}{x-u}\right) \right\} = \int_4^N A_{Regge} \qquad (2.20)$$

This is not useful for our purposes since an exotic trajectory with an intercept of $-\frac{1}{2}$ would give a contribution to the high energy sum of the same order of magnitude as that of the rho trajectory. ($(\partial/\partial_6)_t$ of eq.(2.20) produces eq.(2.14) which we found in the previous section to have the same property).

A sum rule dominated by the $I_t=0$ amplitude may be obtained by taking the (I=0) + 2(I=2) combination of eq.(2.8); this produces the equation for the absorptive part of the $\pi^0\pi^0$ scattering amplitude $A^{00}(s,t) \equiv A^0(s,t) + 2A^2(s,t)$ (cf.eq.(1.10))

$$\int_4^N d\alpha \left\{ A^{00}(\alpha,t)\left(\frac{1}{\alpha-s}+\frac{1}{\alpha-u}\right) - A^{00}(\alpha,u)\left(\frac{1}{\alpha-s}+\frac{1}{\alpha-t}\right)\right\} = \int_4^N A_{Regge} \qquad (2.21)$$

This equation vanishes when t=u. For convenience we take u=0 to relate the amplitudes at arbitrary t in the range (4,-28) to those at t=0.

In the previous section two independent sum rules from eq.(2.10) were noted. We may take the third as the combination (I=0) + 2 (I=2) of eq.(2.10), however this is simply the derivative of eq.(2.21), containing the same partial waves, and having very similar properties to eq.(2.21). We thus do not consider this sum rule any further.

One sum rule from eq.(2.11) has been noted already; there remain two more. At t=u, eqs.(2.11), for each I, reduce to eq.(2.12), which is not now dominated by any one t channel isospin amplitude. However, following Wanders (29) we may subtract eq.(2.13) from eq.(2.12) to obtain a (well known) sum rule dominated by the I_t=0 amplitude:-

$$\int_4^N \frac{d\alpha}{(\alpha-t)^2(\alpha-4+2t)}\left\{ A_s'(\alpha,t)\frac{(3\alpha-4)}{(\alpha-4+2t)^2} - \frac{2}{3}\frac{\partial A_t^0}{\partial t}(\alpha,t) + \frac{10}{3}\frac{\partial A_t^2}{\partial t}(\alpha,t)\right\} = -\int_N^\infty A_{Regge} \qquad (2.22)$$

Eq.(2.22) may be derived by several alternative methods (33, 36, 37). The low energy sum contains no S or P wave contributions.

Taking the combination (I=0) + 2(I=2) of eq.(2.11) produces a rule analagous to eq.(2.21) but now also with no S or P wave contributions. For simplicity we take the limit t → u to obtain+

$$\int_4^N d\alpha \left\{ \frac{\partial A^{00}}{\partial t}(\alpha,t)\left(\frac{2}{(\alpha-4+2t)^3} - \frac{2}{(\alpha-t)^3}\right) + \frac{\partial^2 A^{00}}{\partial t^2}\left(\frac{1}{(\alpha-t)^2} - \frac{1}{(\alpha-4+2t)^2}\right)\right\} = -\int_N^\infty A_{Regge} \qquad (2.23)$$

+We could alternatively take the appropriate combination of $(\partial/\partial s)_u$ of eqs.(2.11).

Eq.(2.25) has been used with t=0 to obtain inequalities for partial waves and resonance widths (18, 36).

We have now presented all the crossing sum rules we shall use in conjunction with FESR's to study the asymptotic t channel isospin zero amplitude.

We assume that the asymptotic $I_t=0$ amplitude may be described in terms of the exchange of pomeron and f Regge trajectories. To determine the t dependence of these exchanges, we first try making the simplifying assumption that the f trajectory is strongly exchange degenerate with that of the rho. Thus we write for the asymptotic amplitude, where a pomeron of intercept unity has been taken:-

$$A_t^0(s,t) = 3A_p\, g(t)\sqrt{s(s-4)} + \frac{3}{2}\gamma(t)\left(\frac{s-4}{s_0}\right)^{\alpha(t)} \qquad (2.24)$$

A simple calculation with the first moment I=0 FESR then immediately leads to trouble, independent of the choice of cutoff. For all phase shift solutions studied the pomeron t structure is such that g(t) is either nearly constant (for the large I=2 amplitudes) or actually grows as $|t|$ increases (for the small I=2 amplitudes). The value found for A_p depends on the isospin two amplitude used, and results in an asymptotic σ_T $(\pi^+\pi^-)$ of 2.5 - 8 mb, which is much smaller than the value expected from factorization arguments.

With the aid of the crossing sum rules we can investigate the t dependence of the pomeron and f exchanges using weaker assumptions. We now replace γ (t) in eq.(2.24) by an unknown function of t, f(t). There are three sum rules (the FESR and eqs.(2.9) and (2.11)), which do not contain derivatives; we may solve between any two of them to determine f(t) and g(t). Eqs.(2.9) and (2.21) are related by eq.(2.13) so we do not solve between these. We notice that the dominant contribution to both the first moment I=0 FESR and to sum rule (2.9) comes from the P wave as $|t|$ increases (see table 2.1). Solving between these two equations may thus be analogous to solving between 2 FESR's of different moments. We find, in fact, unstable cutoff dependent results from this procedure,

from which no conclusions can be drawn+. The sum rule of eq.(2.21) has very different partial waves dominating the low energy sum, but requires an input of the value of the f residue function at t=0, f (0) into the high energy sum in order to obtain a solution with the FESR.

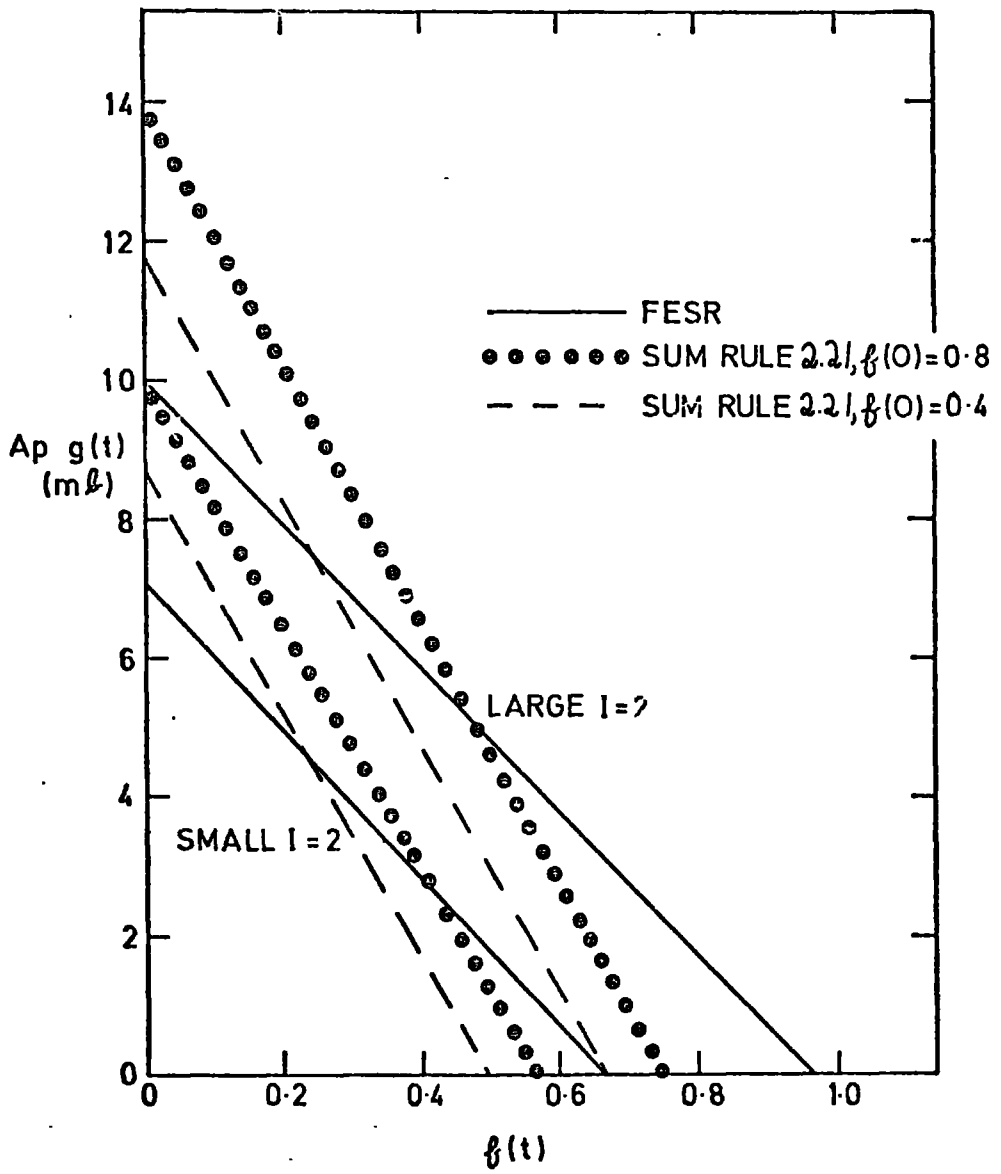

Fig.2.5 Solution of sum rule (2.21) with first moment isospin zero FESR for the pomeron and f residue functions, f(t) and $A_p g(t)$, at t=-0.24GeV^2. Solution B of Estabrooks et al., both extreme isospin two amplitudes, and inputs of f(0)=0.4 and f(0)=0.8 to sum rule (2.21) are used. The solution for f (t) is insensitive to the isospin two amplitude, and results are similar for other phase shift solutions.

+The solution at t=0 is highly dependent on the I=2 low energy amplitude, and also depends on the precise form of the Regge amplitude, for example whether the f energy dependence is $s^{\alpha(0)}$ or $(s-4)^{\alpha(0)}$. No solution at all is obtained for a considerable range of t, however, this result is sensitive to small changes in cutoff and f intercept.

First the FESR is evaluated at t=0 and at a range of values of t down to t = -0.55 GeV^2, to produce an equation relating f (t) to $A_p g(t)$ at each value of t. Sum rule (2.21) with an input of f(0) produces a similar set of equations (at $t \neq 0$); thus at each value of t there are two independent equations relating f(t) and g(t) which may then be solved. In Fig.2.5 the graphical solution at t=-0.24 GeV^2 is shown for phase shift solution B, taking two extreme values of f(0), 0.4 and 0.8. The latter value is approximately that expected from rho-f exchange degeneracy at t=0. The solution is insensitive to small changes in the low energy sum of equation (2.21), thus the uncertainty in the I=0 S wave below 600 MeV is unimportant. The results do not depend strongly on the cutoff either; in fact one can see that results should not change much if the cutoff is taken above the positions of the expected resonances (57) with ℓ =4 and ℓ =5 on the ρ trajectory. (Quantitative estimates of this change are not easy to make as the FESR is not dominated by leading partial waves to the same extent as the crossing sum rules and so possible daughter resonance contributions could become increasingly important). f(t) and g(t) are almost unchanged if the f intercept is varied by 20% from its assumed value of 0.5.

Figs.2.3 and 2.6 display the solutions for f(t) and g(t) obtained with both extreme I=2 amplitudes and with the two chosen values of f(0). The pomeron residue function is much more sensitive to the I=2 amplitude than that of the f. The solutions with the small f(0) and large I=2 amplitudes produce the smoothest form of g(t), with $g(t) \sim e^{bt}$, as is seen in fig. 2.6; f(t) has a zero at $t \simeq -0.55$ GeV^2 and $b \simeq 2.5$ GeV^{-2}.

We now briefly discuss the possibility of using the remaining two I_t=0 dominated sum rules to distinguish between the solutions found above. First consider sum rule (2.22). The low energy sum has contributions from D_0, D_2 and F waves. From table 2.1 it is seen that there is a considerable cancellation between D_0 and F waves, and that the D_2 contribution is significant. Fig.2.7a shows the low energy sum for the three different phase shift solutions, and the high energy sum for four of the possible solutions for the asymptotic I_t=0 amplitude. The D_0 and F wave absorptive parts of the Hyams et al solution are nearly identical to those of the Estabrooks et al solution; the large difference between the

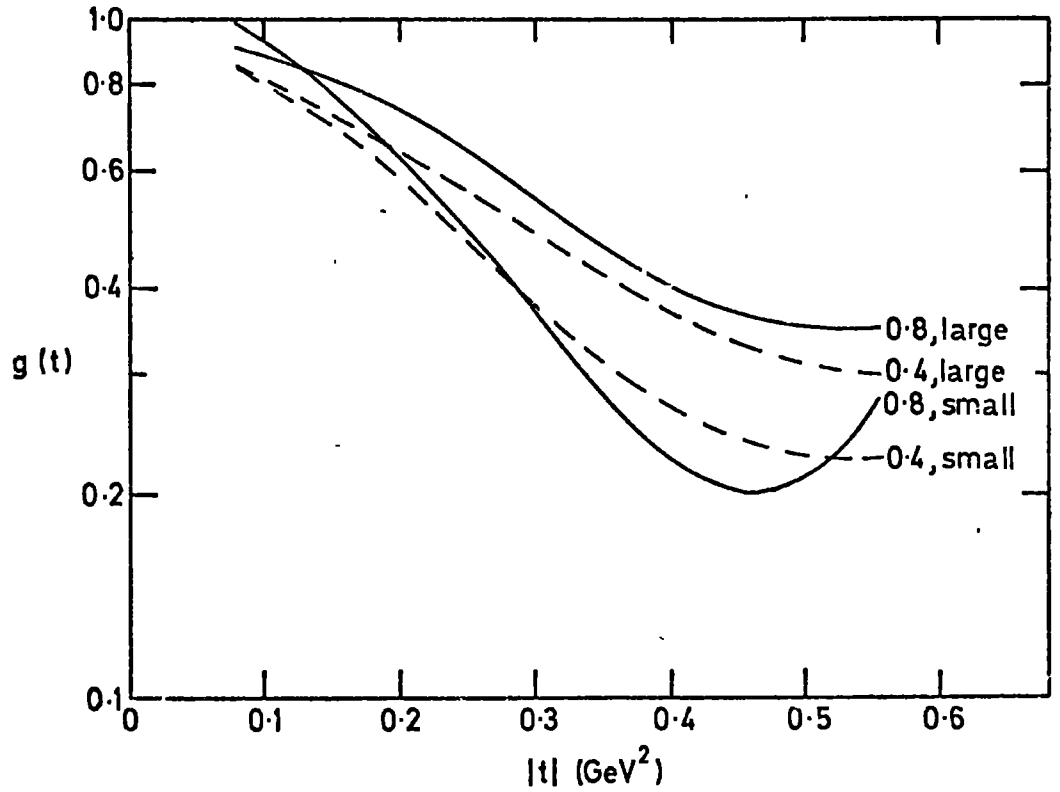

Fig.2.6. Pomeron residue function (normalized to unity at t=0), g(t), for phase shift solution B with the large and small extreme isospin two amplitudes. The solution with $f(0) = 0.4$ and the large isospin two amplitude is closest to the form $g(t) = e^{bt}$.

corresponding low energy sums seen in fig.2.7a arises because of a difference in overall phase between the two solutions, and shows that the sum rule of eq.(2.22) is very sensitive to this. It is thus not clear that useful conclusions can be drawn from the sum rule when applied in this manner (as is attempted in ref.54). While agreement might be obtained with any of the asymptotic solutions, the large I=2 or small $f(0)$ solutions are favoured.

Sum rule (2.23) contains double derivaties and will thus be very sensitive to the t dependence of the amplitudes. Only D_0 and D_2 partial waves contribute to the low energy sum; their contributions are shown in table 2.1. The D_2 contribution is not important, but again the sum rule is sensitive to small changes in the overall phase. In fig.2.7b we show for sum rule (2.23) the low energy sums for the phase shift solutions of ref.(7) and ref.(8), and the high energy sum for four of our suggested solutions for the asymptotic $I_t=0$ amplitude. Agreement is again better for the large I=2, small f(0) solutions but a small change in the phase shifts might produce agreement with other asymptotic solutions.

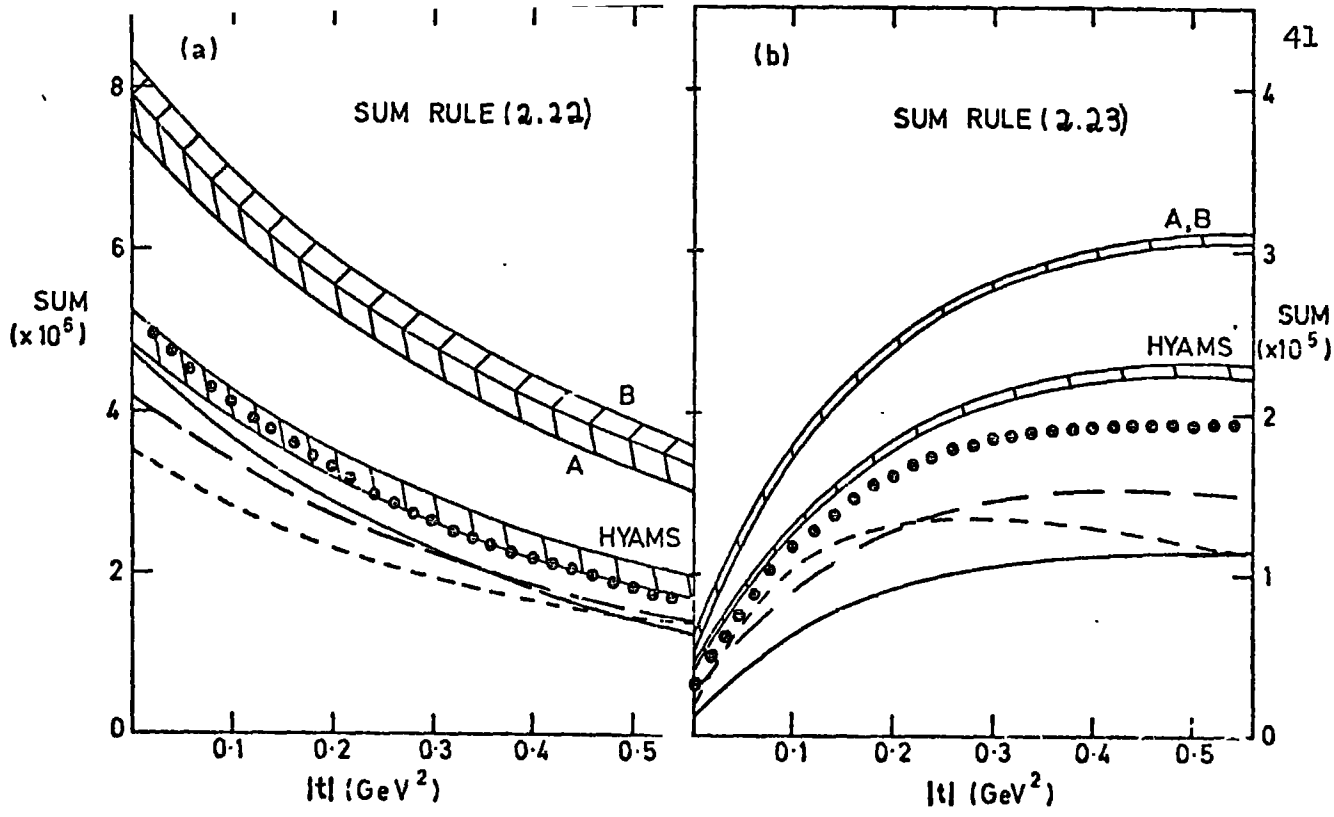

Fig.2.7. (a) sum rule (2.22) and (b) sum rule (2.23). The low energy sums are for the phase-shift solutions of Hyams et al., and solutions A and B of Estabrooks et al.; the width of the bands indicates the uncertainty in the D_2 wave. The high energy sums use the solutions for the asymptotic $I_t = 0$ amplitude with $f(0) = 0.4$ (dotted curve for the large isospin two amplitude solution and full curve for the small isospin two solution) and $f(0) = 0.8$ (long-dashed curve for the large isospin two solution and short-dashed curve for the small isospin two solution). $m_\pi^2 = 1$ units are used.

2.6: Conclusions

We have shown, in this chapter, how the principles of analyticity, crossing and unitarity constrain the pion-pion scattering amplitudes and allow them to be studied in regions inaccessible to phase shift analysis. The Roy equations allow a good deal of information on low energy pion-pion scattering to be obtained if information on higher energy scattering is given. In particular, a one parameter family of solutions for the S wave pion-pion scattering lengths may be obtained; the values found are consistent with the predictions of the totally different theoretical approach of current algebra. The low energy P wave amplitude as determined by the Roy equations, is however in disagreement with the results of all phase shift analyses.

The systematic derivation of physical region crossing sum rules for pion-pion scattering, presented here, is useful in linking together all the crossing sum rules which have been separately derived, by different methods, in the literature, and ensures that none are missed. In conjunction with finite energy sum rules they are of considerable value in studying the asymptotic form of the pion-pion scattering amplitudes, but they are unsuccessful in resolving the ambiguities of phase shift analyses, largely because the isospin two pion-pion scattering amplitude, which is hard to determine experimentally, is poorly known.

We find, using the sum rules, that the imaginary part of the asymptotic t channel isospin one pion-pion scattering amplitude is well described by the exchange of a conventional rho trajectory. If strong rho-f exchange degeneracy is assumed a FESR calculation shows that the pomeron contribution to the t channel isospin zero amplitude is such that the asymptotic total cross section for $\pi^+\pi^-$ scattering is between 2.5 and 8 mb. With the aid of crossing sum rules, the pomeron and f exchange contributions may be separated without this assumption; evidence then points to the breaking of ρ - f exchange degeneracy and, if the isospin two amplitude is very inelastic below 1.8 GeV, the $\pi^+\pi^-$ asymptotic total cross section can be as large as 12.5 mb. Since there are few inelastic channels available, the $\pi^+\pi^+$ scattering amplitude can be expected, however, to be nearly elastic, indicating a much smaller total cross section for $\pi^+\pi^-$ scattering; we also present further direct evidence in chapter 5 that the asymptotic total cross section for pion-pion scattering is near 6 mb. The question as to why the naive factorization arguments (which predict a total cross section for pion-pion scattering of about 15 mb) should fail so badly, will be discussed in the next chapter.

3: MESON-MESON TOTAL CROSS-SECTIONS AND NUCLEON DIFFRACTION DISSOCIATION

In this chapter we present evidence that the total cross section for elastic meson-meson scattering is small, and discuss possible explanations for the apparent failure of the pomeron to factorize. We show how the separation of the contributions to the diffractive production of low mass pion-nucleon systems allows several items of physical interest, including the high energy pion-pion scattering total cross section, to be studied. We conclude the chapter with a brief discussion of how the diffractive component of the $\pi N \to \pi\pi N$ reaction may be found experimentally.

3.1: The meson-meson scattering total cross-section

In the previous chapter we obtained the result that either the isospin two pion-pion scattering amplitude is large and inelastic, or the coupling of the pomeron to pion-pion scattering is smaller than that expected from naive factorization arguments. The available direct experimental evidence also points to a small asymptotic total cross section for meson-meson scattering. This cross-section should be determined most easily from a study of scattering amplitudes which have no s channel resonances and are pomeron dominated in the t channel (such as in $\pi^+\pi^+$ or $\pi^- K^-$ scattering). Such a cross section may be expected to rise rapidly to its asymptotic value; several experiments (52, 58, 59) have found the $\pi^+\pi^+ \to \pi^+\pi^+$ total cross section to be in the 2.5-5 mb. range in the 1.4 - 2 GeV energy region, though larger values would be obtained if the amplitude were very inelastic. The $\pi^- K^-$ total cross section has been determined as 5-6 mb. in the 1.8 - 2.8 GeV energy range (60). It could be that these cross-sections are still rising, as few inelastic channels are available in $\pi^+\pi^+$ or $\pi^+ K^+$ scattering at low energies, and the asymptotic regime may not yet have been reached. We obtain, however, in chapter 5, evidence that the pomeron contribution to the $\pi^+\pi^- \to \pi^+\pi^-$ total cross section is about 6 mb. in the 3 - 4 GeV energy region; there are many available inelastic channels and so there is no reason to suppose that the pomeron has not attained its asymptotic coupling. Another estimate of the pion-pion scattering total

cross section has been obtained by the Stony Brook - Michigan - Batavia - Pittsburgh collaboration (61), who studied the 100 GeV/c $\pi^+ n \rightarrow pX$ inclusive reaction. On the assumption that pion exchange dominates the amplitude at low momentum transfer, a triple- Regge description allows the $\pi^- \pi^+$ total cross section to be extracted. Values of 15 ± 4 mb at 4.5 GeV and 13.5 ± 2.5 mb at 5.6 GeV were found; these cross sections include ρ and f exchange contributions, and the pomeron contribution, and thus the asymptotic $\pi^- \pi^+$ total cross section, is smaller, in the region of 9 mb. The total $\pi^- \pi^+$ cross section was found to lie between 10 and 25 mb. at energies up to 10 GeV, however these results are not so reliable, as the momentum transfer between nucleon and proton is such that pion exchange may no longer dominate the amplitude.

We thus conclude that the coupling of the pomeron to meson-meson scattering is probably considerably smaller than expected. We discuss below possible explanations.

3.2: Factorization of the pomeron

There is good experimental evidence that factorization of the pomeron holds to better than 20%, between meson-baryon and baryon-baryon systems. For instance we find (25):-

$$\frac{\frac{d\sigma}{dt}(\pi^- p \rightarrow \pi^- N(1690))}{\frac{d\sigma}{dt}(\pi^- p \rightarrow \pi^- p)} \simeq \frac{\frac{d\sigma}{dt}(K^- p \rightarrow K^- N(1690))}{\frac{d\sigma}{dt}(K^- p \rightarrow K^- p)} \simeq \frac{\frac{d\sigma}{dt}(\bar{p} p \rightarrow \bar{p} N(1690))}{\frac{d\sigma}{dt}(\bar{p} p \rightarrow \bar{p} p)} \quad (3.1)$$

at 8 and 16 GeV/c, for $|t| < 0.4$ GeV^2. Similarly (25) the ratios of the cross sections of the reactions with $\pi\pi$ or pp at the upper vertices and with either pp, pp π^0, pp $(2\pi^0)$, pp$(3\pi^0)$ at the lower vertices are all about equal at 16 and 19 GeV/c. These results do not however check the simultaneous validity of factorization between meson-meson, meson-baryon, and baryon-baryon processes, and will still hold if either of the two explanations for the small meson-meson cross section, discussed below, is correct. It has been shown in refs.(62, 63) that the π p, pp and Kp elastic scattering data may be well described by including the exchange of a pomeron trajectory of intercept 1.07. If indeed the pomeron intercept is not unity,

factorization can only be applied to the total cross-sections of $\pi\pi$, π p and Kp scattering if all the reactions are considered at the same energy (which must be high enough for pomeron exchange to dominate the amplitude). Writing for the pomeron contributions to the total cross section:-

$$\sigma_T(\pi P) = G_1 s^{0.07}, \quad \sigma_T(PP) = G_2 s^{0.07}, \quad \sigma_T(\pi\pi) = G_3 s^{0.07} \qquad (3.2)$$

with, from refs.(61, 62) G_1 = 15 mb, G_2 = 25 mb, then factorization of the pomeron implies:-

$$G_3 = G_1^2/G_2 = 9\ mb. \qquad (3.3)$$

and thus the pomeron contribution to the total pion-pion scattering cross section is about 10 mb. at 2 GeV, which is nearer the values indicated in section 3.1. The pion-pion scattering cross section will grow asymptotically, and the 'failure of factorization' is an illusion.

Another explanation of the small coupling of the pomeron to meson-meson systems, compared to its coupling to meson-baryon and baryon-baryon systems, has been suggested by Pennington and Gula (64) in terms of dual loop models of the pomeron. The generally accepted model for the dual pomeron in meson-meson scattering, embodying Harari-Freund duality (24) (non resonant s-channel background with t channel vacuum quantum number exchange) is as in fig.3.1a, and for meson-baryon and baryon-baryon as in figs.3.1b, 3.1c (taken from ref.(64)). Such diagrams, where only $q\bar{q}$ or qqq intermediate states are allowed, lead to the usual factorization predictions. The authors of ref.(64) point out that, as $qq\bar{q}\bar{q}$ intermediate states are required in all dual schemes involving baryon-antibaryon scattering, there is no reason why they should not be present in meson-baryon and baryon-baryon scattering also. The pomeron can then couple, in meson-baryon and baryon-baryon scattering, via the diagrams of figs.3.2a, 3.2b in addition to the 'conventional' couplings of figs.3.1b, 3.1c. Thus this model predicts that the pomeron couples more strongly to

meson-baryon and baryon-baryon channels than to meson-meson channels. There are in fact enough free parameters in the model of ref.(64) to accommodate any experimental ratios of the three cross-sections.

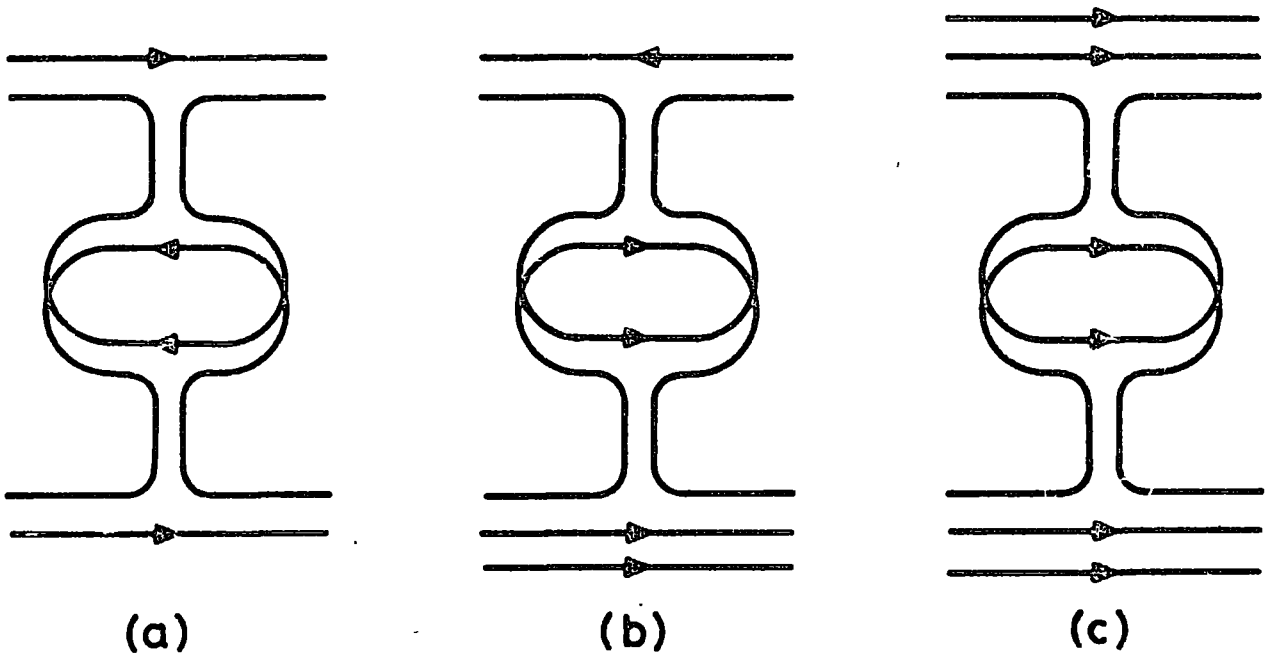

Fig.3.1. Conventional dual quark diagrams for the pomeron in: (a) meson-meson, (b) meson-baryon, (c) baryon-baryon scattering. (Taken from ref.(64))

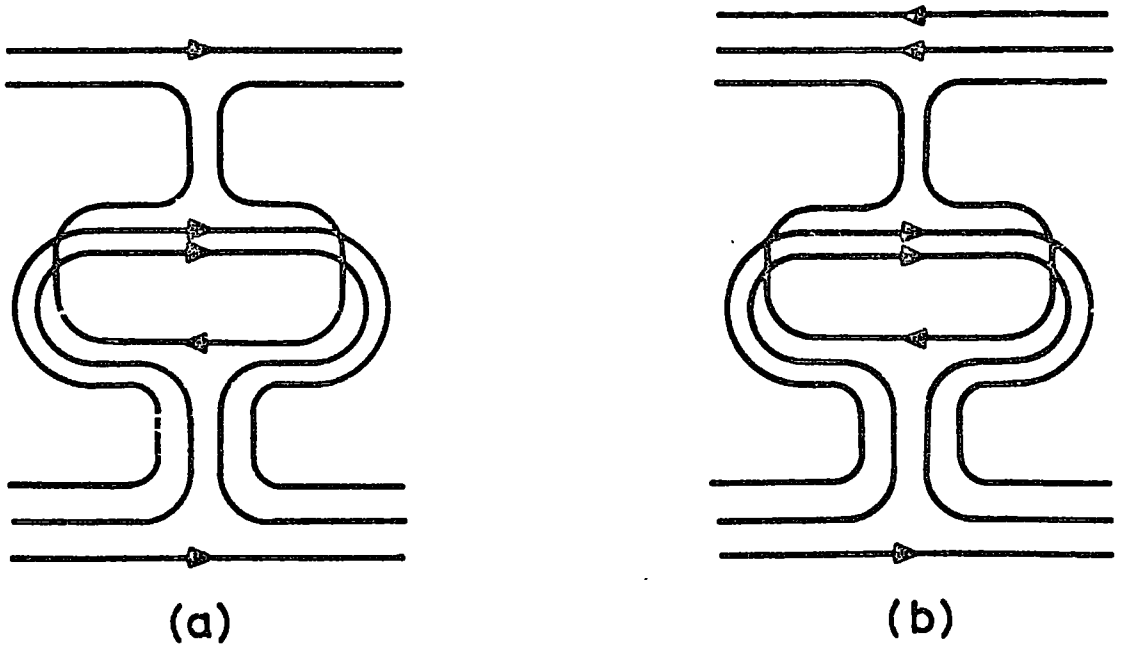

Fig.3.2. Additional dual quark diagrams for the pomeron, when $qq\bar{q}\bar{q}$ states are allowed, in: (a) meson-baryon, and (b) baryon-baryon scattering. (from ref.(64).

3.3: The low πN mass kinematic region of the $\pi N \rightarrow \pi\pi N$ reaction

To obtain direct information on high energy pion-pion scattering, we can consider data from the $\pi N \rightarrow \pi\pi N$ reaction in a kinematic region of the Dalitz plot (fig.1.2) different from that studied in previous chapters. For an incident pion momentum of 16 GeV/c, $t_{\pi\pi} > -0.15$ GeV/c^2 (when pion exchange should be important) implies that $M_{\pi\pi} \lesssim 10$ GeV, and so the region of the Dalitz plot where $M_{\pi\pi} \simeq 3$ GeV and $M_{\pi N} \simeq 4.5$ GeV should give good information on high energy pion-pion scattering, free from interference with N* resonance production. The detailed data available, however, is in the low mass region of the Dalitz plot, where N* resonance production may be important.

In common with other diffraction dissociation reactions, many interesting features are shown by the distributions of the diffractively produced low mass system in the $\pi N \rightarrow \pi(\pi N)$ reaction. From a study of such diffractive processes, it may be deduced that mechanisms corresponding to those shown in

fig.1.3, for $\pi N \rightarrow \pi (\pi N)$ are present. The diagram of fig.1.3a was first suggested (65) to account for the diffractive production of low mass $\pi\rho$ systems in π p $\rightarrow \pi\rho$ p, and is usually referred to as the pion exchange Deck (or Deck-Drell-Hiida)mechanism. As will be discussed in chapters 4 and 5, there is good evidence for the presence of the other mechanisms (the nucleon exchange Deck mechanism and the direct resonance production mechanism) of fig.1.3 in the $\pi N \rightarrow \pi (\pi N)$ reaction, with analogous mechanisms in other diffraction dissociation reactions.

In order to separate the contributions of the diagrams of fig.1.3 to the t channel isospin zero exchange part of the $\pi N \rightarrow \pi (\pi N)$ reaction, it is first necessary to consider the role of duality. The exchange of the pion trajectory, when the momentum transfer between ingoing and outgoing nucleon is small, leads to a mainly real amplitude, as the pion trajectory has an intercept close to zero, and even signature. Since duality only applies to the imaginary parts of amplitudes, pion exchange may not be dual to any resonance. The nucleon exchange amplitude (fig.1.3b), on the other hand, has a large imaginary part and may be dual to the amplitude for the production of N* resonances. Together, these facts suggest that the pion exchange amplitude, with either the resonance production or the nucleon exchange amplitude, should be used to describe the diffractive $\pi N \rightarrow \pi (\pi N)$ reaction.

The presence of resonance bumps in the cross-section for the production of pion-nucleon systems of mass greater than 1.4 GeV/c leads naturally to the choice of the resonance excitation amplitude here (although the nucleon exchange amplitude should also give, on average, a valid description of this part of the amplitude). For pion-nucleon systems of lower mass, the nucleon exchange amplitude is the natural choice to use with the pion exchange amplitude, to describe the diffractive reaction, and its presence is indicated by the data, as will be seen.

In order to take correctly into account the interference between the amplitudes of fig.1.3 it will be necessary to determine how the helicity states of the outgoing nucleon are populated. This is straightforward for the pion and nucleon exchange amplitudes, but, to calculate the resonance excitation diagram of fig.1.3c, a model is needed to describe how

the pomeron couples to the NN* system. We shall motivate the idea that the pomeron may have a vector coupling, in chapter 5.

It is by the different kinematic properties of the processes shown in fig.1.3 that their respective contributions to $\pi N \rightarrow \pi (\pi N)$ diffractive scattering may be identified and separated. It is thus necessary to study the kinematics of a 5-body reaction in some detail; we do this in the next chapter, emphasizing the qualitative features of the data which may be interpreted in terms of the different processes.

First however we show how the isospin zero exchange amplitude has been extracted from experimental data on the $\pi N \rightarrow \pi\pi N$ reaction.

3.4: Isospin and prism plot analysis of $\pi N \rightarrow \pi\pi N$

The cross sections for the seven possible charge configurations of the process $\pi^{\pm} p \rightarrow \pi (N\pi)$ can be expressed in terms of three independent complex amplitudes $M^{I}_{I_E}$ (66 - 68) (in the notation of ref.(66)) where, for the exchanged object, $I_E = 0$ and $I_E = 1$ are considered and where I ($= \frac{1}{2}$ or $\frac{3}{2}$) denotes the isospin of the produced ($N\pi$) system. Six of the seven possible processes may be measured in a bubble chamber experiment and from these may be obtained the required quantity $|M^{\frac{1}{2}}_{0}|^2$, which determines the distributions of the diffractively produced pion-nucleon system. This is the method of isospin analysis.

An alternative method of obtaining information on the diffractive amplitude in, say, the $\pi^{+} p \rightarrow \pi^{+} (p \pi^{o})$ reaction, is the prism plot analysis. This involves the assumption that the reaction proceeds via certain well defined non-interfering channels, each occupying a different region of four-dimensional phase space. Firstly, by examining one or two dimensional samples of the four dimensional distribution, the principal reaction channels are guessed. A Monte-Carlo calculation is then carried out to give the probability of each experimental point to lie in a given channel, and the relative weights of different channels. This process is repeated, re-determining the probability of experimental points to lie in a particular channel by using the newly found weights of the different channels. The process is continued until convergence occurs, keeping a watch for untagged

points to see if new channels are required. Thus, for example, assuming that nucleon diffraction dissociation and the production of dipion resonances, dominate the 16 GeV $\pi^+ p \to \pi^+ \pi^0 p$ reaction, the respective contributions of these processes may be separated. While the assumption of non-overlapping channels cannot be correct, it is seen from the Dalitz plot of fig.1.2. that overlap between low mass dipion and pion-nucleon systems is small, and so results should be reasonable. The results obtained in ref.(69) by means of this technique are consistent with those obtained by the isospin analysis of ref.(66), using the same data.

We shall be concerned in some detail in the following chapters with the distributions of the diffractively produced pion-nucleon system in the 16GeV/c $\pi^- p \to \pi^- (\pi N)$ reaction, obtained from the isospin anaysis carried out by the Aachen-Berlin-Bonn-CERN-Heidelberg collaboration (55) on data from the CERN two metre bubble chamber. These distributions are presented in considerably more detail than in any other publication to date, and a considerable amount of information may be extracted from them.

4: KINEMATICS OF DIFFRACTIVE AMPLITUDES AND A QUALITATIVE INTERPRETATION OF DIFFRACTION DISSOCIATION

In this chapter we discuss the kinematics of a general five body reaction, and consider in some detail the kinematic properties of the pion and nucleon exchange Deck amplitudes for the $2 \to 3$ diffractive scattering process, as exemplified by the $\pi N \to \pi(\pi N)$ reaction. We then show how qualitative features of nucleon diffraction dissociation may be interpreted in terms of the Deck mechanisms, in association with the diffractive production of nucleon resonances.

4.1: Invariants and coordinate systems

For the general $AB \to CDE$ reaction we define, as illustrated in fig.4.1, the Lorentz invariant energies

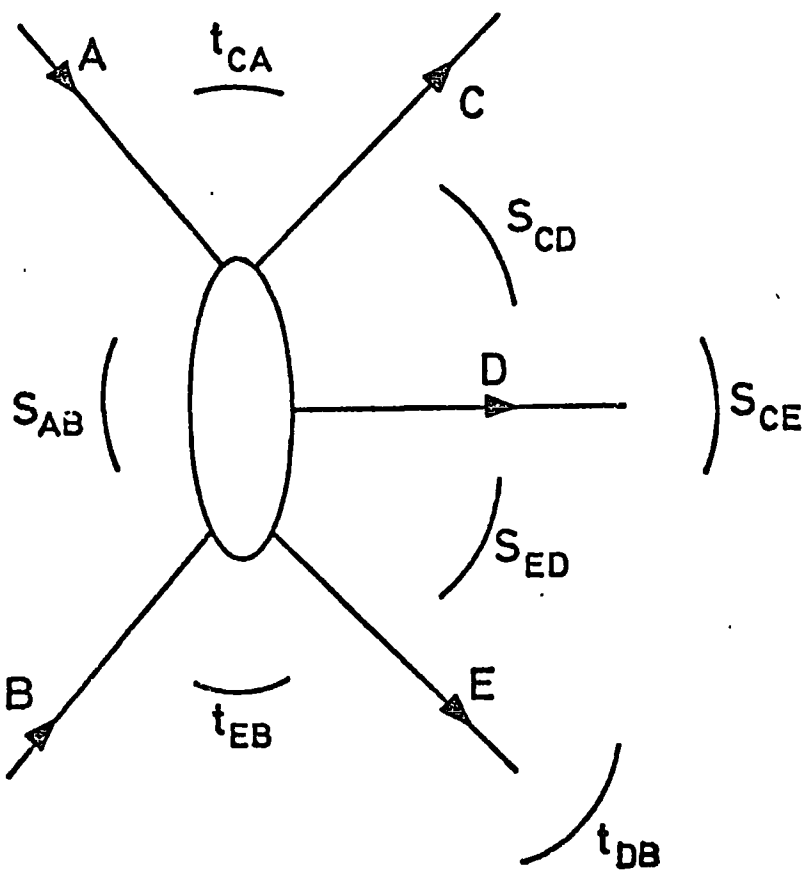

Fig.4.1. Kinematic invariants for general 5 body process.

$s_{xy} = (P_x^\mu + P_y^\mu)(P_{x\mu} + P_{y\mu})$ and momentum transfers $t_{xy} = (P_x^\mu - P_y^\mu)(P_{x\mu} - P_{y\mu})$. A set of five independent invariants may be chosen in several ways from these. Several relations between the invariants of fig.4.1 hold; these are most easily derived by considering a pair of particles together and using the relation for $2 \rightarrow 2$ scattering:-

$$s + t + u = \sum_i m_i^2 \tag{4.1}$$

Thus taking A and B together we have:-

$$s_{AB} + m_C^2 + m_D^2 + m_E^2 = s_{CD} + s_{CE} + s_{DE} \tag{4.2}$$

Taking AC together:-

$$t_{CA} + m_B^2 + m_D^2 + m_E^2 = s_{DE} + t_{DB} + t_{EB} \tag{4.3}$$

and so on.

For the $AB \rightarrow CDE$ reaction we shall in general be interested in the properties of the scattering amplitude as a function of s_{AB}, t_{CA}, s_{ED} and the angles θ, ϕ of particle E in the frame of reference where the centre of mass of particles D and E is at rest. To calculate the amplitudes from a given model, the energies and momenta of all the particles in this frame of reference, as well as the other invariants, will be needed. First we must define the coordinate systems in which θ and ϕ are measured; as several different conventions are in current use we choose ours to agree with that of the Aachen-Berlin-Bonn-CERN-Heidelberg collaboration (66) whose data we shall discuss in detail below. It is usual to use either of two coordinate systems, the so-called s and t channel systems, which are distinguished by the direction chosen for the Z axis in the E D centre of mass system. For the $\pi N \rightarrow \pi\pi N$ reaction we define A=π, B=N, C=π, D=π, E=N. Consider first the t-channel frame (fig.4.2a); we take the Z axis to lie along the direction of momentum of particle B, and define the Zx plane as that containing the momenta of

(a) t channel

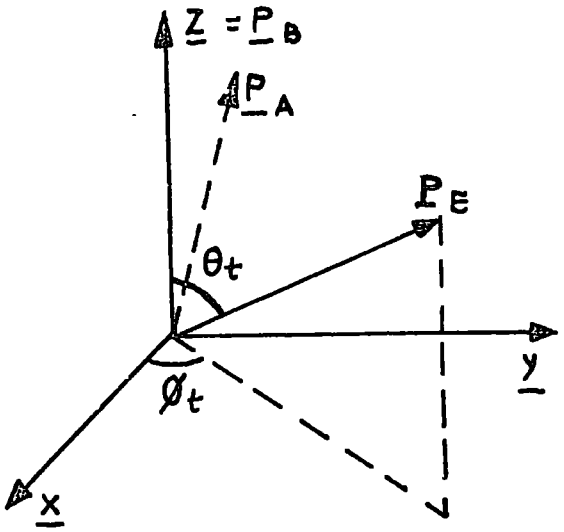

(b) s channel

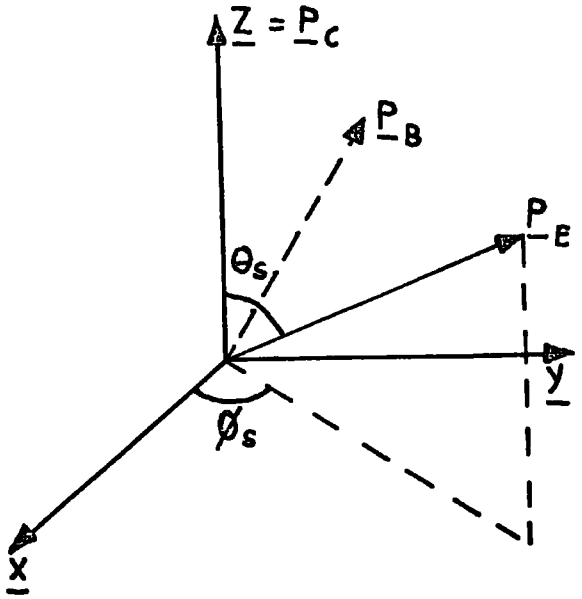

Fig.4.2. Definition of t and s channel coordinate systems.

particles A and B. Define:-

$$\hat{\underline{y}} = \frac{\underline{P}_A \wedge \underline{P}_B}{|\underline{P}_A|\ |\underline{P}_B|} \quad , \quad \hat{\underline{x}} = \hat{\underline{y}} \wedge \hat{\underline{z}} \tag{4.4}$$

Thus $(P_A)_x < 0$ and, for $\phi_t = 0$, incident A(π) and outgoing E(N) are on opposite sides of the Z axis. The polar and azimuthal angles are as depicted in fig.4.2a. This convention is used in refs.(66, 69). Refs.(70 - 72) take $\hat{\underline{y}} \propto \underline{P}_B \wedge \underline{P}_A$ and thus have the azimuthal angle equal to $\phi_t + \pi$. In refs. (73, 74) particle E is defined as the pion and thus the azimuthal angle equals $\phi_t + \pi$ and the polar angle equals $\pi - \theta_t$.

In the s channel we take the Z axis in the direction of momentum of particle C, and the Zx plane as that containing the momenta of particles B and C. Define:-

$$\hat{\underline{y}} = \frac{\underline{P}_B \wedge \underline{P}_C}{|\underline{P}_B|\ |\underline{P}_C|} \quad , \quad \hat{\underline{x}} = \hat{\underline{y}} \wedge \hat{\underline{z}} \tag{4.5}$$

Thus $(P_B)_x < 0$ and, for $\phi_s = 0$, incident B(N) and outgoing E(N) are on opposite sides of the Z axis. The polar and azimuthal angles are then as depicted in fig.4.2b. This is the convention used in refs.(66, 69); other conventions involve taking $\hat{\underline{z}} = -\hat{\underline{P}}_C$ (73, 74) or $\hat{\underline{y}} \propto \underline{P}_C \wedge \underline{P}_B$ (71).

4.2: Energies, momenta and angles

In this section we describe how to relate the quantities of physical interest, in the s or t channel, to the invariants and to each other. We work throughout in the frame where the centre of mass of particles D and E is at rest, and assume we are given the invariants S_{AB}, t_{CA}, and S_{ED}, with the angles θ_t and ϕ_t.

Consider particle R, mass $\sqrt{S_{ED}}$, decaying to particles E and D. 4-momentum conservation may be written:-

$$P_R - P_E = P_D \tag{4.6}$$

Squaring then gives us immediatly the energy of particle E:-

$$E_E = \frac{S_{ED} + M_E^2 - M_D^2}{2\sqrt{S_{ED}}} \tag{4.7}$$

and interchanging the labels D and E gives:-

$$E_D = \frac{S_{ED} + M_D^2 - M_E^2}{2\sqrt{S_{ED}}} \tag{4.8}$$

To obtain the energy of particle C, E_C, square the equation:-

$$P_A + P_B = P_C + P_R \tag{4.9}$$

Thus:-

$$E_C = \left(S_{AB} - S_{ED} - M_C^2\right)/2\sqrt{S_{ED}} \tag{4.10}$$

Rewriting eq.(4.9) as $P_A - P_C = P_R - P_B$, and squaring, we have:-

$$E_B = \left(S_{ED} + M_B^2 - t_{CA}\right)/2\sqrt{S_{ED}} \tag{4.11}$$

and from conservation of energy:-

$$E_A = E_C + E_D + E_E - E_B \tag{4.12}$$

The momenta of the particles are obtained from the usual relation:-

$$|\underline{P}_x| = + \sqrt{E_x^2 - M_x^2} \tag{4.13}$$

We shall also need the invariants S_{CD} and t_{EB}.
$t_{EB}(= (P_E - P_B)^2)$ is obtained immediately in terms of known quantities:-

$$t_{EB} = M_E^2 + M_B^2 - 2E_E E_B + 2|\underline{P}_E||\underline{P}_B| \cos\theta_t \tag{4.14}$$

To calculate S_{CD}, we first need the angle $\chi_t (0 < \chi_t < \pi)$ between $\underline{P}_B$ and $\underline{P}_A$, defined by

$$t_{CA} = m_C^2 + m_A^2 - 2E_C E_A + 2|\underline{P}_A|^2 + 2|\underline{P}_A||\underline{P}_B| \cos\chi_t \qquad (4.15)$$

(where $\underline{P}_C = \underline{P}_A + \underline{P}_B$ has been used).

Using $\underline{P}_D = -\underline{P}_E$, we find:-

$$S_{CD} = m_C^2 + m_D^2 + 2E_C E_D + 2|\underline{P}_B||\underline{P}_D| \cos\theta_t + 2\underline{P}_A \cdot \underline{P}_E \qquad (4.16)$$

With our definition of the t channel coordinate system $P_A^x < 0$ and so:-

$$S_{CD} = m_C^2 + m_D^2 + 2E_C E_D + 2|\underline{P}_B||\underline{P}_D| \cos\theta_t + 2|\underline{P}_A||\underline{P}_E| \cos\theta_t \cos\chi_t - 2|\underline{P}_A||\underline{P}_E| \sin\chi_t \sin\theta_t \cos\phi_t \qquad (4.17)$$

with $\sin\chi_t = +\sqrt{1 - \cos^2\chi_t}$.

The only remaining problem is to determine the s channel angles in terms of the invariants. We obtain θ_s directly from :-

$$S_{CD} = m_C^2 + m_D^2 + 2E_C E_D + 2|\underline{P}_C||\underline{P}_D| \cos\theta_S \qquad (4.18)$$

Defining χ_S as the angle between $\underline{P}_B$ and $\underline{P}_C$ $(0 < \chi_s < \pi)$, we obtain $\cos\phi_s$ from the equation:-

$$t_{EB} = m_B^2 + m_E^2 + 2E_E E_B - 2|P_E||P_B|(\sin\chi_S \sin\theta_S \cos\phi_S - \cos\theta_S \cos\chi_S) \qquad (4.19)$$

where $P_B^x < 0$ has been used.

χ_s is obtained from :-

$$t_{CA} = m_c^2 + m_A^2 - 2E_c E_A + 2|\underline{p}_c|^2 - 2|\underline{p}_c||\underline{p}_B| \cos\chi_s \qquad (4.20)$$

Note that we still do not know the sign of ϕ_s. To determine this, we need to evaluate the invariant $\varepsilon_{\alpha\beta\gamma\delta} P_A^\alpha P_B^\beta P_C^\gamma P_D^\delta$ in both s and t channels. We show in Appendix (3A) that in fact $0 < \phi_t < \pi$ if only if $0 < \phi_s < \pi$, for any values of the other independent variables.

4.3: Kinematic properties of Deck model amplitudes

We discuss in this section the distributions of a pion-nucleon system produced by the Deck mechanism in the $\pi N \to \pi\pi N$ reaction. We shall consider the Deck amplitudes in more detail in chapter 5; for our present purposes is sufficient to write for the pion exchange Deck amplitude (fig.1.3a):-

$$A \sim \frac{(a s_{CD} + b\sqrt{s_{CD}})}{t_{EB} - m_\pi^2} e^{b t_{CA}} \qquad (4.21)$$

For the nucleon exchange Deck amplitude (fig.1.3b) the denominator is replaced by $t_{DB} - m_N^2$.

It is necessary to carry out a detailed calculation to determine properly the kinematic properties of these amplitudes, however a general idea of what to expect may be obtained without resorting to the computer.

First note that the amplitude is largest when s_{CD} is large and thus, by eq.(4.2) when s_{DE} (and s_{CE}) is small; also the amplitude is large only when t_{CA} and t_{EB} or t_{DB} is small. These properties result in a particularly large cross-section for the production of low mass pion-nucleon systems.

The exact calculation shows that $\frac{d\sigma}{dt_{CA}}$ (Deck) falls more steeply with t_{CA} when the mass of the pion-nucleon system is near its threshold value, than when larger, and that this effect is more pronounced for the pion than for the nucleon exchange Deck amplitude. This kinematic effect arises as,

when $S_{ED} \simeq (m_E + m_D)^2$, we may write, approximately:-

$$t_{EB} \simeq m_E^2 + m_B^2 - 2 m_E E_B \tag{4.22}$$

$$t_{DB} \simeq m_D^2 + m_B^2 - 2 m_D E_B \tag{4.23}$$

Equs. (4.3) and (4.11) then give immediately:-

$$t_{DB} \simeq \frac{t_{CA} m_D + m_E m_B^2}{m_D + m_B} - m_E m_D \tag{4.24}$$

and:-

$$t_{EB} \simeq \frac{t_{CA} m_E + m_D m_B^2}{m_D + m_E} - m_E m_D \tag{4.25}$$

Specializing to the π N $\rightarrow \pi\pi$ N reaction of fig.(4.1) we find to first order in m_π / m_N:-

$$1/(t_{EB} - m_\pi^2) \simeq 1/(t_{CA} - 2 m_\pi^2) \tag{4.26}$$

and:-

$$1/(t_{DB} - m_N^2) \simeq m_N / m_\pi (t_{CA} - 2 m_N^2) \tag{4.27}$$

Thus in the amplitude of eq.(4.21) the t_{CA} dependence is enhanced by the t_{EB} or t_{DB} dependence of the propagator, the enhancement being greater for the pion exchange Deck amplitude.

An important feature arising from the peripherality of the amplitude with t_{EB} (or t_{DB}), is a preference for the reaction to be coplanar, resulting in an anisotropy of the azimuthal angular distributions. Consider first the pion exchange Deck amplitude. Since the amplitude is large only when t_{EB} is small, the nucleon is a spectator in pion-pion

scattering and has little momentum available to offset any non-coplanarity between the outgoing dipion system and the incoming pion-nucleon system. The degree of coplanarity will become greater as the energy of the pion in the outgoing pion-nucleon centre of mass frame increases, and so we may expect an increasing anisotropy of the azimuthal angular distributions as the mass of the pion-nucleon system increases from its threshold value. The outgoing pions will tend to move in opposite directions, and so the differential cross sections will be largest for $\phi \simeq \pi$. Similarly, for the nucleon exchange Deck amplitude, we have a 'spectator pion' in pion-nucleon scattering and can expect peaks in the azimuthal angular distributions at $\phi = 0$. This anisotropy means that helicity of the nucleon is not conserved in either the s or t channel, as we demonstrate in appendix 4E.

The spectator aspect of the nucleon (pion) also results in a tendency for the outgoing nucleon (pion) to be aligned with the incoming nucleon, in the t channel, leading to a peak in the polar angular distributions at $\theta_t = 0(\pi)$. This effect is in fact suppressed for small t_{CA} and S_{ED}, as has been demonstrated by Berger (70). For $S_{AB} \gg S_{ED}$ and $t_{CA} \simeq 0$, the following approximate relations hold:-

$$S_{CD} \simeq S_{AB} \frac{(t_{EB} - m_D^2)}{S_{ED} - m_B^2} \tag{4.28}$$

$$S_{CE} \simeq S_{AB} \frac{(t_{DB} - m_E^2)}{S_{ED} - m_B^2} \tag{4.29}$$

The pion or nucleon pole thus cancels out of the S_{CD}(or S_{CE}) dependent part of the amplitude, removing the t_{EB} and thus the θ_t dependence. The pole remains in the $\sqrt{S_{CD}}$ or $\sqrt{S_{CE}}$ dependent part of the amplitude. In fact the exact calculation shows that the relations (4.28, 4.29) soon break down as S_{ED} increases from its threshold value and $|t_{CA}|$ increases, and prominent peaks appear in the polar angular distributions.

4.4: Qualitative features of diffraction dissociation

We discuss, in this section, how the qualitative features of inelastic diffraction dissociation processes may be understood in terms of the Deck effect, in association with the direct diffractive production of resonances.

In all inelastic diffraction dissociation reactions a large enhancement of the cross-section is observed, when the mass of the diffractively produced system is near its threshold value, and less than that of the lowest mass resonance observed in formation experiments. This can be immediately understood in terms of the kinematic effects of the Deck model, discussed in section 4.3. Enhancements are also observed when the mass is greater and, if the selection $\cos \theta_t < 0$ is made on the data to suppress the pion Deck amplitude, are considerably more pronounced. This effect is seen in fig.4.3, from ref.(75), for the $\pi^- p \to \pi^- (n\pi^+)$ and $pp \to p (n\pi^+)$ reactions; the peaks in the cross section may clearly be interpreted as due to the direct diffractive production of the N(1470), N(1520) and N(1690) resonances. Resonance effects are also seen in fig.4.4 (from ref.(66)), where selections on t_{CA} are made on the (πN) mass distributions of the 16 GeV diffractive $\pi N \to \pi (\pi N)$ reaction. The low mass enhancement dominates when t_{CA} is small, but at larger t_{CA}, when the contribution to the amplitude from the Deck mechanism becomes less important, the mass spectrum peaks in the region of the N(1470), N(1520) and N(1690) resonances. The solid curves in fig.4.4. are a fit made by the authors of ref.(66) to their data using an incoherent sum of the Deck amplitude with the amplitude for the diffractive production of N(1520) and N(1690) resonances. The most general production and decay mechanism of a spin J nucleon resonance in the $\pi N \to \pi (\pi N)$ reaction leads to angular distributions of the outgoing πN system of the form:-

$$\frac{d\sigma}{d\theta_t} \propto \sum_{n=0}^{n=J-\frac{1}{2}} a_n \cos 2n\theta_t \qquad (4.30)$$

$$\frac{d\sigma}{d\phi_t} \propto \sum_{n=0}^{n=J-\frac{1}{2}} b_n \cos 2n\phi_t \qquad (4.31)$$

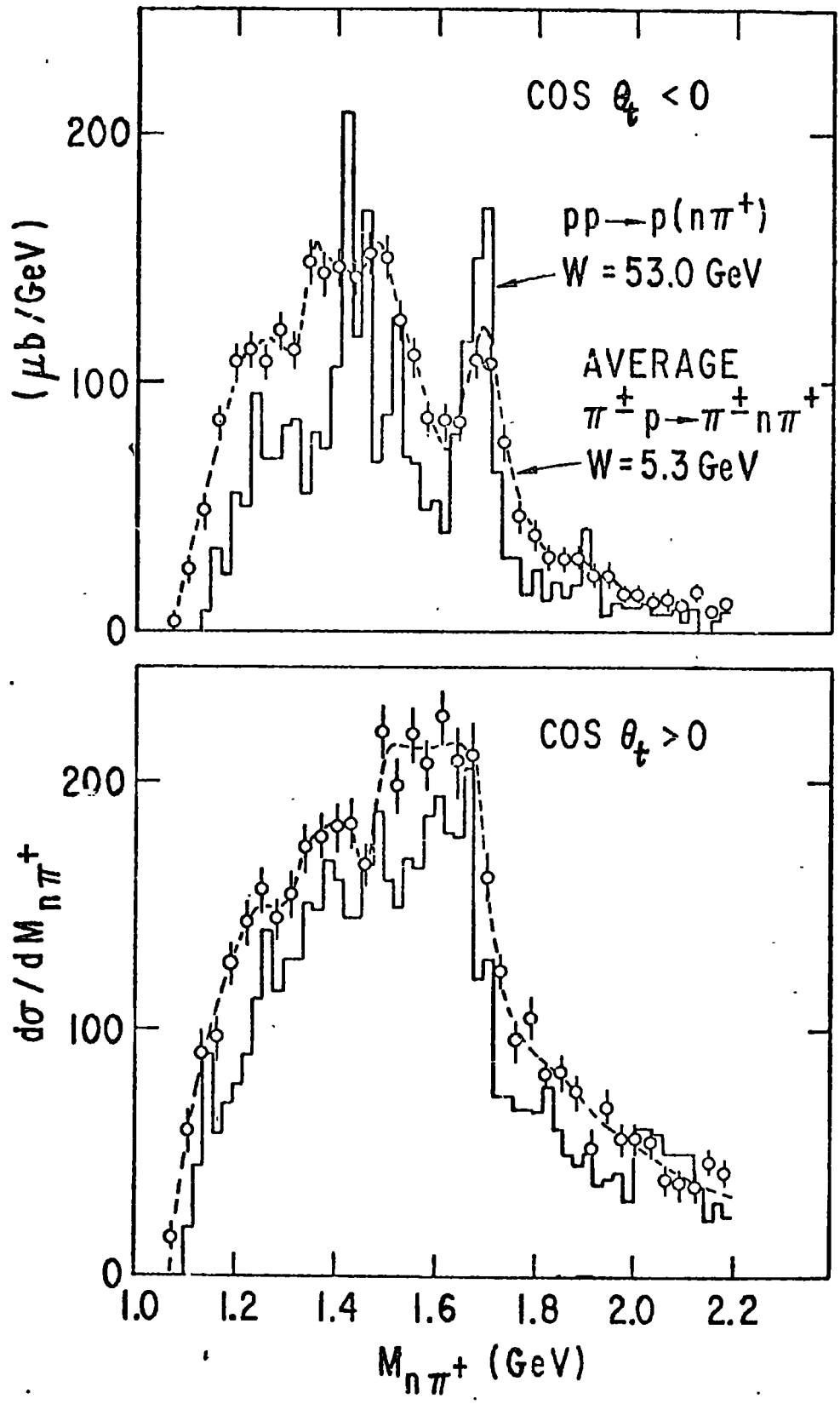

Fig.4.3. (From ref.(75)). Mass distributions of the diffractively produced $(n\pi^+)$ System in 53GeV $pp \rightarrow p(n\pi^+)$ (histogram) and in 5.3 GeV $\pi^\pm p \rightarrow \pi^\pm (n\pi^+)$. Resonance peaks, more pronounced for $\cos\theta_t < 0$, are visible.

These distributions are symmetric about $\theta = \frac{\pi}{2}$ and $\phi = \frac{\pi}{2}$, thus, as we shall see below, resonance production cannot be the only process occurring in the diffractive production of high mass π N systems.

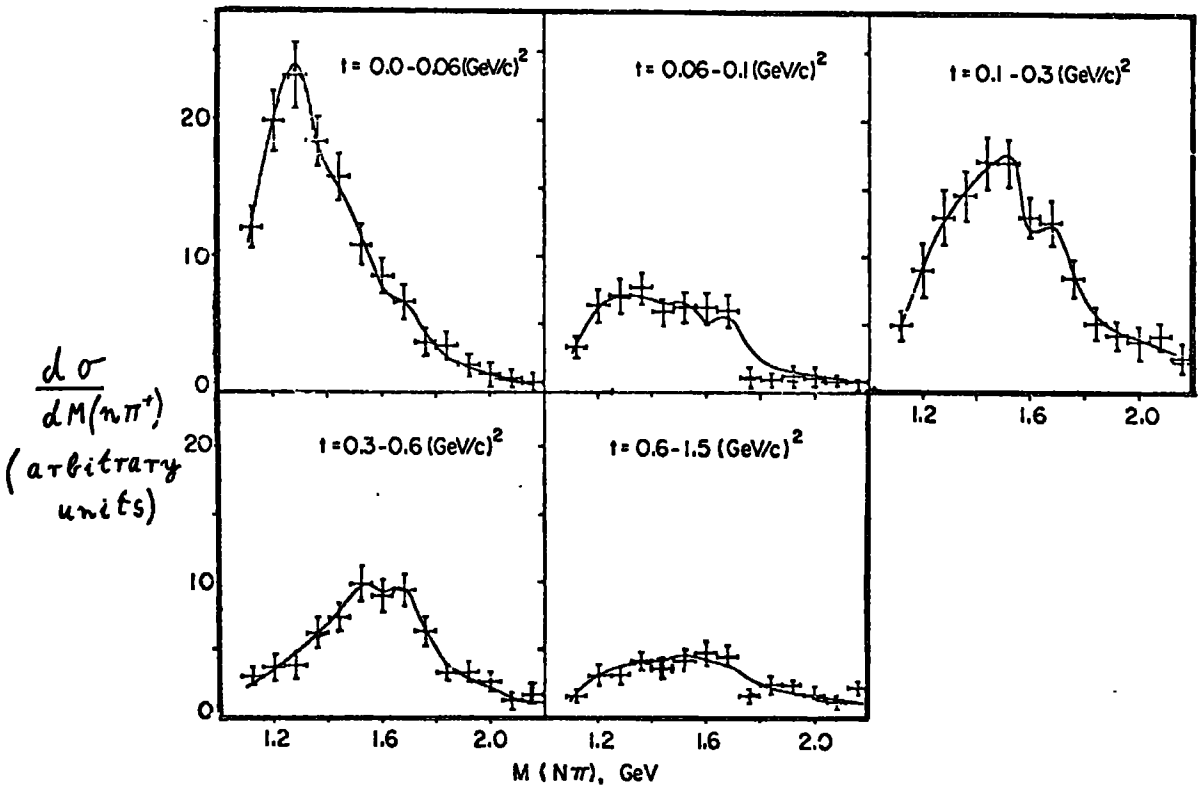

Fig.4.4. Mass distributions of the diffractively produced $n\pi^+$ system in 16 GeV $\pi^- p \to \pi^-(\pi^+ n)$, for different intervals of t_{CA}. (from ref.(66)) The solid curves are a fit to the data, made in ref.(66), using an incoherent sum of pion Deck plus resonance production amplitudes.

We now consider data on the angular distributions of diffractively produced pion-nucleon systems.

We examine the distributions $\frac{d\sigma}{d(\cos\theta_t)}$ and $\frac{d\sigma}{d\phi_t}$ of the diffractively produced pion-nucleon system in the 16 GeV $\pi N \to \pi\pi N$ reaction, in the t channel, for t_{CA} both less than and greater than -0.06 GeV^2. We consider the distributions in five mass bins, as shown in figs.4.5, 4.6 (taken from ref.66) where the cross sections for the diffractive production of a $\pi^+ n$ system in the $\pi^- p \to \pi^-\pi^+ n$ reaction are plotted[+]. The solid lines are our fits and predictions, discussed in the next chapter.

Consider the data in the resonance region. The most notable feature is the large peak in $\frac{d\sigma}{d(\cos\theta_t)}$, present for $|t_{CA}| > 0.06$ GeV^2 but almost absent for $|t_{CA}| < 0.06$ GeV^2. This combined with a $\frac{d\sigma}{d\phi_t}$ distribution which rises to a maximum around $\phi_t = \pi$, is a clear indication of the pion exchange Deck effect. However, the peaks at $\cos\theta_t = -1$, as well as the size of the cross-section near $\phi_t = 0$) cannot be reproduced by this alone; the obvious interpretation is that resonance production and decay is also occurring.

The situation is less clear in the lower mass region. Peaks in $\frac{d\sigma}{d(\cos\theta_t)}$ at $\cos\theta_t = 1$ are still present in the $t > 0.06$ GeV^2 data, but are less pronounced, as is expected from the kinematic properties of the pion exchange Deck amplitude. Peaks in $\frac{d\sigma}{d\phi_t}$ at $\phi_t = \pi$ confirm the presence of this amplitude. The peaks in $\frac{d\sigma}{d(\cos\theta_t)}$ at $\cos\theta_t = -1$ indicate the presence of nucleon exchange Deck amplitude, however this cannot be very large as there are no peaks in $\frac{d\sigma}{d\phi_t}$ at $\phi_t = 0$.

Similar considerations have been applied to the $NN \to N(\pi N)$ reaction by the Fermilab-Northwestern-Rochester-SLAC collaboration,(76) who estimated that about equal amounts of pion and nucleon exchange were present in the amplitude near the threshold for (πN) production. Another strong indication of the

---

[+]The diffractive part of the $\pi^- p \to \pi^-\pi^+ n$ reaction is extracted from data on the general $\pi N \to \pi\pi N$ reaction by means of an isospin analysis, as discussed in the previous chapter.

presence of both these exchange mechanisms is obtained from a study of cross-over systematics carried out by the Aachan-Berlin-Bonn-CERN-Heidelberg collaboration, for the diffractive production of low mass $\pi^- \Delta^{++}$ systems in the $\pi^{\pm} p \to \pi^{\pm}\pi^-\Delta^{++}$ reactions (77). Their arguments are as follows.

Suppose the diffractive $\pi^{\pm} p \to \pi^{\pm}\pi^-\Delta^{++}$ amplitude is dominated by both pion and Δ Deck exchange amplitudes.

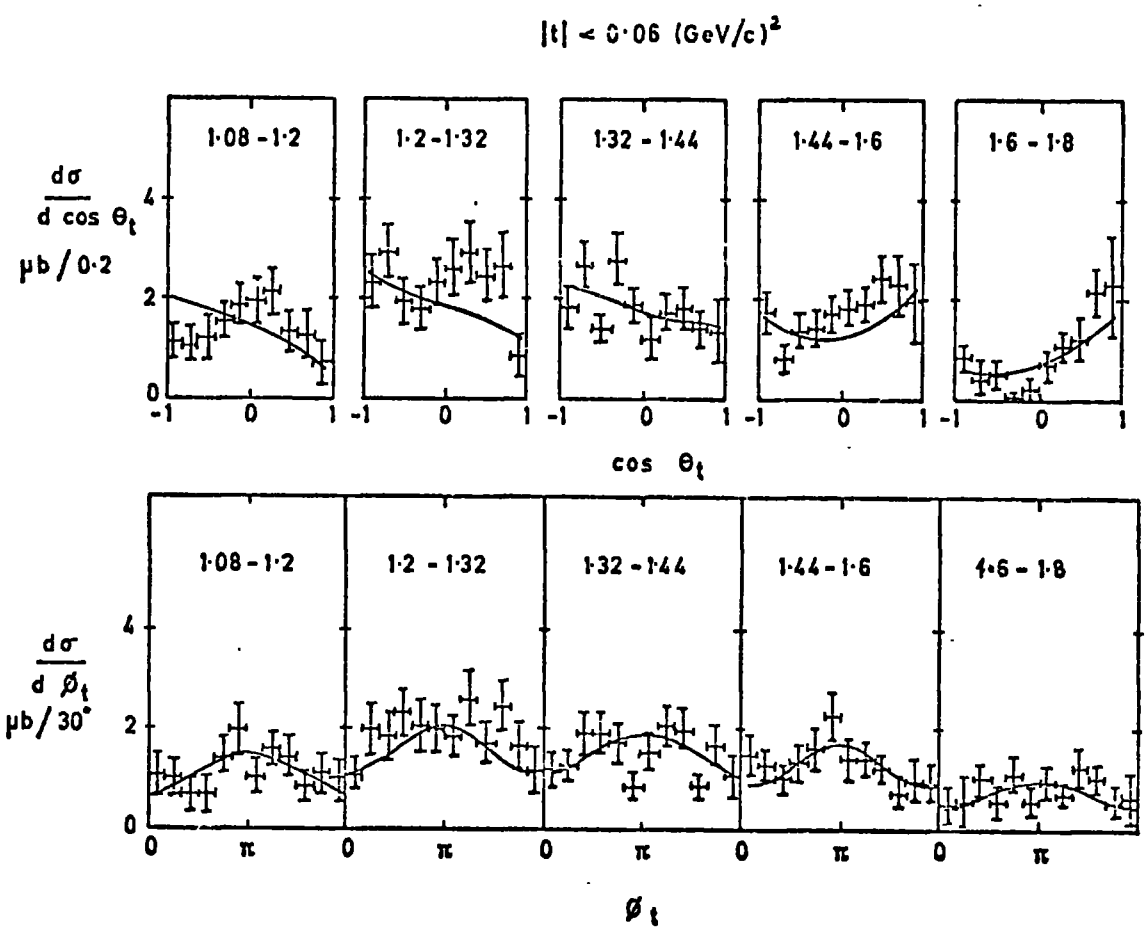

Fig.4.5. t-channel angular distributions of the diffractively produced $\pi^+ n$ system in the $\pi^- p \to \pi^- \pi^+ n$ reaction, for different intervals of $\pi^+ n$ mass (GeV/c^2) and with $|t_{CA}| < 0.06$ $(GeV)^2$. The data is from ref.(66) and the solid curves are the fits (of chapter 5) for $\pi^+ n$ mass > 1.2 GeV/c^2 and predictions for $\pi^+ n$ mass < 1.2 GeV/c^2.

We would then expect the $0 < \phi_s < \frac{\pi}{2}$ region of phase space[+] to be dominated by Δ^{++} exchange, and the $\frac{\pi}{2} < \phi_s < \pi$ region to be dominated by π^- exchange. The $\pi^+ \Delta^{++}$ channel is exotic, and so we expect, for $0 < \phi_s < \frac{\pi}{2}$, the slope of the differential cross section of the π^+ induced process, $\frac{d\sigma^+}{dt}$, to be less than that of the π^- induced process, and for $\frac{d\sigma^+}{dt}$ $(t = 0)$ to be less than $\frac{d\sigma^-}{dt}$ $(t = 0)$. Likewise, for $\frac{\pi}{2} < \phi_s < \pi$, when the amplitude will contain the pion-pion scattering sub-process, with the $\pi^- \pi^-$ channel exotic, we expect $\frac{d\sigma^+}{dt}(0) > \frac{d\sigma^-}{dt}(0)$ and that the slope of the former

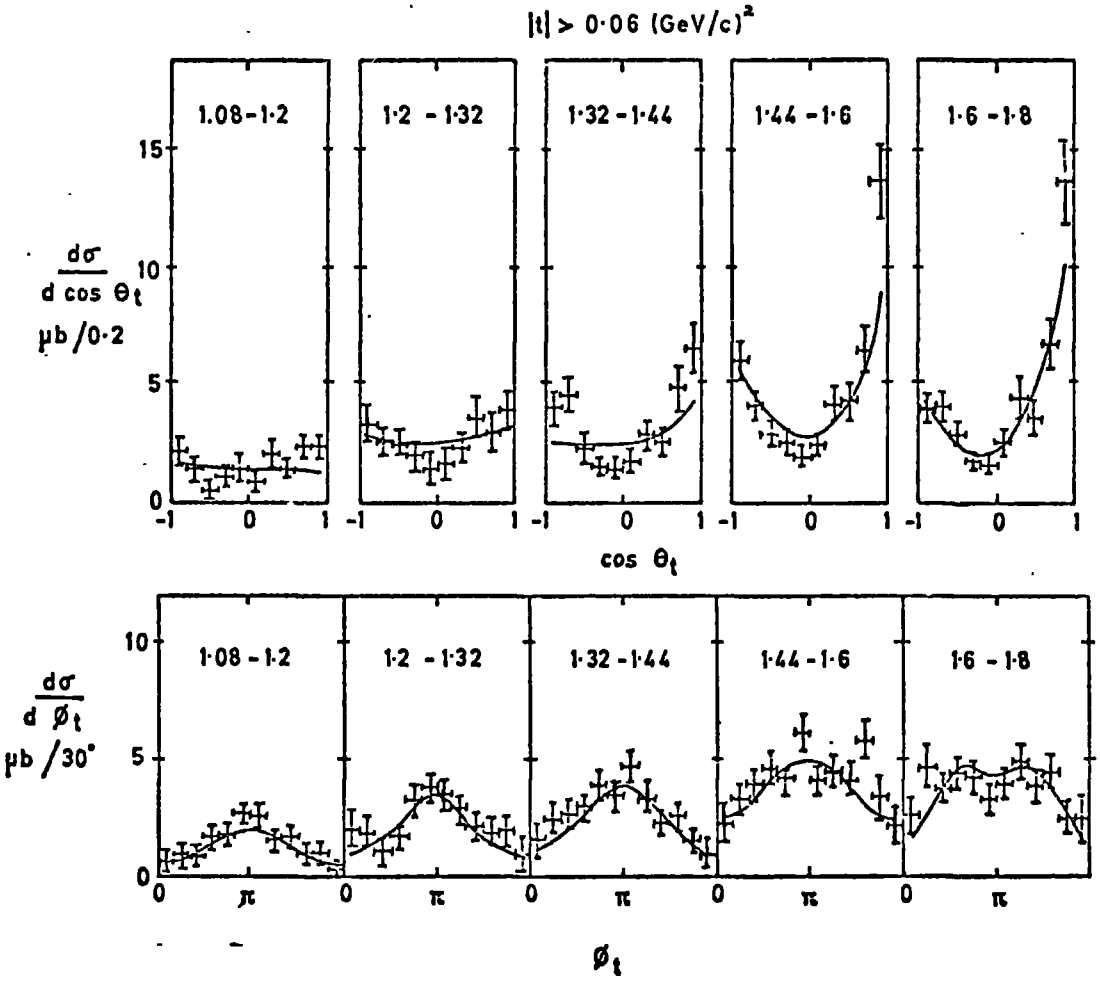

Fig.4.6. As fig.4.5, but with $|t_{CA}| > 0.06$ (GeV/c)^2.

[+]We use our definition of ϕ, which differs by π from that in ref.(77)

will now be greater. Thus cross-overs may be expected in plots of these distributions. These predictions are nicely confirmed by the experimental results, as shown in fig.4.7 (from ref.77); indeed the cross-overs even appear to occur at values of 't' close to those at which cross-overs are seen in real $\pi\pi$ and πp scattering. It would be interesting to check that the same cross-overs are observed when the appropriate selection on θ, instead of ϕ, is made.

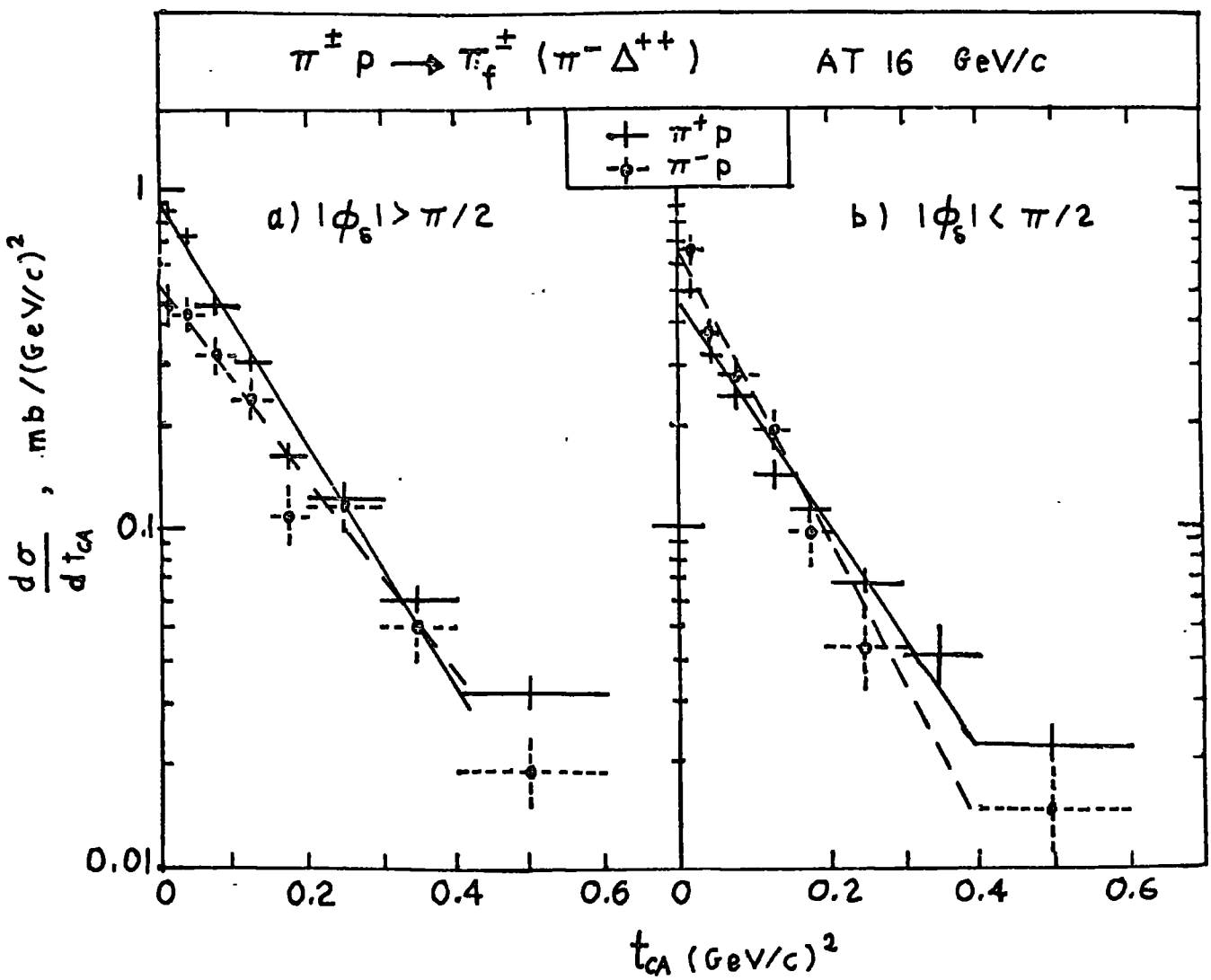

Fig.4.7. t distributions of the diffractively produced $\pi^- \Delta^{++}$ system in 16 GeV/c $\pi^{\pm} p \rightarrow \pi^{\pm} (\pi^- \Delta^{++})$ for ϕ_s both greater and less than $\frac{\pi}{2}$, showing the change in the sign of the crossover. (from ref.(77)).

It is likely that these ideas are also capable of resolving the problem of the crossover in diffractive Q ($K^*\pi$) production, which has cast doubt on the Deck model in the past. In the beam diffraction dissociation reactions $\bar{K}^0 p \to (K^{*-}\pi^+)p$ and $K^0 p \to (K^{*+}\pi^-)p$ the cross-over of $\frac{d\sigma}{dt}$, for data integrated over azimuthal angle, is found to be in the opposite direction to that expected if the pion exchange Deck amplitude dominates.(78, 79). However if, as we now suspect, K* exchange is present also, it is necessary to consider separately the data corresponding to two different regions of ϕ, and we may then find that in fact the model and the data are in agreement. An alternative but more artificial solution to the Q problem has been proposed in ref.(80), where the B - ω exchange diagram is enlisted to cancel the effects of the pion exchange Deck diagram and so reverse the sign of the cross-over (for all azimuthal angles). It seems rather unlikely that this diagram will give a large enough contribution, with the correct phase, but it may well be present in addition to the K* exchange. The final choice between these two ideas lies in a re-analysis of the experimental data, so that $\frac{d\sigma}{dt}$ may be plotted in the two regions $\phi < \frac{\pi}{2}$ and $\phi > \frac{\pi}{2}$.

A problem arises with the Deck model when we consider the cross section for the production of a low mass diffractive system, as a function of t_{CA}. The data of ref.(66) shows that the cross-section for the diffractive production of a low mass pion-nucleon system is particularly large for $|t_{CA}| < 0.06$ GeV^2 and falls rapidly as $|t_{CA}|$ increases, but only slowly for $|t_{CA}| > 0.3$ GeV^2. In fig.4.8 (from ref.(75)) we show the relation between the mass of the diffractively produced system and the slope, b, (writing $\frac{d\sigma(t)}{dt} = \frac{d\sigma(o)}{dt} e^{bt}$) for the $\pi p \to (3\pi)p$ and $pp \to (p\pi^-)p$ reactions, and observe a rapid change of slope with mass. This 'mass-slope correlation' cannot be explained simply by the Deck enhancement of the t_{CA} dependence (81, 82) and may be partly due to peripherality of the inelastic diffraction dissociation process in impact parameter space. As discussed in ref.(83) a target proton which appears as a ring in impact parameter space will give rise to a sharp decrease in $\frac{d\sigma}{dt_{CA}}$ to a minimum at $t_{CA} \simeq -0.2$ GeV^2, in the

part of the (π N) production amplitude which conserves helicity in the s channel. This dip arises from the first zero of the Bessel function $J_o(R\sqrt{-t})$ (with R≈1 fermi) and can only be important for low mass π N systems, when the non-flip amplitude is large. Furthermore, this effect will be most important in the nucleon exchange part of the amplitude. We may see this by calculating $\frac{d\sigma}{d\phi_s}$ for low mass, small t_{CA} π N systems; the nucleon exchange Deck amplitude gives rise to a much less sharply peaked distribution than the pion exchange amplitude and thus has a larger non-flip component.

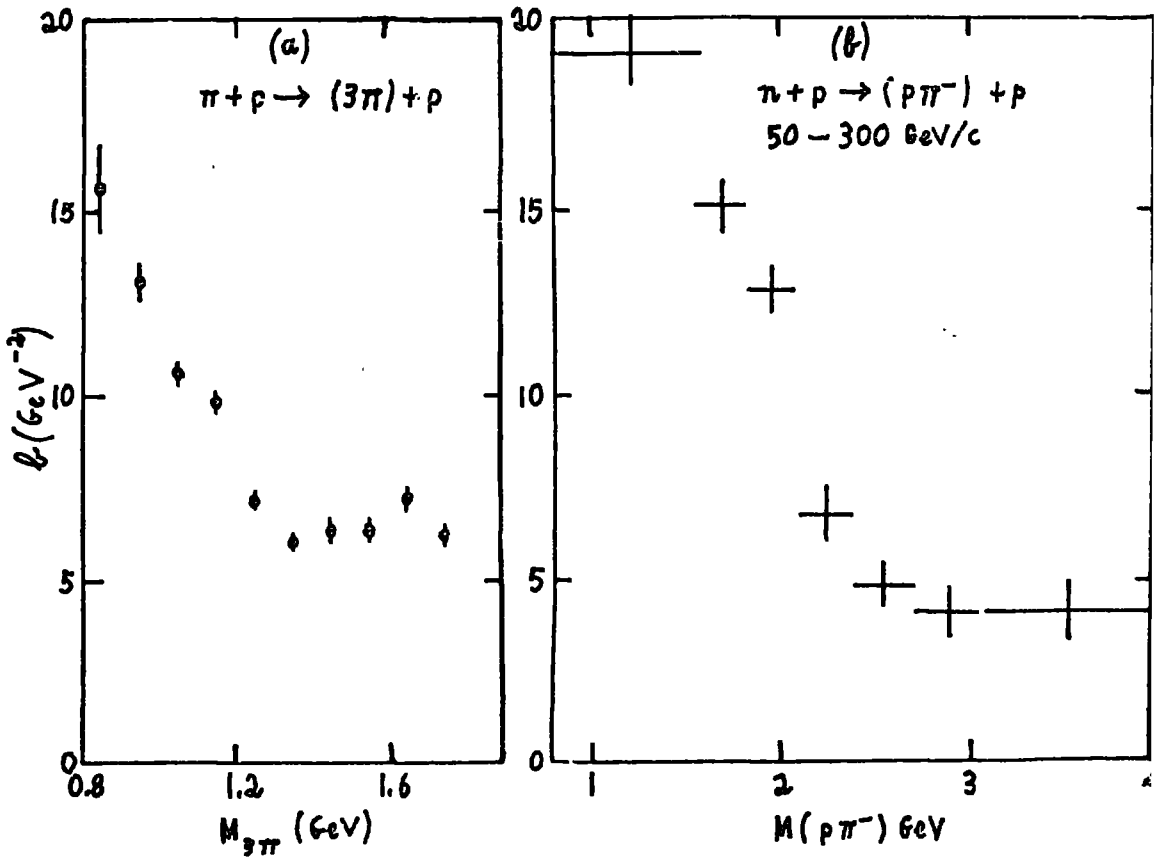

Fig.4.8. Mass-slope correlation for the diffractive reactions: (a) π P → $(3\pi)_p$ in the 5-20 GeV/c momentum range and (b) np → $(p\pi^-)p$ at 50 - 300 GeV/c. (From ref. (75)).

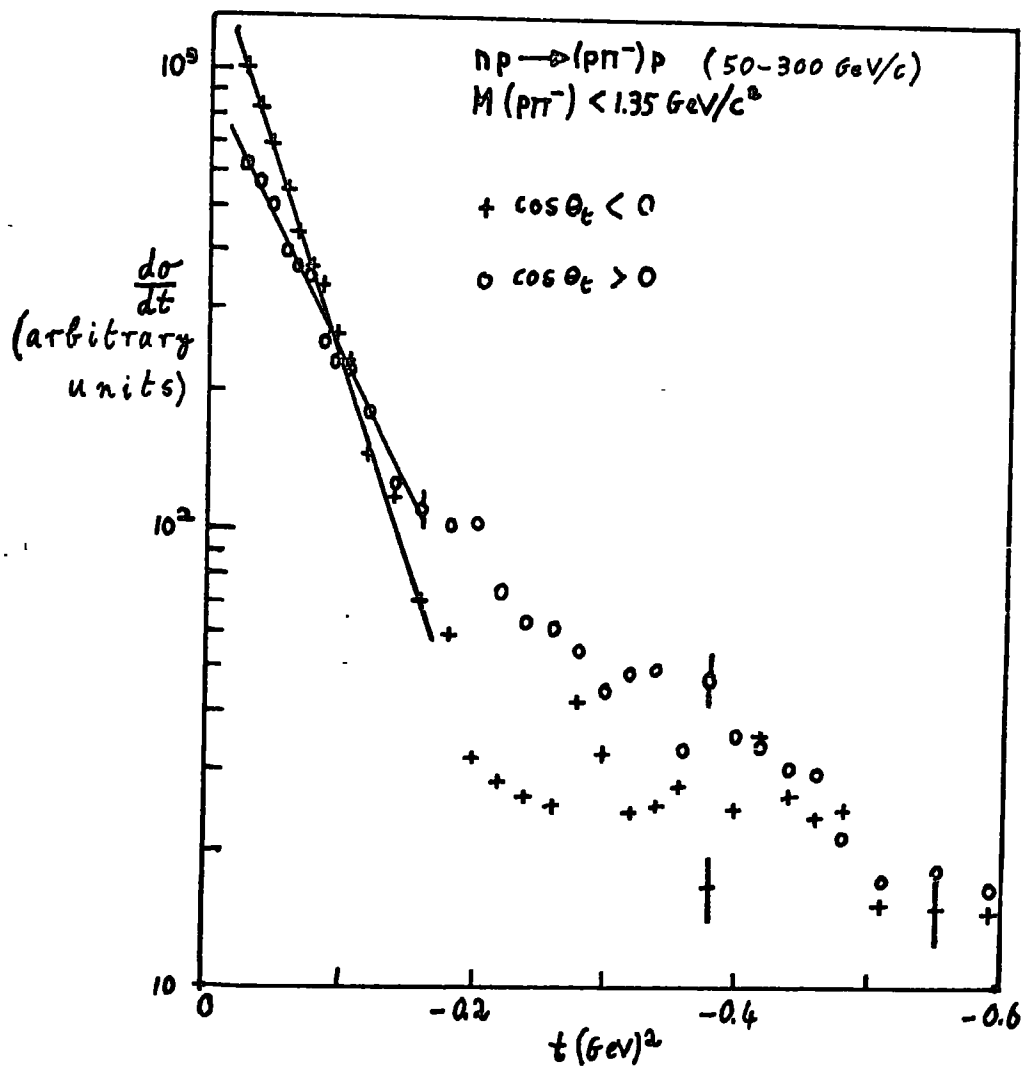

Fig.4.9. Differential cross-sections for the process np → $(p\pi^-)p$ for $\cos\theta_t > 0$ and $\cos\theta_t < 0$. (from ref. (83)).

This idea is supported if a selection is made on θ_t when studying $d\sigma/dt$, so as to separate the pion and nucleon Deck exchange contributions. In Fig.4.9 (from ref.(83)) it is seen that $d\sigma/dt$ falls more steeply with t_{CA} for the nucleon Deck amplitude (which dominates when $\cos\theta_t < 0$) than for the pion Deck amplitude, (which dominates when $\cos\theta_t > 0$); the simple Deck model predicts the opposite effect, as is seen from eqs.4.26, 4.27. This suggests, that absorption of the nucleon Deck amplitude is important and leads to an enhanced t_{CA} dependence of $d\sigma/dt_{CA}$, when the mass of the produced pion-nucleon system is low. Berger and Pirila (84) have carried out a detailed study of absorptive effects in nucleon diffraction dissociation, and obtained predictions in agreement with experiment.

When the mass of the diffractively produced system is great enough, resonance production will lead to a flattening of the slope of $d\sigma/dt$; this effect contributes to the comparitively large cross section for producing high mass ($N\pi$) systems at large t, seen in fig.4.4.

A good qualitative understanding of inelastic nucleon diffraction dissociation has thus been obtained, in terms of the pion and baryon Deck exchange mechanisms with the direct diffractive production of resonances. In the next chapter we present a simple quantitative model based on these ideas, to describe the angular distribution data of ref.(66).

5: A RESONANCE-DECK INTERFERENCE MODEL FOR $\pi N \to \pi\pi N$ DIFFRACTIVE SCATTERING

5.1: The Model

In this chapter, angular distributions of the pion-nucleon system produced in the diffractive $\pi N \to \pi(\pi N)$ reaction at 16 GeV/c (66) are interpreted quantitatively in terms of a simple model. Taking full account of spins and interference, we take the amplitude, for the production of a pion-nucleon system of mass in the resonance region, as a coherent sum of pion exchange Deck amplitude with the amplitude for production and decay of the dominant isospin $\frac{1}{2}$ nucleon resonances. We take these [+] as the 1470 ($\frac{1}{2}^+$), 1520 ($\frac{3}{2}^-$) and 1690 ($\frac{5}{2}^+$), as suggested by Morrison's rule (85) and the spin-parity analysis of ref.(86). We calculate how the helicity states of the resonances are populated by taking the pomeron to couple as a spin one object, and test various models for the required three coupling constants. Duality gives a reason for neglecting baryon exchange and provides a counter to Fox's (87) argument that, were the pomeron like a photon, then the sum of the three possible diffraction dissociation amplitudes would equal zero, in the forward direction. Below the resonance region we take the diffractive amplitude as a coherent sum of pion and baryon exchange Deck amplitudes. We obtain a very good quantitative description of the data in the N* resonance region and, with a naive inclusion of absorptive effects, a good description in the low pion-nucleon mass region also. We obtain information on high energy $\pi^- \pi^+ \to \pi^- \pi^+$ scattering and our best description of the data is found using a parametrization of isospin zero exchange consistent with the results of chapter 2. The pomeron contribution to the $\pi^- \pi^+ \to \pi^- \pi^+$ cross section is found to be about 6 mb at energies of 3 - 5 GeV.

[+]We do not explicitly include the 1470 in our fits as its decay angular distributions are isotropic, and cannot be separated from those of the 1520.

Similar but less detailed Deck plus resonance models have been proposed elsewhere. Berlad et al.(73, 88) discuss qualitative features of the $\pi\pi N \to \pi(\pi N)$ reaction at 3.5 GeV in terms of such a model. The authors of ref.(66) interpret their data in a similar manner but do not consider angular distributions; neither studies takes into account spins or interference.

A detailed partial wave analysis of the pion Deck contribution to the $pp \to pn\pi^+$ reaction has been carried out by Uehara et al.(89) who also consider qualitatively the consequences of interference of the amplitude with six pion-nucleon resonances, on the assumption that t-channel helicity is conserved in their production. Ansorge et al.(90) fit the moments of the pion-proton angular distribution for the $np \to pp\pi$ reaction, at 9-24 GeV/c, by decomposing the pion exchange Deck amplitude into partial waves and adding in five resonances. A reasonable description of the data is obtained with the inclusion of resonances violating Morrison's rule, and approximate t channel helicity conservation is found to be obeyed. No attempt is made to explain t distributions or to include baryon exchange amplitudes.

Ochs et al.(91) have presented a qualitative interpretation of the momentum distributions in 14 GeV diffractive $\pi p \to \pi(N\pi)$ and $\pi p \to \pi(\pi\Delta)$ reactions, in terms of pion and baryon exchange in addition to resonance production. Spin effects are neglected, and interference is only included in a very crude manner. Evidence is found for pion and baryon exchange in about equal amounts, in addition to a background attributed to resonance production and decay.

5.2: The Deck and resonance production amplitudes

First consider the pion exchange Deck amplitude (fig.1.3a). We write for this:-

$$A_{\nu\mu}(\pi) = A_t^0(\pi\pi)(\sqrt{2}g)\, s^{(-0.02-t_{EB})} \cdot \frac{\bar{u}_\nu(n)\gamma_5 u_\mu(p)}{t_{EB} - m_\pi^2} \qquad (5.1)$$

$g^2/4\pi = 14.6$, and the Dirac spinors are normalised as in appendix 4A. We calculate the isospin zero exchange $\pi^-\pi^+ \to \pi^-\pi^+$ amplitude, $A_t^0(\pi\pi)$ as if it were on

shell, and parametrize it in terms of pomeron and f exchange:-

$$A^{0}_{t}(\pi\pi) = \frac{32\pi}{\sqrt{2}}\Big[A_p S_{CD} e^{b_p t_{CA}} . i . e^{\frac{i\pi}{2}\alpha'_p t_{CA}} - \frac{1}{2}\Big(1 + e^{-i\pi\alpha_f(t_{CA})}\Big)\Big(a + b\, t_{CA}\Big) S_{CD}^{\alpha_f(t_{CA})}\Big] \qquad (5.2)$$

with $\alpha_f(t) = 0.5 + 0.9t$ and $\alpha'_p = 0.22\ \text{GeV}^{-2}$. The 32π factor converts the normalization of chapter 2 to that of appendix 1, and the $1/\sqrt{2}$ arises because the outgoing pions are distinguished (see eq.(1.19)). We take, consistent with the results of chapter 2, $0.1 < A_p < 0.3$ ($4\text{mb.} < \sigma_T(\pi^-\pi^+ \to \pi^-\pi^+) < 12\text{mb.}$) and $2.5 < b_p < 5.5\ \text{GeV}^{-2}$. As discussed in chapters 1 and 2, a FESR calculation of the asymptotic pion-pion scattering amplitudes from low energy phase shift data relates the pomeron and f residue functions at $t = 0$, A_p and a. We find $a \simeq 3(C - A_p)$ where $0.3 < C < 0.5$, within the uncertainties (largely those of the low energy isospin two amplitude) of the $\pi\pi$ phase shift data. The parameter b is chosen so that the f residue function has a zero at $t = -0.6\ \text{GeV}^2$, (as found in chapter 2) but in fact results are very insensitive to this parameter and are virtually unchanged if a zero at $t = -0.4\ \text{GeV}^2$ is taken.

In appendix 4B the coupling $\bar{u}_{\frac{1}{2}}(n)\gamma_5 u_{\frac{1}{2}}(p)$ is explicitly calculated and the other couplings are listed.

Consider next the nucleon exchange Deck amplitude. We write for this amplitude (fig.1.3b):-

$$A_{\nu\mu}(N) = G.A(\pi N).\sqrt{2}g.S_{DE}^{\alpha(t_{DB})} e^{-\frac{i\pi}{2}\left(\alpha(t_{DB})-\frac{1}{2}\right)} . \frac{\bar{u}_\nu(N)\gamma_5 u_\mu(p)}{\not{k}_\pi - \not{k}_p - m_N} \qquad (5.3)$$

where $\alpha(t) = -0.35 + 0.85t$. We take the off shell $\pi^- n \to \pi^- n$ scattering amplitude $A(\pi N)$ as equal to the on shell $\pi^+ p \to \pi^+ p$ amplitude. We use the parametrization for this from the data fit of ref.(62) where it is assumed that the pomeron -N-N coupling is scalar.

We argue that, because of duality, we cannot include simultaneously this amplitude and the resonance production

amplitude in the N*resonance region. As discussed in chapter 4, there is considerable evidence that resonance production does take place, and so we should only need the nucleon exchange amplitude when the pion-nucleon mass is low. We can, however, test semi-local duality by using the nucleon exchange amplitude instead of the resonanceproduction amplitude in the higher pion-nucleon mass region; we mention the results of attempting this in the next section.

It is not clear how nucleon exchange should be parametrized when the pion-nucleon sub-energy is very low. We find that contributions from the amplitude are only large when $t_{DB} > 0$, near the nucleon pole, and so it makes little difference whether we use the above simple pole description or a more sophisticated parametrization including nonsense wrong-signature zeros. The inclusion of the Regge phase is arguable, but slightly improves the data fits. In appendix 4C we show how to evaluate the various helicity amplitudes of eq.(5.3), and list them.

In the kinematic regions of the $\pi^- p \to \pi^- \pi^+ n$ reaction which concern us, both S_{CD} and S_{CE} lie principally in the region of 12-30 GeV^2, and so both pion-pion and pion-nucleon scattering sub-processes should be well described by Regge parametrizations.

We assume that, in addition to the pion-exchange Deck effect, direct excitation of the $N^{1+}_{\frac{1}{2}}(1470)$ and $N^{3-}_{\frac{1}{2}}(1520)$ resonances takes place in the $1.44 < M_{\pi N} < 1.6$ GeV mass region, and of the $N^{5+}_{\frac{1}{2}}(1690)$ in the $1.6 < M_{\pi N} < 1.8$ GeV mass region (fig.1.3c).

We need to calculate how the N* helicity states are populated, and thus require a model for the pomeron-N-N* coupling. If we assume that the pomeron if 'f dominated' and so couples like the f meson, and that the f and ω are exchange degenerate we would expect the pomeron to couple like the ω meson. The ω couples like the isoscalar part of the photon, thus the pomeron may also couple in this manner (92). This is the motivation for our assumption that we may take the most general coupling of the pomeron to be vector. The coupling for the excitation of a spin J, helicity λ

resonance is then of the form:-

$$T^{J}_{\lambda\mu} \propto \bar{u}^{J\lambda}_{\alpha_1\alpha_2\ldots\alpha_{J-\frac{1}{2}}} \left(g_1 P_{\alpha_1} P_{\alpha_2} \ldots P_{\beta} + g_2 \gamma_{\beta} P_{\alpha_1} P_{\alpha_2} \ldots P_{\alpha_{J-\frac{1}{2}}} + g_3 g_{\alpha_1\beta} P_{\alpha_2} \ldots P_{\alpha_{J-\frac{1}{2}}} \right) u_{\mu} Q^{\beta} \qquad (5.4)$$

$\bar{u}^{J\lambda}_{\alpha_1\alpha_2\ldots\alpha_{J-\frac{1}{2}}}$ is the Rarita-Schwinger spinor for a spin J fermion of helicity λ , $P = \frac{1}{2}(P_B+P_{N^*})$, $Q = \frac{1}{2}(P_A+P_C)$. We work in the DE centre of mass with the t channel coordinate system; for an incoming proton of helicity $+\frac{1}{2}$, N* states of spin projection $+\frac{1}{2}$ are populated by g_1, of $\pm\frac{1}{2}$ by g_2, and of $\pm\frac{1}{2}$ and $+\frac{3}{2}$ by g_3. We outline, in more detail, this formalism for spin $\frac{3}{2}$ and spin $\frac{5}{2}$ particles in appendix 4D and show explicitly how to calculate the helicity amplitudes $T^{J}_{\lambda\mu}$. These t-channel helicity amplitudes vanish if $|\lambda| - |\mu| > 1$.

For a nucleon resonance of spin J and helicity λ the amplitudes $A_{\nu\lambda}$ for decay to a pion and a nucleon of helicity ν can be calculated as a function of the centre of mass angles and N* mass in terms of one coupling, as we show in appendix 4E. We write for the full resonance excitation and decay amplitude:-

$$A_{\nu\mu}(res) = \sum_{\lambda} A_{\nu\lambda}\, T^{J}_{\lambda\mu} \sqrt{A_P}\, S_{AB}\, e^{\frac{i\pi}{2}\alpha'_P t_{CA}} \cdot \frac{i}{M^2_{N^*} - S_{DE} - iM_{N^*}\Gamma} \qquad (5.5)$$

$\alpha'_P = 0.22\ \text{GeV}^{-2}$ and Γ , the total N* width, is taken as 140 MeV for both N(1520) and N(1690). All normalization constants, including the $N^* \to \pi N$ width, are absorbed in the pomeron-N-N* couplings of eq.(5.4). The N(1470) has isotropic decay angular distributions and so its contribution to these distributions cannot be separated from that of the N(1520); we thus do not include the N(1470) in our fits.

There are several models for the N* couplings, which we test. T-channel helicity conservation (a scalar pomeron) would imply simply that $g_2=g_3=0$. If, on the other hand, the pomeron couples like the isoscalar part of the photon, we would expect the preference for helicity $\frac{3}{2}$ $N^* \to \gamma N$ decay,

over helicity $\frac{1}{2}$ state decay (93) to be preserved in diffractive production. Now the couplings calculated in appendix 4D are precisely those for the decay $N^* \to \gamma N$, if we replace the 4-vector Q by the photon polarization vector ε. The $T_{\frac{1}{2}\frac{1}{2}}$ amplitude then vanishes, and we have the requirement for the other helicity $\frac{1}{2}$ amplitude, $T_{\frac{1}{2}-\frac{1}{2}}$ to vanish, from eq.(4D 19)

$$g_3 = \frac{g_2 |\underline{P}_N|^2}{E_N + m_N} = g_2 (E_N - m_N) \tag{5.6}$$

In the N* centre of mass, $E_N = \frac{1}{2m_N^*}(m_N^{*2} + m_N^2)$ for photo-decay, and so:-

$$g_3 = \frac{g_2}{2m_N^*} (m_N^* - m_N)^2 \tag{5.7}$$

which gives $g_3 = 0.11 g_2$ for the N(1520) and $g_3 = 0.17 g_2$ for the N(1690). Of course, as the couplings in this model have been continued in mass and spin from m=0, J=1 to the Regge region, it is not obvious that either the coupling relationship eq.(5.7) or the conserved nature of the current will be preserved. However, it is in any case interesting to see if the couplings g_2 and g_3 are required at all. Another suggestion arises from a quark model approach, see eg.ref.(94), which predicts s channel helicity conservation at the pomeron $N\bar{N}$ vertex, or in general $g_1 = 0$. We also test this possibility in our fits to the data.

In this resonance region we argue, by duality, that the nucleon exchange amplitude is automatically included with the resonance production amplitude. The pion exchange amplitude, which is mainly real, must however be included in addition.

5.3: Description of data by model

In the N(1520) and N(1690) regions, where we consider pion Deck with resonance production mechanisms, we take:-

$$\frac{d\sigma}{d\Omega\, dt_{cA}\, dm_{BD}} = \frac{|P_D|}{(32\pi^2 P_{LAB} m_B)^2} \times \left| \sum_{\mu=\pm\frac{1}{2}} \sum_{\nu=\pm\frac{1}{2}} \left[A_{\nu\mu}(\pi) + A_{\nu\mu}(res) \right] \right|^2 \tag{5.8}$$

and when the mass of the pion-nucleon system is lower, we replace the resonance production amplitude $A_{\nu\mu}(res)$ by the nucleon exchange Deck amplitude $A_{\nu\mu}(N)$. (We show how to obtain the general expression for the differential cross section of a $2 \rightarrow 3$ scattering process in appendix 1B.) The sum over spin, with parity conservation, implies that in general the cross sections $d\sigma/d\phi$ must be symmetric about $\phi = \pi$, as is demonstrated in appendix 4E.

We calculate the differential cross sections in five

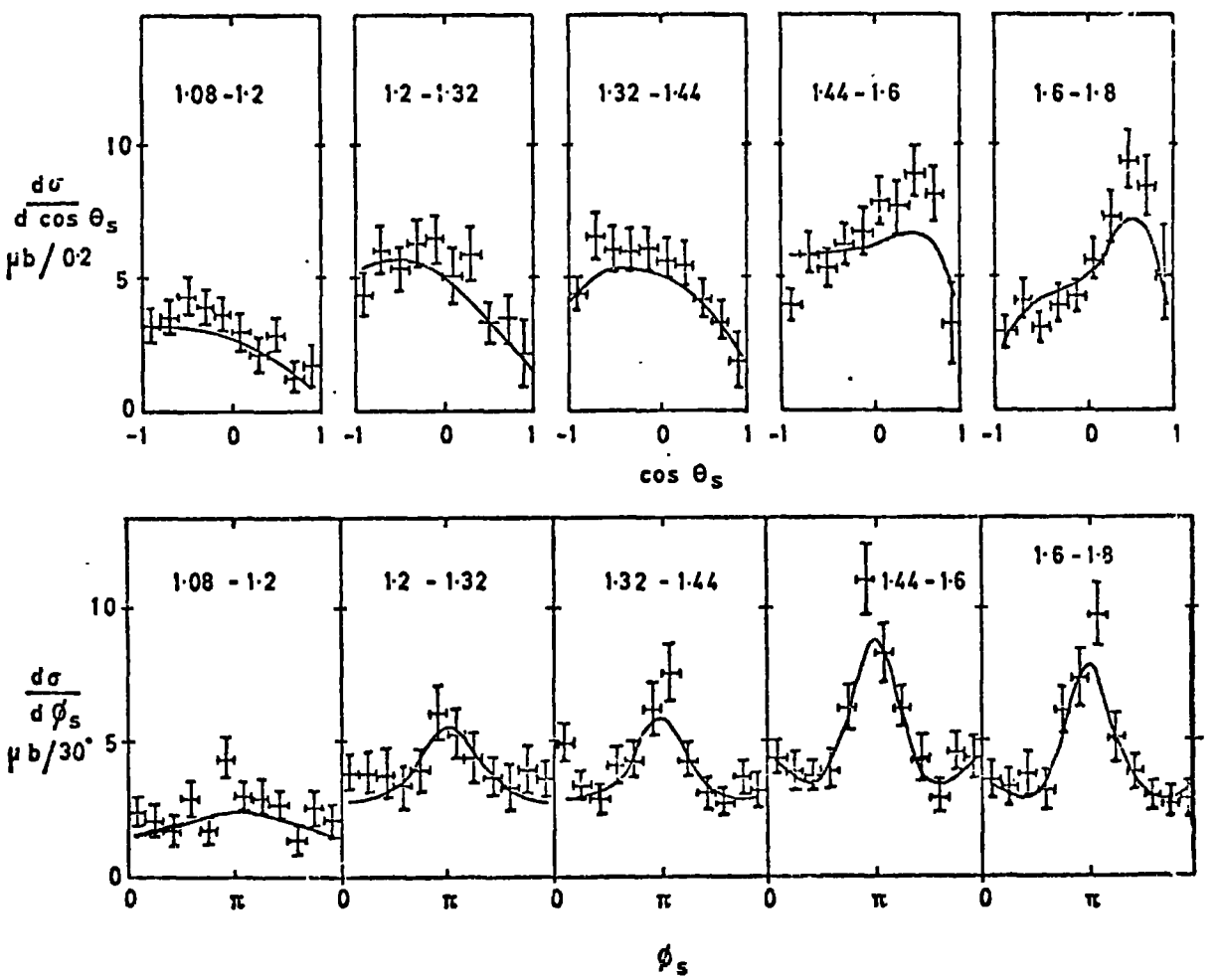

Fig.5.1. s-channel angular distributions of the diffractively produced $\pi^+ n$ system in the $\pi^- p \Rightarrow \pi^- \pi^+ n$ reaction for different intervals of ^+n mass. The data in from ref.(66) and the solid curves are the predictions of the model.

different regions of pion-nucleon mass between 1.08 and 1.8 GeV. In each region we evaluate eq.(5.8) at three values of S_{ED}, 12 values of ϕ (15^o to 345^o), 10 values of $\cos\theta$(-0.9 to +0.9) and 14 values of t_{CA} (6 values below -0.07 GeV^2, 8 values between -0.07 and -1.5 GeV^2), and integrate over all variables but one to obtain the appropriate angular distributions.

In each of the four mass regions between 1.2 and 1.8 GeV we fit simultaneously to the $\frac{d\sigma}{d(\cos\theta_t)}$ and $\frac{d\sigma}{d\phi_t}$ distributions, for t_{CA} both less than and greater than -0.06 GeV^2, by minimizing χ^2. We find the best set of pion-pion scattering parameters in the resonance region, and use these in the low pion-nucleon mass region. We then check our results by predicting the t channel angular distributions in the mass region 1.08-1.2 GeV, and the s channel angular distributions (integrated over t_{CA}) in all five mass regions.(To obtain the s channel angular distributions we simply transform each pair of s channel angles into the t channel, as described in chapter 4, and then calculate the amplitude as before, letting the s channel angles run over the values listed above)

In the N(1520) and N(1690) regions of the pion-nucleon mass spectrum, we obtain a good description of the data, as depicted in figs.4.5 and 4.6; all the qualitative features are reproduced. We do not, however, find sufficiently sharp peaks in $\frac{d\sigma}{d(\cos\theta_t)}$ near $\cos\theta_t=1$ for $t > 0.06$ GeV^2. [+] We show in fig.5.1 our prediction for the s channel angular distributions; again agreement with the data is good.

Interference effects are not large in this mass region, as the pion exchange amplitude predominantly flips the nucleon helicity and tends to populate the $\phi_t \simeq \pi$, $\cos\theta_t \simeq 1$ regions of phase space whereas the resonance production and decay amplitudes contain both flip and non-flip parts, and

---

[+]This is not simply a binning effect and could be due to an incomplete separation of non-diffractive amplitudes in the isospin analysis of ref.(66), resulting in a contamination of the data with some isospin 1 (ρ) exchange. This would increase the proportion of S_{CD} dependent data, and thus enhance the peak, as described in the previous chapter.

populate all phase space. Nevertheless, the fits are significantly improved by taking the interference effects into account.

In the N(1520) region, the three suggested models for the coupling constants give an equally good description and cannot be distinguished (the pion-pion scattering parameters determined simultaneously are also virtually unaffected by the choice of model). In the N(1690) region a good description cannot be obtained with t channel helicity conservation, and our best fit is obtained with all three couplings free, when we find $g_3/g_2=0.12$, compared with a photodecay value of 0.17 (eq.(5.7)). We can also obtain an acceptable description with the quark model prediction $g_1=0$. The pion-pion scattering parameters of eq.(5.2) which produce the best fit over the two mass regions are

$$\begin{aligned} A_p &= 0.16 \quad (\sigma_T(\pi^-\pi^+ \to \pi^-\pi^+) = 6.5\ mb) \\ b_p &= 3.9\ GeV^{-2} \\ a &= 0.87 \quad (C = 0.45) \end{aligned} \tag{5.9}$$

A reasonable description cannot be obtained with a pomeron corresponding to σ_T in the range 12-18 mb. The parameters of our fits are shown in table 5.1[+]. We also show in this table the results of fitting the data in this mass region using a sum of pion and nucleon exchange Deck amplitudes with no resonance contributions. Although a much poorer description of the data is obtained, results are sufficiently good to lend support to the idea that nucleon exchange is dual to resonance production. The best results are obtained with completely unabsorbed nucleon exchange and a pomeron corresponding to $\sigma_T(\pi\pi) \simeq 8$ mb.

[+]Two points which contribute large values to χ^2 are ignored in the values tabulated. The point at $\cos\theta_t=-0.3$, $t<0.06$ GeV^2 for $\frac{d\sigma}{d(\cos\theta\, t)}$ in the N(1690) region contributes ~ 50, and that at $\cos\theta_t=0.9$, $t>0.06$ for $\frac{d\sigma}{d(\cos\theta\, t)}$ in the N(1520) region contributes ~ 10.

We now consider the model applied to the low pion-nucleon mass kinematic region. We first attempt to describe the t channel angular distributions, in the two pion-nucleon mass bins lying between 1.2 and 1.44 GeV, in terms of a sum of pion and nucleon exchange Deck amplitudes. We fix the pion-pion scattering parameters at the values given by eq.(5.9)[+] and take G, of eq.(5.3), (which determines the size of the nucleon Deck contribution) as the only variable parameter, the same in both mass regions. We are unable to obtain a good description of the data.

As mentioned above, this may indicate the need for absorptive corrections. We may naively include absorption of the nucleon exchange amplitude, eq.(5.3), by multiplying this amplitude by the factor $(\alpha' + J_0 (R\sqrt{-t_{pB}}))/(1+\alpha')$, where α' is a free parameter and R is taken as $\simeq 1$ fermi. We find a considerably improved description, with $\alpha'=0$, although the $\frac{d\sigma}{d(\cos\theta_t)}$ distributions are still not correct.

We can make numerous other modifications to the amplitude but none of them lead to significantly improved descriptions of the data. A more thorough consideration of absorption including spin effects could possibly further improve results, but we do not attempt this here. The parameters of our fits are given in table 5.1. We show in figs.4.5 and 4.6 our best descriptions of the data, as well as a prediction of the t-channel angular distributions for the mass region 1.08-1.2 GeV and the s channel distributions for all three mass bins (in fig.5.1). The predictions agree well with the data, in general.

Interference between pion and nucleon exchange Deck amplitudes is large in this low pion-nucleon mass region, as the kinematic regions where each is important overlap considerably. Thus our results, indicating a fairly small nucleon Deck contribution, are not necessarily at variance with those of refs.(76, 91), where interference was not taken into account, and where the pion and nucleon Deck amplitudes were estimated to contribute about equally.

In fig.5.2 we show the $\frac{d\sigma}{dt_{CA}}$ distributions in four

---

[+]Again we do not obtain a good description if we use a larger pomeron coupling.

$\pi^+ n$ Mass (GeV)	Model	Resonance Couplings	σ_π	σ_{res}	σ_N	σ_{TOT}	σ_{TOT}(expt.)	χ^2/point
		$g_1 : g_2 : g_3$						
	π Deck quark (g_1=0)	0 : 11 : 1	32	28	-	58		1.23
	+ photo (g_2/g_3=9.0)	1.4 : 9 : 1	32	27	-	58		1.19
1.44 - 1.6	Resonances TCHC ($g_2=g_3$=0)	1 : 0 : 0	32	28	-	58	62	1.23
	π + N Deck	———	37	-	15	55.5		1.8
	π Deck all free	-4.1 : 8.3 : 1	23	24.5	-	49		1.0
	+ quark	0 : 3.3 : 1	23	24.5	-	49		1.3
1.6 - 1.8	Resonances TCHC	1 : 0 : 0	23	22	-	47	52.5	2.2
	π + N Deck	———	30	-	14	42.5		2.6
1.2 - 1.32	π + N Deck	———	31	-	8	45	48	1.0
1.32 - 1.44	π + N Deck	———	31	-	9	45	49	2.3

Table 5.1

Parameters of fits to the 16 GeV $\pi N \to \pi\pi N$ data. Cross sections, in microbarns, are for the production of a diffractive $\pi^+ n$ system in the $\pi^- p \to \pi^- \pi^+ n$ reaction, with mass in the given range. σ_π, σ_{res} and σ_N are the cross sections for the production by the π Deck, resonance excitation and N Deck mechanisms, taken separately. σ_{TOT} is the total cross section found in the fits, where interference is taken into account.

mass regions between 1.08 and 1.8 GeV, as determined by our model. In qualitative agreement with data, there is a strong mass-slope correlation, largely due to the increasing proportion of resonance excitation amplitude as the mass of the pion-nucleon system increases. We consistently predict rather smaller cross sections at large t_{CA} than are found in ref.(66); our model is probably too simple to describe this region correctly.

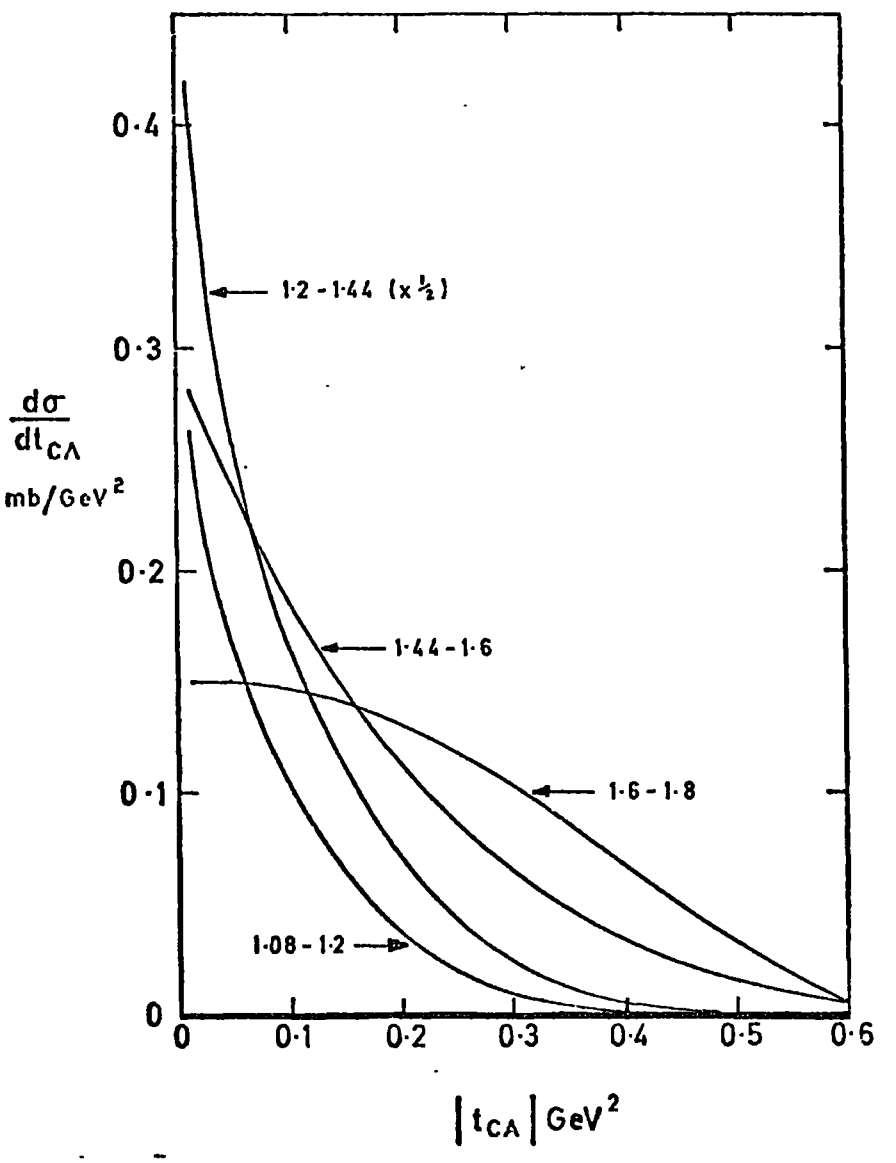

Fig.5.2. Momentum transfer distributions of the diffractively produced (π^+n) system in the $\pi^-p \to \pi^-\pi^+n$ reaction, as predicted by the model, for different intervals of (π^+n) mass (GeV/c^2).

5.4: Summary of results

In this chapter, we have shown that a good quantitative description of the angular distributions of the high mass pion-nucleon system, diffractively produced in the 16 GeV/c $\pi N \to \pi (\pi N)$ reaction, may be obtained from our model, which takes the amplitude as the pion exchange Deck amplitude coherently added to the amplitude for direct excitation of N(1520) and N(1690) resonances by a 'photon-like' pomeron exchange. The resonance couplings we obtain are consistent with simple quark model ideas or, for N(1520) production only, with t channel helicity conservation. However, results do not support t channel helicity conservation in N(1690) production, and the total amplitude for the production of high mass pion-nucleon systems strongly violates helicity conservation in both s and t channels. We also obtain information on the high-energy pion-pion scattering amplitudes, finding a description of the t channel isospin zero amplitude consistent with the results of chapter 2, and a pomeron contribution to the pion-pion scattering total cross-section of about 6 mb in the 3 - 5 GeV energy region. The use of the nucleon exchange amplitude instead of the resonance excitation amplitude in the high pion-nucleon mass region produces a reasonable description of the data, lending support to the idea of duality between nucleon exchange and resonance excitation. For the production of low mass pion-nucleon systems, our model of simple pion exchange Deck amplitude coherently added to nucleon exchange Deck amplitude does not reproduce the data well unless some attempt is made to include absorptive effects; this suggests that absorption may indeed be the clue to understanding effects arising in this low mass region. We find interference to be large between pion and nucleon exchange amplitudes and that, separately, the pion and nucleon Deck total cross sections are in the approximate ration of 3.5 to 1.

Although our model does not predict quite large enough cross sections for diffractive (πN) production at large t, the t dependence of the model is generally in good qualitative agreement with data, and a large slope-mass correlation is predicted.

6: CONCLUSIONS

This thesis has illustrated some of the features of strong interaction phenomenology by means of two studies based on the π N $\rightarrow \pi\pi$ N reaction.

In the first two chapters we showed how the general principles of S-matrix theory can be applied to the simplest possible strong interaction process, pion-pion scattering, on which information may be obtained from a study of the π N $\rightarrow \pi\pi$N reaction in the appropriate kinematic region. These principles constrain the pion-pion scattering amplitudes considerably, when given a certain amount of experimental information, and provide a means of studying the amplitudes in energy regions not easily accessible to phase shift analysis. A thorough application of the crossing principle, by means of physical region crossing sum rules, yielded the information that high energy pion-pion scattering may, as expected, be described in terms of Regge and pomeron exchange, that the asymptotic pion-pion scattering cross section is probably rather small, and that the rho and f trajectories, coupling to pion-pion scattering, are apparently not strongly exchange degenerate. We found that a lack of good experimental information about low energy isospin two pion-pion scattering is the main barrier to obtaining better knowledge of high energy pion-pion scattering by means of the sum rule approach.

It would be interesting to extend the work of chapter 2 to relate the scattering of all in particles in the SU(3) pseudoscalar octet, by writing the crossing sum rules for U or V spin multiplets instead of for the isospin multiplet. The chief difficulty lies in the large mass differences between the particles in the octet, resulting in different thresholds for different scattering processes.

The second part of the thesis illustrates the use of strong interaction phenomenology in organizing data and understanding its general features in terms of simple ideas (without, however, obtaining any deep theoretical understanding or finely detailed predictions). We recalled evidence to demonstrate that double exchange processes (the Deck effect), with resonance excitation, explain qualitatively well a good deal of inelastic diffraction dissociation data. We then

showed in detail, taking spins and interference properly into account, that the pion exchange Deck mechanism, with resonance production and decay, affords a good description of the diffractive production of a pion-nucleon system of mass between 1.4 and 1.8 GeV in the 16 GeV/c π N $\rightarrow$ π π N reaction. The diffractive production of lower mass pion-nucleon systems in this reaction can be accounted for rather less well by taking the amplitude for the reaction as a sum of pion and nucleon exchange Deck amplitudes; it is necessary to make the model more complicated by including 'absorption'. The two main results to emerge from this calculation, are that the pomeron NN* coupling may, consistently with the data, be described as vectorlike, and that the pion-pion scattering total cross section at high energy is about 6 mb. This latter result, taken with the other evidence for a small meson-meson scattering total cross section, emphasizes the fact that the pomeron is not a simple factorizable Regge pole of intercept unity.

The work of chapters 4 and 5 can clearly be extended to other inelastic diffractive reactions as good angular distribution data becomes available; in particular the model for the pomeron coupling should be further tested, and the πp $\rightarrow$ ($\pi\pi\pi$)p reaction can be studied to resolve the problem of the existence or otherwise of the A_1 meson, by studying the angular distributions of the $\pi\pi$ ($\pi\pi$) system.

This thesis has demonstrated the remarkable amount of physics contained in the π N $\rightarrow$ π π N scattering process. It has illustrated the role of strong interaction phenomenology in extracting much interesting information from data, and in interpreting many physical effects in terms of a few simple ideas. The work described is a step along the path towards a good general description of strong interactions, to await a deeper understanding in terms of fundamental theory.

APPENDIX 1

A: S-matrix and state normalization

We define the transition matrix in terms of the S-matrix by:-

$$S_{fi} = 1 + (2\pi)^4 i\, \delta^4(P_f - P_i)\, T_{fi} \tag{1A1}$$

with the covariant state normalization:-

$$\langle p' | p \rangle = 2E\, \delta^3(\underline{p} - \underline{p}')\, (2\pi)^3 \tag{1A2}$$

The phase space element is:-

$$\prod_{\substack{\text{final state} \\ \text{particles}}} \frac{d^3 p_i}{(2\pi)^3 2E_i} \tag{1A3}$$

With the flux factor $1/4m_B|\underline{p}_L| = 1/4\sqrt{s}\,|\underline{p}_{CM}|$, we have the cross section for the $AB \rightarrow 1 \ldots n$ reaction as

$$\sigma = \frac{1}{4 m_B |\underline{p}_L|} \int \prod_i \frac{d^3 p_i}{(2\pi)^3 2E_i} \cdot (2\pi)^4\, \delta_4\Big(\sum p_i - p_A - p_B\Big) \times \\ \times \left| \langle p_1 \ldots p_N | T | p_A p_B \rangle \right|^2 \tag{1A4}$$

where m_B is the mass of target particle B and $\underline{p}_L$ is the laboratory beam momentum.

For a $2 \rightarrow 2$ reaction,

$$\frac{d^3 p_1 \cdot d^3 p_2}{2E_1 \cdot 2E_2 \cdot (2\pi)^2}\, \delta^4(p_1 + p_2 - p_A - p_B) = \frac{1}{(2\pi)^2}\, \delta^4(p - p_1 - p_2)\, \frac{d^4 p\, |\underline{p}_1^{CM}|}{4\sqrt{s}}\, d\Omega_1^{CM} \tag{1A5}$$

and so

$$\frac{d\sigma}{d\Omega} = \frac{1}{64\pi^2 s}\, \frac{|\underline{p}_1^{CM}|}{|\underline{p}_A^{CM}|}\, |T|^2 \tag{1A6}$$

B: Differential cross section 2 → 3 reaction

For three particles in the final state, the phase space integral is, from eq.(1A4):-

$$I = \int \frac{d^3P_1\, d^3P_2\, d^3P_3}{8E_1E_2E_3(2\pi)^5}\ \delta^4\left(P_1 + P_2 + P_3 - P_A - P_B\right) \tag{1B1}$$

To cast this into a more useful form, consider particles 1 and 2 together as 'R', and insert into eq.(1B1) the identity:-

$$1 = \int d^4P_R\ \delta^4\left(P_R - P_1 - P_2\right) \equiv \int d^3P_R \frac{ds_R}{2E_R}\ \delta^4\left(P_R - P_1 - P_2\right) \tag{1B2}$$

Rearranging, we then have:-

$$I = \int \frac{d^3P_R}{2E_R}\ \frac{d^3P_3}{2E_3\cdot(2\pi)^2}\ \delta^4\left(P_R + P_3 - P_A - P_B\right) \times \tag{1B3}$$

$$\times \int \frac{d^3P_1}{2E_1}\ \frac{d^3P_2}{2E_2(2\pi)^2}\ \delta^4\left(P_R - P_1 - P_2\right)\frac{ds_R}{2\pi}$$

Using eq.(1A5):-

$$I = \int \frac{1}{(2\pi)^2}\frac{|\underline{P}_1^{CM}|}{4\sqrt{s_R}}\, d\Omega_1 \cdot \frac{1}{(2\pi)^2}\frac{|\underline{P}_R|}{4\sqrt{s}}\, d\Omega_R\, \frac{ds_R}{2\pi} \tag{1B4}$$

$\underline{p}_1^{CM}$ and Ω_1, are the momenta and solid angles of particle 1 in the R centre of mass frame; $\underline{p}_R$ and Ω_R are the momenta and solid angles of R in the AB centre of mass frame.

Since the AB → R3 reaction is coplanar, we may integrate over ϕ_R. Using $d(\cos\theta_R) = \frac{dt_{A3}}{2|\underline{p}_R|^2}$, we have:-

$$I = \frac{1}{(2\pi)^4}\int \frac{|\underline{P}_1^{CM}|\, d\Omega_1\, dt_{A3}\, ds_R}{8\sqrt{s_R}\cdot 4|\underline{P}_R|\sqrt{s}} \tag{1B5}$$

and so the differential cross section, from eq.(1A4), is:-

$$d\sigma = \frac{1}{(32\pi^2|\underline{P}_L| m_B)^2} \times |\underline{P}'_{CM}| \times d\Omega_1 \, dt_{A3} \, dM_R |T|^2 \qquad (1B6)$$

APPENDIX 2

A: The $\pi^0\pi^0$ Roy equation

The $\pi^0\pi^0$ scattering amplitude, T(s,t,u) obeys a twice subtracted fixed t dispersion relation for $s \geqslant 0$ and $4 \geqslant t \geqslant -28$.(17) The s - u crossing property, T(s,t,u) = T(u,t,s), allows a subtraction constant to be removed (18) and so we may write the once subtracted relation:-

$$T(s,t_0) = T(0,t_0) + \frac{s}{\pi}\int_4^\infty A(x,t_0)\left(\frac{1}{(x-s)x} - \frac{1}{(x-4+s+t_0)(x-4+t_0)}\right)dx \qquad (2A1)$$

(The subtraction point s_0=0 has been chosen in eq.(1.8))

To remove the 't' dependence of the subtraction constant we first use s - t and t - u crossing to write:-

$$T(0,t_0,4-t_0) = T(4-t_0,0,t_0) \qquad (2A2)$$

A rigorously valid fixed t dispersion relation may now be written for $T(4-t_0, 0, t_0)$. Subtracting at s = 4 (t_0 = 0) we have:-

$$T(4-t_0,0,t_0) = T(4,0) - \frac{t_0}{\pi}\int_4^\infty A(x,0)\left(\frac{1}{(x-4+t_0)(x-4)} - \frac{1}{(x-t_0)x}\right)dx \qquad (2A3)$$

T(4, 0) is just the (constant) scattering length a^{00}. Substituting eq.(2A3) into eq.(2A1) leads to:-

$$T(s,t_0) = a_{00} + \frac{s(t_0+s-4)}{\pi}\int_4^\infty A(x,t_0)\left(\frac{t_0-4+2x}{(x-s)(x)(x-4+s+t_0)(x+t_0-4)}\right)dx$$
$$- + \frac{t_0(t_0-4)}{\pi}\int_4^\infty A(x,0)\left(\frac{2x-4}{(x-t_0)(x)(x-4+t_0)(x-4)}\right)dx \qquad (2A4)$$

eq.(2A4) is valid for $0 \leqslant s < \infty$, $4 \geqslant t \geqslant -28$. For s > 4 the left hand side is replaced by Re $T(s,t_0)$ and the right

hand side by a principal value integral. To obtain the integral (Roy)equation for the partial wave amplitudes, $A(\alpha,t)$ and $A(\alpha,o)$ are expanded using eq.(1.17). The partial waves are projected from $T(s,t)$ using :-

$$f_\ell^I(s) = \frac{1}{2}\sqrt{\frac{s-4}{s}} \int_{-1}^{1} T(s,t,u)\, P_\ell(z)\, dz \qquad (2A5)$$

Since $Z = 1+2t/(s-4)$, we can obtain $f_\ell(s)$ for $4 < s \lesssim 32$. However since $T(s,t,u) = T(u,t,s)$ the integral can be rewritten as over the range of Z from zero to one, and the Roy equation can then be used for $4 \lesssim s \lesssim 60$. In practice, iterative calculations are performed with amplitudes which may not obey the s-u crossing property, and errors (usually small) may be introduced by using the half range integration.(41) The extended Roy equations of ref.(49) do not suffer from this problem. To impose three channel crossing on the full amplitude, write eq.(2A4) for $T(s, 4-s-t_o, t_o)$ and equate to eq.(2A4) (thus imposing t - u crossing). The resulting equation is the supplementary condition (crossing sum rule) for the $\pi^o\pi^o$ scattering Roy equation.

APPENDIX 3

A: The sign of the s-channel azimuthal angle

We can determine $\cos \phi_s$ as described in chapter 4 but do not immediatly know the sign of ϕ_s.
Consider the invariant:-

$$K = \varepsilon_{\alpha\beta\gamma\delta} P_A^{\alpha} P_B^{\beta} P_C^{\gamma} P_D^{\delta} \tag{3A1}$$

By 4-momentum conservation:-

$$K = \varepsilon_{\alpha\beta\gamma\delta} P_A^{\alpha} P_B^{\beta} P_D^{\gamma} P_E^{\delta} \tag{3A2}$$

and antisymmetry implies:-

$$K = \varepsilon_{\alpha\beta\gamma\delta} P_A^{\alpha} P_B^{\beta} P_D^{\gamma} \left(P_D + P_E\right)^{\delta} \tag{3A3}$$

In the DE centre of mass, $P_D+P_E = (\sqrt{s_{DE}}, 0,0,0)$ and so:-

$$\begin{aligned} K &= \sqrt{s_{DE}} \left(\underline{P}_A \wedge \underline{P}_B\right) . \underline{P}_D \\ &= -\sqrt{s_{DE}} \left(\underline{P}_A \wedge \underline{P}_B\right) . \underline{P}_E \end{aligned} \tag{3A4}$$

And so, in the t channel:-

$$K = -\sqrt{s_{DE}} \, |\underline{P}_A| \, |\underline{P}_B| \sin\chi_t \sin\theta_t \sin\phi_t \tag{3A5}$$

Since $0 < \theta_t < \pi$, $0 < \chi_t < \pi$, we have:-

$$\text{sign}(\phi_t) = -\text{sign}(K) \quad \text{for} \quad 0 < |\phi_t| < \pi \tag{3A6}$$

Using $\underline{P}_A+\underline{P}_B = \underline{P}_C$, we have from eq.(3A4):-

$$K = -\sqrt{s_{DE}} \left(\underline{P}_C \wedge \underline{P}_B\right) . \underline{P}_E \tag{3A7}$$

in the s channel:-

$$K = -\sqrt{s_{DE}} \, |\underline{P}_C| \, |\underline{P}_B| \sin\chi_s \sin\theta_s \sin\phi_s \tag{3A8}$$

$$\therefore \quad \text{sign } \phi_s = - \text{ sign } (K) \tag{3A9}$$

$$\text{and so} \quad \text{sign } \phi_s = \text{sign } \phi_t \tag{3A10}$$

$\therefore 0 < \phi_t < \pi$ if and only if $0 < \phi_s < \pi$.

Appendix 4

A: Dirac Formalism

We use the Bjorken-Drell (95) convention for the Dirac γ matrices:-

$$\gamma_0 = \begin{pmatrix} 1 & 0 & 0 & 0 \\ 0 & 1 & 0 & 0 \\ 0 & 0 & -1 & 0 \\ 0 & 0 & 0 & -1 \end{pmatrix}, \underline{\gamma} = \begin{pmatrix} \underline{0} & \underline{\sigma} \\ -\underline{\sigma} & \underline{0} \end{pmatrix}, \quad \gamma_5 = \begin{pmatrix} 0 & 0 & 1 & 0 \\ 0 & 0 & 0 & 1 \\ 1 & 0 & 0 & 0 \\ 0 & 1 & 0 & 0 \end{pmatrix} \tag{4A1}$$

$\underline{\sigma}$ is the usual Pauli matrix vector.
The Dirac spinors for a spin $\frac{1}{2}$ particle of momentum $\underline{p}$ and polar angles θ , ϕ are:-

$$u_{\frac{1}{2}}(p) = \sqrt{E+m} \begin{pmatrix} \cos(\theta/2) \\ \sin(\theta/2)\, e^{i\phi} \\ (|\underline{p}|/(E+m))\cos(\theta/2) \\ (|\underline{p}|/(E+m))\sin(\theta/2)e^{i\phi} \end{pmatrix} \tag{4A2}$$

$$u_{-\frac{1}{2}}(p) = \sqrt{E+m} \begin{pmatrix} -\sin(\theta/2)\, e^{-i\phi} \\ \cos(\theta/2) \\ (|\underline{p}|/(E+m))\sin(\theta/2)\, e^{-i\phi} \\ -(|\underline{p}|/(E+m))\cos(\theta/2) \end{pmatrix}$$

B: The Pion exchange coupling

We wish to calculate the π NN coupling appearing in fig.1.3, $\bar{u}(\underline{p}_E)\gamma_5 u(\underline{p}_B)$, in the πN (DE) centre of mass frame, using the t channel coordinate system (fig.4.2a)

The incoming nucleon (B) has its helicity along the Z axis, while the outgoing nucleon (E) has its helicity at angles (θ, ϕ). We calculate the 'non-flip' coupling and state the results for the others.

Consider $T_{\frac{1}{2}\frac{1}{2}}(\pi) \propto \bar{u}_{\frac{1}{2}}(p_E)\,\gamma_5\,u_{\frac{1}{2}}(p_B)$

$$= u^{+}_{\frac{1}{2}}(p_E)\,\gamma_0\gamma_5\,u_{\frac{1}{2}}(p_B) \qquad (4B1)$$

using equs.(4A1, 4A2):-

$$T_{\frac{1}{2}\frac{1}{2}} \propto \left(\sqrt{E_E+M}\right)\left(\sqrt{E_B+M}\right)\left(\cos\frac{\theta}{2},\ \sin\frac{\theta}{2}e^{-i\phi},\ \frac{|p_E|}{E_E+M}\cos\frac{\theta}{2},\ \frac{|p_E|}{E_E+M}\sin\frac{\theta}{2}\right)\begin{pmatrix}\frac{|p_B|}{E_B+M}\\0\\0\\0\end{pmatrix} \qquad (4B2)$$

$$\therefore\ T_{\frac{1}{2}\frac{1}{2}} \propto \left(\sqrt{E_E+M}\right)\left(\sqrt{E_B+M}\right)\left(\frac{|p_B|}{E_B+M}-\frac{|p_E|}{E_E+M}\right)\cos\frac{\theta}{2} \qquad (4B3)$$

We find, likewise, that

$$T_{\frac{1}{2}-\frac{1}{2}} \propto -\left(\sqrt{E_E+M}\right)\left(\sqrt{E_B+M}\right)\left(\frac{|p_B|}{E_B+M}-\frac{|p_E|}{E_E+M}\right)\sin\frac{\theta}{2}e^{-i\phi} \qquad (4B4)$$

and

$$T_{-\frac{1}{2}-\frac{1}{2}}(\theta) = -T_{\frac{1}{2}\frac{1}{2}}(\theta)$$

$$T_{-\frac{1}{2}\frac{1}{2}}(\theta,\phi) = T_{\frac{1}{2}-\frac{1}{2}}(\theta,-\phi) \qquad (4B5)$$

We may check these results by calculating explicitly

$$\frac{1}{2}\sum_{\mu\nu=\pm\frac{1}{2}}|T_{\mu\nu}|^2 = -t_{EB} \qquad (4B6)$$

which is the same result as obtained by writing

$$\frac{1}{2}\sum_{\substack{\mu\nu\\=\pm\frac{1}{2}}}|T_{\mu\nu}|^2 = \frac{1}{2}\,\mathrm{Trace}\left((\not{p}_E+M)\gamma_5(\not{p}_B+M)\gamma_5\right)$$

$$= -2M^2 + 2p_E^{\mu}p_{B\mu} = -t_{EB}$$

C: The Nucleon exchange coupling

This is the coupling appearing in the diagram of fig.1.3b and is to be evaluated in the π N (DE) centre of mass, using t-channel axes. We write:-

$$T(N) \propto \bar{u}(P_E) \frac{1}{\not P_B - \not P_D - M} \gamma_5 u(P_B) \tag{4C1}$$

which may be rewritten:-

$$T(N) \propto \bar{u}(P_E) \frac{(\not P_B - \not P_D + M)}{t_{DB} - M^2} \gamma_5 u(P_B) \tag{4C2}$$

which, with the aid of the Dirac equation, reduces to:-

$$T(N) \propto -\bar{u}(P_E) \not P_D \gamma_5 u(P_B) \tag{4C3}$$

It is now trivial, but tedious, to calculate the spin amplitudes, using eqs.4A1 and 4A2. We find:-

$$T_{\frac{1}{2}-\frac{1}{2}} \propto \sqrt{(E_B+M)(E_E+M)}\, \sin\frac{\theta}{2}\, e^{i\phi} \left(E_D \left(\frac{|\underline{P}_B|}{E_B+M} - \frac{|\underline{P}_E|}{E_E+M} \right) - |\underline{P}_D| \left(1 - \frac{|\underline{P}_B||\underline{P}_E|}{(E_B+M)(E_E+M)} \right) \right) \tag{4C4}$$

$$T_{\frac{1}{2}\frac{1}{2}} \propto \sqrt{(E_B+M)(E_E+M)}\, \cos\frac{\theta}{2} \left(E_D \left(\frac{|\underline{P}_B|}{E_B+M} + \frac{|\underline{P}_E|}{E_E+M} \right) + |\underline{P}_D| \left(1 + \frac{|\underline{P}_B||\underline{P}_E|}{(E_B+M)(E_E+M)} \right) \right) \tag{4C5}$$

$$\text{and} \quad T_{-\frac{1}{2}-\frac{1}{2}}(\theta) = -T_{\frac{1}{2}\frac{1}{2}}(\theta), \quad T_{-\frac{1}{2}\frac{1}{2}}(\theta,\phi) = T_{\frac{1}{2}-\frac{1}{2}}(\theta,-\phi) \tag{4C6}$$

Away from the threshold for pion-nucleon production, when $E_\pi \simeq |\underline{p}_\pi|$, we find, either by explicit calculation or by the use of trace methods:-

$$\frac{1}{2}\sum_{\substack{\mu\nu \\ =\pm\frac{1}{2}}} |T_{\mu\nu}(N)|^2 \simeq \frac{2E_0^2}{(t_{DB}-M^2)^2}\left(E_E + |\underline{p}_E|\right)\left(E_\theta + |\underline{p}_B|\cos\theta\right) \qquad (4C7)$$

D: N* resonance production couplings

We first summarize the formalism needed for the description of spin $\frac{3}{2}$ and spin $\frac{5}{2}$ particles. The wave function for a spin $\frac{3}{2}$ particle is written as the direct product of a spin one and a spin $\frac{1}{2}$ wave function:-

$$\left|\tfrac{3}{2},\lambda\right\rangle = \sum_{\substack{m,m' \\ m+m'=\lambda}} \left|1\ m\right\rangle\left|\tfrac{1}{2}\ m'\right\rangle \times \text{Clebsch} \qquad (4D1)$$

Thus $$u_\mu^{\pm\frac{3}{2}} = \varepsilon_\mu^{\pm 1}\, u^{\pm\frac{1}{2}} \qquad (4D2)$$

and $$u_\mu^{\pm\frac{1}{2}} = \frac{1}{\sqrt{3}}\,\varepsilon_\mu^{\pm 1}\, u^{\mp\frac{1}{2}} + \sqrt{\frac{2}{3}}\,\varepsilon_\mu^{0}\, u^{\pm\frac{1}{2}} \qquad (4D3)$$

The spin $\frac{5}{2}$ wave functions are obtained from the direct product of a spin one and a spin $\frac{3}{2}$ wave function :-

$$\left|\tfrac{5}{2},\lambda\right\rangle = \sum_{\substack{m,m' \\ m+m'=\lambda}} \left|1\ m\right\rangle\left|\tfrac{3}{2}\ m'\right\rangle \times \text{Clebsch} \qquad (4D4)$$

Thus:-

$$u_{\mu\nu}^{\pm\frac{5}{2}} = \varepsilon_\mu^{\pm 1}\, u_\nu^{\pm\frac{3}{2}} \tag{4D5}$$

$$u_{\mu\nu}^{\pm\frac{3}{2}} = \sqrt{\frac{2}{5}}\,\varepsilon_\mu^{0}\, u_\nu^{\pm\frac{3}{2}} + \sqrt{\frac{3}{5}}\,\varepsilon_\mu^{\pm 1}\, u_\nu^{\pm\frac{1}{2}} \tag{4D6}$$

$$u_{\mu\nu}^{\pm\frac{1}{2}} = \sqrt{\frac{3}{5}}\,\varepsilon_\mu^{0}\, u_\nu^{\pm\frac{1}{2}} + \sqrt{\frac{3}{10}}\,\varepsilon_\mu^{\pm 1} u_\nu^{\mp\frac{1}{2}} + \frac{1}{\sqrt{10}}\,\varepsilon_\mu^{\mp 1} u_\nu^{\pm\frac{3}{2}} \tag{4D7}$$

In the N* rest frame, the spin one polarization vectors ε^i are:-

$$\varepsilon^0 = (0,\ 0,\ 0,\ 1) \tag{4D8}$$

$$\varepsilon^{\pm 1} = \frac{1}{\sqrt{2}}(0,\ \mp 1,\ -i,\ 0) \tag{4D9}$$

Now consider π N $\to \pi'$ N* scattering. If the pomeron is taken to couple as a natural parity spin one particle, as in chapter 5, then the most general pomeron -N-N*$^{5/2}$ coupling, for the production of an N* of spin projection λ , may be written:-

$$C^\beta = \bar{u}_\nu^\lambda(p')\left(g_1 P^\beta P^\nu + g_2 \gamma^\beta P^\nu + g_3 g^{\beta\nu}\right) u(p) \tag{4D10}$$

where $$p = \frac{1}{2}\left(P_N + P_{N^*}\right) = \frac{1}{2}\left(E_N + M_{N^*},\ \underline{P}_N\right) \tag{4D11}$$

In the N* centre of mass frame of reference.
The other independent 4-vector may be taken as

$$Q = \frac{1}{2}\left(P_\pi + P_{\pi'}\right) = \frac{1}{2}\left(E_\pi + E_{\pi'},\ \underline{P}_\pi + \underline{P}_{\pi'}\right) \tag{4D12}$$

For the production of $N^*\frac{5}{2}$ states, the most general coupling is of the form:-

$$C^\beta = \bar{u}^\lambda_{\mu\nu}(p')\left(g_1 p^\beta p^\mu p^\nu + g_2 \gamma^\beta p^\mu p^\nu + g_3 g^{\beta\mu} p^\nu\right) \qquad (4D13)$$

Noting that

$$p^\nu \varepsilon^{\pm 1}_\nu = 0 \qquad (4D14)$$

we see that only the $\varepsilon_\nu{}^0$ parts of eqs.(4D6, 4D7) contribute to C^β, and thus the pomeron couplings for a spin $\frac{5}{2}$ N* are simply proportional to those for a spin $\frac{3}{2}$ N*, and are obtained immediately.

For the production of a spin $\frac{3}{2}$ N*, of helicity $\frac{1}{2}$, we write:-

$$T^{\frac{3}{2}\frac{1}{2}}_{\frac{1}{2}} = Q_\beta\left(\frac{1}{\sqrt{3}}\,\varepsilon^{1*}_\mu\,\bar{u}_{-\frac{1}{2}}\left(g_1 p^\beta p^\mu + g_2\gamma^\beta p^\mu + g_3 g^{\beta\mu}\right)u_{\frac{1}{2}}\right.$$
$$\left. + \sqrt{\frac{2}{3}}\,\varepsilon^{0*}_\mu\,\bar{u}_{\frac{1}{2}}\left(g_1 p^\beta p^\mu + g_2\gamma^\beta p^\mu + g_3 g^{\beta\mu}\right)u_{\frac{1}{2}}\right) \qquad (4D15)$$

By eq.(4D14) the first term vanishes, and so, from the second term:-

$$T^{\frac{3}{2}\frac{1}{2}}_{\frac{1}{2}} = -\sqrt{\frac{2}{3}}\sqrt{2m_N^2(E_N+m_N)}\left(\frac{1}{2}g_1 P_\beta Q^\beta\left|\underline{P}_N\right| + \right.$$
$$\left. + \frac{1}{2}g_2\left|\underline{P}_N\right|\left(Q_0 - \frac{\left|\underline{P}_N\right| Q_z}{E_N+m_N}\right) + g_3 Q_z\right) \qquad (4D16)$$

which can immediately be expressed in terms of known N* centre of mass angles, energies and momenta. We find:-

$$T^{\frac{3}{2}-\frac{1}{2}}_{-\frac{1}{2}} = T^{\frac{3}{2}\frac{1}{2}}_{\frac{1}{2}} \qquad (4D17)$$

and similarly:-

$$T_{\frac{1}{2}}^{\frac{3}{2}\frac{3}{2}} = -T_{-\frac{1}{2}}^{\frac{3}{2}-\frac{3}{2}} = \frac{g_3}{2} Q_\alpha \sqrt{2 m_{N^*}(E_N + m_N)} \qquad (4D18)$$

$$T_{\frac{1}{2}}^{\frac{3}{2}-\frac{1}{2}} = -T_{-\frac{1}{2}}^{\frac{3}{2}\frac{1}{2}} = \sqrt{\frac{2}{3}} \sqrt{2 m_{N^*}(E_N + m_N)} \times \qquad (4D19)$$

$$\times \left(\frac{|\underline{P}_N|^2}{2(E_N + m_N)} g_2 - \frac{g_3}{2} \right)$$

E: N* → π N decay, helicity conservation and azimuthal angular distributions

The amplitude for the decay of an N* resonance of spin J, and spin component λ to a pion, and a nucleon of helicity ν and polar angles (θ , ϕ) is given by:-

$$M_{\nu\lambda}^{J} \propto D_{\lambda\nu}^{J^*}(\phi, \theta, -\phi) A_\nu^J = d_{\lambda\nu}^J(\theta) e^{i(\lambda-\nu)\phi} A_\nu^J \qquad (4E1)$$

The rotation functions $d_{mm'}^J(\theta)$ are calculated from the general formula, due to Wigner, given in appendix A2 of ref.(15). Parity conservation in the decay implies

$$A_\nu^J = (-1)^{J-\frac{1}{2}} A_{-\nu}^J \eta_\pi \eta_{N^*} \eta_N \qquad (4E2)$$

where η_x is the intrinsic parity of particle X.
Since we assume that only natural parity N* resonances are produced, eq.(4E2) implies that:-

$$A_\nu^J = -A_{-\nu}^J \qquad (4E3)$$

Since $\nu = \pm \frac{1}{2}$, the decay only involves one coupling constant. The angular distribution of the outgoing pion-nucleon system is given by:-

$$W(\theta, \phi) \propto \left| \sum_{\mu\nu} T^{J\lambda}_{\mu} M^{J}_{\nu\lambda} \right|^2 \qquad (4E4)$$

(where μ , ν take values $\pm \frac{1}{2}$). This will be independent of ϕ unless more than one N* helicity state is populated. Thus if an anisotropy is observed in the azimuthal angular distribution in a given frame of reference, helicity is not conserved in the production of a pion-nucleon system in that frame of reference.

For the overall amplitude for N* production and decay, $T_{\nu\mu} = \sum_{\lambda} T^{J\lambda}_{\mu} M^{J}_{\nu\lambda}$, we find, by eqs. 4D17 - 4D19 and 4E4,

$$T_{-\frac{1}{2}-\frac{1}{2}}(\theta, \phi) = -T_{\frac{1}{2}\frac{1}{2}}(\theta, -\phi) \qquad (4E5)$$

$$T_{\frac{1}{2}-\frac{1}{2}}(\theta, \phi) = T_{-\frac{1}{2}\frac{1}{2}}(\theta, -\phi)$$

These relations also hold for the pion and nucleon exchange Deck amplitudes (eqs.4B5, 4C6) and are in fact a general consequence of parity invariance. The angular distribution must therefore, from eq.(4E4), obey:-

$$W(\theta, \phi) = W(\theta, -\phi) \qquad (4E6)$$

REFERENCES

1. J.Iliopoulis, Lectures given at the International School of Elementary Particle Physics, Basko Polje 1975.

2. S.Weinberg, Proc.II Int.Conf.on Elementary Particle Physics, Aix-en-Provence 1973.

   T.Applequist, R.Barbeiri, Proc.1975 Cargèse Summer School, Cargèse, 1975.

3. S.D.Bjorken, Symposium summary, Proc.Int.Symposium on lepton and photon interactions, Stanford 1975.

4. M. Froissart, Phys.Rev.123 (1961) 1053.

5. R.J.Eden et.al., 'The Analytic S-Matrix', Cambridge University Press 1966.

6. S.Weinberg, Phys. Rev.Lett. 17 (1966) 616.

   S.L.Adler, R.F.Dashen, 'Current Algebras', Benjamin (1968)

7. P.Estabrooks, A.D.Martin, Nucl.Phys. B95 (1975) 322.

8. B.Hyams et.al., Nucl,Phys. B64 (1973) 134.

9. W.Männer, Proc.IV Int.Conf. on Experimental Meson Spectroscopy, Boston 1974.

10. S.D.Protopopescu et al., Phys.Rev. D7 (1973) 1279.

11. P.Baillon et al., Phys.Lett. 38B (1972) 555.

12. W.D.Apel et.al., contributed paper to Palermo Conference on High Energy Physics, 1975.

13. J.L.Petersen, Phys.Reports 2C (1971) 155.

    D.Morgan, "Questions in $\pi\pi$ scattering and related processes", Rutherford Lab.report RPP/T/27 (1972).

    B.R.Martin, D.Morgan, G.Shaw, 'Pion-Pion interactions in particle physics', Academic Press (1976).

14. L.D.Soloviev et.al., Phys.Lett. 24B (1967) 181.

    R.Dolen et.al., Phys.Rev.Lett. 19(1967) 402,
    Phys.Rev.166 (1968) 1768.

    K.Igi et.al., Phys.Rev.Lett. 18 (1969) 625.

15. A.D.Martin, T.D.Spearman, 'Elementary Particle Theory', North Holland, 1970.

16. S.Mandelstam, Phys.Rev.112 (1958) 1344.

17. A.Martin, Nuovo Cimento 42A (1966) 930.

18. G.Wanders, Nuovo Cimento 63A (1969) 108.

19. G.Grayer et.al., Nucl.Phys. B75 (1974) 189.

20. E.C.Titchmarsh, 'The Theory of Functions', Oxford University Press, 1950.

21. H.Lehmann, Nuovo Cimento 10 (1958) 579.

22. S.M.Roy, Phys.Letters 36B (1971) 353.

23. P.H.Frampton, 'Dual Resonance Models', W.A.Benjamin, 1974.

J.Scherk, Rev.Mod.Phys. 47 (1975) 123.

S.Mandelstam, Phys.Reports 13C (1974) 261.

G.Veneziano, Phys.Reports 9C (1974) 1.

24. H.Harari, Phys.Rev.Lett. 20 (1968) 1395.

P.G.O.Freund, Phys.Rev.Lett. 20 (1968) 235.

25. E.Predazzi, Lectures given at the International School of Elementary Particle Physics, Basko Polje 1975.

26. P.D.B.Collins et.al., Nucl.Phys. B80 (1974) 135.

27. M.Gell-Mann, Phys.Rev.Lett. 8 (1962) 263.

V.N.Gribov,I.Y.Pomeranchuk, Phys.Rev.Lett. 8 (1962) 343.

28. C.D.Froggatt,J.L.Petersen, Nucl.Phys. B91 (1975) 454.

29. R.C.Johnson, A.D.Martin, M.R.Pennington, 'Does the ρ' couple to $\pi\pi$? A question of analyticity', CERN preprint TH-2153 (1976).

30. T.Shimada, University of Tokyo thesis. (unpublished)

31. A.Martin, Nuovo Cimento 47A (1967) 265; 58A (1968) 303; 63A (1969) 167.

32. G.Wanders,Springer Tracts in Modern Physics 57 (1971) 22.

33. P.Grassberger, H.Kuhnelt, Nucl.Phys.B70 (1973) 536.

34. D.H.Lyth, Nuovo Cimento Lett. 2 (1969) 724.

35. G.Wanders, Nuovo Cimento 63A (1969) 108.

36. R.Roskies, Phys.Rev. D2 (1970) 247, 1649.

37. S.Krinsky, Phys.Rev.D4 (1971) 1046.

38. M.K.Pidcock, Nucl.Phys. B83 (1974) 253.

39. C.Schmid, Phys.Rev.Lett. 20 (1968) 628.

40. G.Kaiser, Nucl.Phys. B43 (1972) 345.

41. D.Atkinson, T.Pool, Nucl.Phys. B81 (1974) 502.

42. J.L.Basdevant, C.D.Froggatt, J.L.Petersen, Phys.Lett. 41B (1972) 173, 179; Nucl.Phys. B72 (1974) 413.

43. J.C.Le Guillou, A.Morel, H.Navelet, Nuovo Cimento 5A (1971) 659.

44. D.Morgan, G.Shaw, Phys.Rev. D2 (1970) 520.

45. M.R.Pennington, S.D.Protopopescu, Phys.Rev. D7 (1973) 1429.

46. D.Morgan, G.Shaw, Nucl.Phys. B43 (1972) 365.

47. Geneva-Saclay collaboration, P.Extermann et.al., paper submitted to 1975 Palermo Conf. on High Energy Physics.

48. J.L.Petersen, Lectures at Internationale Universitätwoche für Kernphysik, Schladming 1974.

J.L.Basdevant et.al., Nucl.Phys. B98 (1975) 285.

49. G.Mahoux, S.M.Roy, G.Wanders, Nucl.Phys. B70 (1974) 297.

50. A.K.Common, M.R.Pennington, Nuovo Cimento 25A (1975) 219.

51. M.R.Pennington, Ann.Phys. 92 (1975) 164.

52. W.Hoogland et.al., Nucl.Phys. B69 (1974) 266.

53. J.P.Dilley, R.Teshima, Nucl.Phys. B46 (1972) 275.

54. P.Grassberger, Nucl.Phys. B70 (1974) 141.

55. J.L.Basdevant, C.Shomblond, Phys.Lett. 45B (1973) 48.

56. E.P.Tryon, Phys.Rev. D8 (1973) 1586, D11 (1975) 698.

57. J.A.Shapiro, Phys.Rev. 179 (1969) 1345

58. N.B.Durusoy et.al., Phys.Lett. 45B (1973) 517.

59. D.Cohen et.al., Phys.Rev. D7 (1973) 661.

60. M.Bardadin-Otwinoska et.al., Nucl.Phys. B72 (1974) 1.

61. J.Hanlon et.al., 'The inclusive reactions pn → pX and $\pi^+ n \rightarrow pX$ at 100 GeV/c', Fermilab preprint FERMILAB-Pub.-76/28-EXP (1976).

62. P.D.B.Collins, F.D.Gault, A.Martin, Nucl.Phys. B83 (1974) 241.

63. P.D.B.Collins, F.D.Gault, A.Martin, Nucl.Phys. B80 (1974) 135.

64. M.R.Pennington, A.Gula, Nucl.Phys. B96 (1975) 535.

65. R.T.Deck, Phys.Rev.Lett. 13 (1964) 169.

S.D.Drell, K.Hiida, Phys.Rev.Lett. 7 (1961) 199.

66. H.Grässler et.al., Nucl.Phys. B95 (1975) 1.

67. K.Boesebeck et.al., Nucl.Phys. B40 (1972) 39.

68. J.V.Beaupré et.al., Nucl.Phys. B66 (1973) 93.

69. M.Deutschmann et.al., Nucl.Phys. B86 (1975) 221.

70. E.Berger, 'A critique of the Reggeized Deck Model', Argonne preprint ANL - HEP - PR - 75 - 06 (1975).

71. D.Evans et.al., Nuovo Cimento 14A (1973) 651.

72. K.Gottfried, J.D.Jackson, Nuovo Cimento 33 (1964) 309.

73. G.Berlad et.al., Nucl.Phys. B75 (1974) 93.

74. G.Berlad et.al., Nucl.Phys. B78 (1974) 29.

75. M.Derrick, 'Diffractive Processes', Argonne preprint ANL - HEP - CP - 75 - 52 (1975).

76. J.Biel et.al., Phys.Rev.Lett. 36 (1976) 504, 507.

77. P.Bosetti et.al., Nucl.Phys. B103 (1976) 189.

78. E.Berger, Proc.Int.Colloquim on Multiparticle Reactions, Oxford 1975.

79. G.W.Brandenburg et.al., Nucl.Phys. B45 (1972) 397.

80. G.Cohen-Tannoudji et.al., Nucl.Phys. B95 (1975) 445.

81. H.Miettinen, P.Pirilä, Phys. Lett. 40B (1972) 127.

82. G.Vassiliadus et.al., Nucl.Phys. B103 (1976) 1.

83. H.Miettinen, Proc.Palermo Conf. on High Energy Physics (1975).

84. E.L.Berger, P.Pirilä, Phys.Rev.D12 (1975) 3448; 'Absorptive effects in the diffractive dissociation of nucleons', Argonne report ANL-HEP-PR-75-34 (1975.

85. D.R.O.Morrison, Phys.Rev. 165 (1968) 1699.

86. Y. Oh et.al., Phys.Lett. 42B (1972) 497.

87. G.C.Fox, Experimental Meson Spectroscophy, A.I.P.Conf.Proc. (1972)

88. G.Berlad et.al., Nucl.Phys. B78 (1974) 29.

89. M.Uehara et.al., 'Partial wave analysis for low mass N π system produced in diffraction dissociation', Kyushu preprint KYUSHU-75-HE-6 (1975).

90. R.E.Ansorge et.al., 'Spin parity analysis of diffractive $n \rightarrow p\pi^-$ and the question of a parity change rule', Cambridge preprint (1975).

91. W.Ochs et.al., Nucl.Phys. B102 (1976) 405.

92. P.D.B.Collins, F.D.Gault, to be published.

93. G.Von Gehlen, Proc 6th International Conf. on Electron and Photon Interactions at High Energies, Bonn 1973.

94. P.V.Landshoff, J.C.Polkinghorne, Nucl.Phys. B32 (1971) 541.

95. J.D.Bjorken, S.Drell, Relativistic Quantum Mechanics, McGraw-Hill, 1965.